國立臺灣大學獸醫專業學院獸醫學系

碩士論文

Department of Veterinary Medicine
School of Veterinary Medicine
National Taiwan University

Master Thesis

分析傳染性腹膜炎貓隻積液中之貓冠狀病毒及抗體及其與第二型嚴重急性呼吸綜合症冠狀病毒之間的關聯性

Feline coronavirus and antibodies in effusions of cats with feline infectious peritonitis and their potential cross-reactivity with SARS-CoV-2

甘曜銘

Yao-Ming Kan

指導教授：陳慧文 博士

Advisor: Hui-Wen Chen, D.V.M., Ph.D.

中華民國 112 年 7 月

July 2023

doi:10.6342/NTU202301829

序言

兩年的研究生活稍縱即逝，眼看碩士階段即將告一段落，心中難免不捨。首先要感謝的是我的指導老師——陳慧文教授，是您當初的一席話帶我踏進了獸醫基礎研究領域，並近一步地瞭解病毒以及感染免疫的奧妙。順著近年 COVID-19 大流行以及冠狀病毒研究的熱潮，加上過程中您學術知識、經驗和研究熱情的深刻影響，使我在就學期間能夠克服困難，不斷進步取得成果。在這邊，也要感謝各位口試委員與教授不吝惜提供寶貴意見，讓論文得以更臻完善。再來，要感謝實驗室的研究團隊，尤其是同梯的軍達、艾艾，有你們的時光總是不無聊，帶給我無比充實的實驗室生活。專業知識與實驗技術則要感謝已畢業的學長姐耀云、孟錡，與實驗室同仁敬元、紫珣、光雯的耐心指導，對於論文數據收集扮演重要角色。接下來，要感謝系壘的學弟妹們，讓我可以發揮運動所長，在課業之餘能夠打球放鬆，使思緒更加流暢。家人們的鼓勵也是我最強大的後盾，儘管父母、胞弟及寵物犬小不點遠在台南，但不時的電話關心總是能一解思鄉情懷，加添向前邁進的動力。此外，最要感謝鈺欣，在論文撰寫期間，不斷地給予陪伴與支持，甚至每週末從台中上台北協助生活起居，使我能全力地投入研究當中。最後，感謝這段期間遇到的每個人，從小到大求學階段皆為南部記憶的我，因為有你們，才能更深刻地體會北部生活，令眼界更加開闊。未來的路上，秉持著各位帶給我的豐富知識與見解，期望能更上一層樓，在畢業後未知領域持續前進。《荀子・勸學》：「鍥而舍之，朽木不折；鍥而不捨，金石可鏤。」

2023 年 春 甘曜銘 謹誌

doi:10.6342/NTU202301829

中文摘要

貓傳染性腹膜炎 (FIP) 是由貓冠狀病毒 (FCoV) 其中一種生物型，貓傳染性腹膜炎病毒 (FIPV) ，引起之貓致命性疾病。而對於 FIPV 感染期間的病理免疫機制，尤其是抗體依賴增強作用 (ADE) 缺乏研究，這導致該病毒疫苗開發方面存在不確定因素。此外，貓對於近年造成全球威脅的第二型嚴重急性呼吸道綜合症冠狀病毒 (SARS-CoV-2) 也具有感受性，當貓同時感染這兩種冠狀病毒，FIPV 和 SARS-CoV-2 之間的潛在交叉反應便成了一大議題。本研究旨在通過對 FIP 患貓的積液樣本中的病毒和抗體進行分析，以增加我們對 FIP 病理發生機制和冠狀病毒交叉反應的了解。從 2022 年 1 月開始，46 個疑似 FIP 貓腹水樣本經 PCR 和免疫螢光試驗 (IFA) 的重複驗證確診為陽性。而首先，我們對這些陽性案例的特徵進行分析以揭示 FIP 的危險因子，發現了 2 歲以下以及白蛋白與球蛋白比值 (A/G ratio) 小於等於 0.4 的貓隻與 FIP 陽性有著顯著關聯。隨後，我們成功地在 36 個陽性 FIP 積液樣本中進行了 FCoV 片段的序列分析，其中 36 個屬於基因一型，僅有一個檢體同時存在基因一型和二型 FCoV，相對於基因二型 FCoV，基因一型 FCoV 親緣樹狀圖顯示出高度多樣性。再者，積液當中的細胞激素 TNF-α 及 IL-6 濃度，雖在 FIP 陽性與陰性病例之間並無顯著差異，但仍使我們更進一步瞭解該疾病的免疫機制。此外，通過從 FIP 患貓積液中純化之免疫球蛋白 G (IgG) 和建立的體外 FIPV ADE 測試模型，檢測到了 FIP 陽性積液樣本中的 ADE 現象。另一項研究探討了 FCoV 和 SARS-CoV-2 之間的潛在交叉反應，結果顯示，來自兔隻抗 SARS-CoV-2 核殼蛋白 (Nucleocapsid) 的多株抗體 (pAb) 通過西方墨點法 (Western blot) 和酵素連結免疫吸附試驗（ELISA）與 FCoV 產生反應，但在 FIPV ADE 測試模型沒有觀察到 ADE 現象。為進一步研究這兩種病毒之間的關係，將人類 COVID-19 康復血清引入測試，發現兩名患者的血清與 FCoV 的刺突蛋白 (Spike) 亞單位 1 (subunit 1) 和核殼蛋白產生交叉反應。同時，一人的血清樣本甚至略微增強 FIPV 的感染狀態，是為 ADE 現象，也初步證實了兩種病毒的交叉反應。此外，將 FIP 貓積液中的 IgG 與 SARS-CoV-2 的刺突蛋白、核殼蛋白及其片段進行測試，發現

doi:10.6342/NTU202301829

IgG 能夠與 SARS-CoV-2 的刺突蛋白亞單位 2 (subunit 2) 和核膜蛋白的所有片段結合，這再次證明了 FCoV 和 SARS-CoV-2 之間的雙向交叉反應。本研究首次報告了 FIP 貓積液中 IgG 引發的 ADE 現象，並發現 FCoV 和 SARS-CoV-2 之間的潛在交叉反應，為未來 FIPV 之感染研究提供了更近一步的見解。

關鍵字：貓傳染性腹膜炎、貓冠狀病毒、抗體依賴增強作用、交互作用、第二型嚴重急性呼吸道症候群冠狀病毒

doi:10.6342/NTU202301829

Abstract

Feline infectious peritonitis (FIP) is a fatal disease in cats caused by feline infectious peritonitis virus (FIPV), a biotype of feline coronavirus (FCoV). The lack of research on antibody-dependent enhancement (ADE) during FIPV pathogenesis has resulted in uncertainties in vaccine development. Moreover, cats are susceptible to severe acute respiratory syndrome coronavirus-2 (SARS-CoV-2), another coronavirus posing a pandemic threat, and the potential cross-reactivity between these two coronaviruses remains unclear. This study aimed to increase our knowledge of FIP pathogenesis and coronavirus cross-reactivity by characterizing the virus and antibodies in FIP-diseased effusion samples. From January 2022, 46 FIP-confirmed samples were collected using PCR and IFA simultaneously. The signalments of these cases were firstly analyzed to reveal the FIP risk factors, which discovered that the cats with age equal to or lower than two y/o and A/G ratio equal to or lower than 0.4 were significantly correlated to FIP-positive cases. Subsequently, materials related to FIP pathogenesis in FIP effusions were investigated. FCoV fragments were successfully sequenced in 36 positive samples, with 35 cases belonging to genotype I and only one co-infected with genotype I and II FCoV. The phylogenetic analysis of the type I FCoV sequences revealed high diversity. Although there was no significant difference in the level of TNF-α and IL-6 in the effusions between FIP-positive and FIP-negative cases, this finding contributes to a better understanding of

doi:10.6342/NTU202301829

the immune mechanisms underlying FIP. The ADE phenomenon was also detected in FIP-positive effusion samples through IgG purified from FIP cat's effusions and the established *in vitro* FIPV ADE test model. Another investigation explored the potential cross-reactivity between FCoV and SARS-CoV-2. Results revealed that only rabbit-derived anti-SARS-CoV-2 nucleocapsid pAb reacted with FCoV through western blot and ELISA, but no ADE phenomenon was observed. To further study the relationship between these two viruses, human COVID-19 convalescent serum was introduced into the test, which surprisingly demonstrated that serum from two patients cross-reacted with FCoV spike subunit 1 (S1) and nucleocapsid proteins—meanwhile, one human serum sample even slightly enhanced FIPV infection. Also, the IgG from FIP cat effusions was incubated with SARS-CoV-2 spike, nucleocapsid proteins, and their truncated fragments. The IgG was found capable of binding to the spike subunit 2 (S2) and all fragments of nucleocapsid protein of SARS-CoV-2, which proved the two-way cross-reactivity between FCoV and SARS-CoV-2. This study is the first to report the *in vitr*o ADE phenomenon elicited from IgG in FIP effusions and discovered potential cross-reactivity between FCoV and SARS-CoV-2, providing valuable insights for future FIPV studies.

Keywords: Feline infectious peritonitis, feline coronavirus, antibody-dependent enhancement, cross-reactivity, SARS-CoV-2

doi:10.6342/NTU202301829

Contents

doi:10.6342/NTU202301829

doi:10.6342/NTU202301829

doi:10.6342/NTU202301829

doi:10.6342/NTU202301829

doi:10.6342/NTU202301829

List of Figures

doi:10.6342/NTU202301829

doi:10.6342/NTU202301829

List of Tables

doi:10.6342/NTU202301829

Chapter 1 Introduction

1.1 Feline coronavirus

1.1.1 The structure of Feline Coronavirus

Feline coronavirus, FCoV in abbreviation, can be found ubiquitous and lead to infection in domestic, outdoor, and wildlife cat species (Hofmann-Lehmann et al., 1996; Paul-Murphy et al., 1994; Stout et al., 2021). The seropositive rate in domestic cats was indicated to be up to 60%, and even 90% in cats from multi-cat environments (Pedersen, 2009, 2014b), which pointed out the importance of discussing this virus. FCoV belongs to the family coronaviridae, subfamily orthocoronavirinae, genus alphacoronavirus, which is together with the other three genera, betacoronavirus, gammacoronavirus, and deltacoronavirus (Woo et al., 2023). In the genus alphacoronavirus, porcine transmissible gastroenteritis virus (TGEV) and canine coronavirus (CCoV) are the more similar viruses to FCoV, which is in the same subgenus tegacovirus. However, some human alphacoronaviruses, like Human coronavirus NL63 (HCoV-NL63) and Human coronavirus 229E (HCoV-229E), were found distantly related since they are in different subgenus, which is duvinacovirus and setracovirus for each (Payne, 2017; Woo et al., 2023).

FCoV is an enveloped virus with a symmetrically spherical shape in a diameter of about 100 nm and a crown-like appearance with projections or spikes ranging from 12 to

doi:10.6342/NTU202301829

24 nm, which is the origin of the name, coronavirus (Bárcena et al., 2009; Fehr and Perlman, 2015). Four structural proteins comprise FCoV, including envelope (E), spike (S), membrane (M), and nucleocapsid (N) protein (Jaimes and Whittaker, 2018). The outer envelope with the M protein and the N protein provides protection and stabilization for the genome inside the virus. The S protein was found to be the pathogenic factor when it binds to the receptor of the host cells (Perlman et al., 2020). Besides, the S protein can be divided into Subunit 1 (S1) and Subunit 2 (S2). The S1 part is functioned as the receptor binding domain (RBD), comprising the functional amino-terminal (N-terminal) domain (NTD) and the carboxyl-terminal (C-terminal) domain (CTD). The fusion peptide (FP), heptad repeats (HR1 and HR2), transmembrane domain (TM), and the internal domain (ID) composes the S2 part, which is responsible for the viral fusion and entry (Le Poder, 2011). The N protein of FCoV, like human coronavirus (HCoV) N protein, was responsible for the replication, transcription, and viral genome packaging (Tilocca et al., 2020), and was demonstrated to be the target of detection methods due to the abundant epitopes exhibited to possess great antigenicity. The same epitopes on the FCoV N protein are also found to be shown simultaneously in genotype I and genotype II FCoV because of the highly conserved sequence of the N protein (Gao et al., 2023; Satoh et al., 2011; Severance et al., 2008; Takano et al., 2014; Tekes and Thiel, 2016).

doi:10.6342/NTU202301829

1.1.2 The genome of Feline Coronavirus

The genome of FCoV is a single, nonsegmental, positive-stranded RNA sequence of approximately 29k bases, which contains the 5'-untranslated region (UTR), replicase, structural, accessory genes, and the 3'-UTR. The 5'-UTR is around 310 nucleotides (nts) long and includes the conserved core-transcription regulatory sequence (TRS) motif (5'-CUAAAC-3') (De Groot et al., 1988; Dye and Siddell, 2005). The 3'-UTR comprises about 275 nts, and a poly (A) tail follows after it. Besides, two-thirds of the genome is occupied by replicase genes, which is consisted of open reading frames (ORFs) 1a and 1b and can be translated to the polyproteins (pp) 1a and 1ab. Subsequently, the virus-encoded 3C-like and papain proteases tailor the pp 1a and 1ab to become 16 kinds of non-structural proteins (nsps) responsible for the cell-host function and replication-transcription complex formation (Ziebuhr, 2005; Ziebuhr et al., 2000). The remaining genome in the 3'-terminus can encode the four structural proteins, serially from 5' to 3' terminus, the S, E, M, and N protein; and five kinds of accessory proteins, containing 7a, 7b, 3a, 3b, and 3c, which can be classified into two groups: accessory protein 7 and 3; and distributed at two different locations of the genome: the ORF 3 is located between S and E genes, and the ORF 7 follows the downstream of N gene (Gao et al., 2023; Haijema et al., 2007; Tekes et al., 2008). The function of accessory 3 proteins and accessory 7

doi:10.6342/NTU202301829

proteins were also shown to be part of FCoV replication and virulence during *in vivo* infection (Gao et al., 2023; Haijema et al., 2004).

1.1.3 Genotypes of Feline Coronavirus

Due to the result of the antigenicity test, FCoV can be subclassified into genotype I FCoV and genotype II FCoV (Decaro et al., 2021). Based on the epidemiological analysis of FCoV infection, genotype I FCoV causes most of the naturally infected cases in the U.S.A, Japan, and Europe, with a prevalence of 80% to 98%. Instead, the genotype II FCoV was seldom detected in these areas (Benetka et al., 2004; Gao et al., 2023; Kummrow et al., 2005; Shiba et al., 2007). The recent reports from Taiwan also showed similar results (Luo et al., 2020; Yen and Chen, 2021). The genotype II FCoV, which results from the homologous recombination between canine coronavirus (CCoV) and the genotype I FCoV, can be propagated well in cell culture, providing a good infection model for further experiments (Herrewegh et al., 1998). However, unlike genotype II FCoV, genotype I FCoV is hard to study due to the difficulty of being cultured in cell lines. And it was indicated only to yield low virus titer in feline primary macrophages (Pedersen et al., 1981), which let most studies discuss the genotype II FCoV, despite the widespread of genotype I FCoV to the worldwide range (Amer et al., 2012). Also, the method to distinguish these two genotypes of FCoV was developed. Based on one paper

doi:10.6342/NTU202301829

discussing the FCoV genotyping, a Reverse Transcriptase Polymerase Chain Reaction (RT-PCR) was conducted, and the target fragment is at the 3'-terminus of the S2 subunit of the S protein (Addie et al., 2003). Some papers even found that there was still a high diversity in the partial sequence of the genotype I FCoV S protein, which was correlated with the high prevalence of the virus in these years and needed to be monitored continuously (Luo et al., 2020; Yen and Chen, 2021). Furthermore, the feline aminopeptidase (fAPN), which is distributed on many kinds of tissue cells, was indicated to be the receptor of the genotype II FCoV, though the receptor of genotype I FCoV was still unclear (Cham et al., 2017; Tresnan and Holmes, 1998; Tresnan et al., 1996; Wang et al., 2014). Some reports showed that the fDC-SIGN, feline Dendritic Cell-Specific Intercellular adhesion molecule-3 Grabbing Nonintegrin, might be employed by both genotypes of FCoV as the coreceptor in vitro, and this was believed to be a hint for further research to find out the receptor for the genotype I FCoV (Gao et al., 2023; Regan et al., 2010; Regan and Whittaker, 2008; Tekes and Thiel, 2016).

1.1.4 Biotypes of Feline coronavirus

In addition to that, all the two genotypes of FCoV can also be divided into two biotypes, feline enteric coronavirus (FECV) and feline infectious peritonitis virus (FIPV), with different levels of pathogenicity (Tekes and Thiel, 2016). FIPV has a higher

doi:10.6342/NTU202301829

virulence and is the cause of the lethal disease, feline infectious peritonitis (FIP), which mainly occurs in younger kittens (Wolfe and Griesemer, 1966). In contrast, the clinical signs in cats with FECV infection are only mild enteritis (Desmarets et al., 2016). The tropism of both biotypes of FCoV also differs. The intestinal epithelial cells and mesenteric lymph nodes are the primary targets of FECV (Pedersen et al., 1981). However, FIPV can proliferate in a wide range of cells, including feline peritoneal macrophages, monocytes, lymphocytes, plasma cells, and neurocytes, which showed better infection efficiency of FIPV than FECV (Pedersen, 2009; Stoddart and Scott, 1989). Some surveillance reports even found that the amino acid location 1058 at the spike sequence was vital in distinguishing both biotypes. The result revealed that 1058M was mostly in FECV, but 1058L was almost in FIPV (Gao et al., 2023; Le Poder, 2011).

1.1.5 Epidemiology and phylogenetic analysis of feline infectious peritonitis virus infection in Taiwan and other countries

FIP cases have been distributed worldwide, which is endemic in isolated areas. Although the FIPV could be shed in cat feces, it was not transmitted horizontally, consistent with its sporadic incidence (Bank-Wolf et al., 2014; Tekes and Thiel, 2016). The countries with FIP cases include the U.S.A (Rohrbach et al., 2001), China (Yin et al., 2021), Japan (Soma et al., 2013), Korea (Yang et al., 2022), Austria (Benetka et al., 2004),

doi:10.6342/NTU202301829

Taiwan (Luo et al., 2020), and so on. Among these reports, the positive rate of FCoV infection from FIP-suspected samples varies, which ranges from 8.8% (Benetka et al., 2004) to 85.8% (Yin et al., 2021). The vast range may result from the detection method differences. As to the genotype distribution of the FCoV in these FIP-positive samples, genotype I FCoV was indicated to be the predominant strain. According to three previous reports from Taiwan, genotype I FCoV infection distribution remains high. 45% to 88.7% of the FIP-positive cases were singly infected with genotype I FCoV, though the result showed a decreasing trend in these years (Lin et al., 2009b; Luo et al., 2020; Yen and Chen, 2021). About the phylogenetic analysis, the spike fragment from genotype I FCoV had a higher diversity than that from genotype II FCoV. From a report investigating FCoV infection status in Taiwan from 2003 to 2007, the highest nucleotide divergence among the sequences collected from the FIP-positive samples was 11.7% for the genotype I FCoV group and 3.1% for the genotype II FCoV group (Lin et al., 2009b). Also, from another result analyzed in 2021, the lowest similarity among the genotype I FCoV internal sequence was only 85.5%. Instead, genotype II FCoV sequence fragment was also close to each other within the collected samples and even similar to sequences from previous reports in Taiwan (Yen and Chen, 2021). The result represents that genotype I FCoV spike has been mutating in these years, which may become the target for future surveillance to avoid the mutation becoming highly virulent or infecting other species.

doi:10.6342/NTU202301829

1.2 Feline infectious peritonitis

1.2.1 Characteristics of feline infectious peritonitis

Feline infectious peritonitis (FIP) is known as a fatal illness caused by FIPV and has some pathological features, such as granulomatous serositis and protein-rich fibrinous effusions within body cavities (Hayashi et al., 1977; Hirschberger et al., 1995; Pedersen, 1987; Weiss and Scott, 1981). Regarding the origin of FIPV, some reports found that the persistent infection of FECV may have a 5% probability of causing FIP in cats, which was hypothesized that FIPV might be originated from mutated FECV (Chang et al., 2011; Haijema et al., 2007; Poland et al., 1996; Vennema et al., 1998). Besides, both genotypes of FCoV can lead to FIP. Among them, the genotype I FCoV is indicated to be responsible for most FIPV natural infection cases (Addie et al., 2003; Benetka et al., 2004; Hohdatsu et al., 1992; Kennedy et al., 2002). Some specific cat signalments were also mentioned as the risk factors for FIP. About age, FIP was found to be most prevalent at the age of cats smaller than two years old, despite the low incidence rate in the aged cats' group (Foley et al., 1997; Pedersen, 2009; Rohrbach et al., 2001). Male and purebred cats were also revealed to be more susceptible to FIPV infection. According to the cat breed analysis, British Shorthair cats were more concerned about FIPV infection. In addition, the lousy breeding environment of cats may enhance the probability of being infected by FIPV,

doi:10.6342/NTU202301829

including the high cat density and unsanitary treatment (Kiss et al., 2000; Pedersen, 2009; Worthing et al., 2012).

1.2.2 Clinical signs of feline infectious peritonitis

The FIP cats can perform common clinical signs, including dehydration, fatigue, inappetence, diarrhea, and fever. Sometimes, jaundice and increased urination frequency also show in these diseased cats. Generally, FIP can be subclassified into wet and dry forms according to the pathological features (Addie et al., 2020; Sykes, 2013).

Dry-form FIP is a slowly progressive disease, which typically takes weeks or months to develop the symptoms after the initial infection. Granulomas are one of the featured lesions of dry-form FIP, mainly influencing abdominal organs, such as kidneys, liver, mesenteric lymph nodes, and the junction between the ileocecal valve and the colon. In about 60% of cases, damage to the central nervous system and ocular organs is observed, with another 40% exhibiting abdominal lesions that may or may not be linked to the central nervous system and ocular lesions. The spinal cord lesions may cause ataxia, forelimb numbness, paralysis, and even epilepsy. The visual damage is characterized by chorioretinitis and uveitis, which may result in distorted pupil shape and finally form glaucoma (Gao et al., 2023; Pedersen, 2009).

doi:10.6342/NTU202301829

Wet-form FIP is mainly characterized by abdominal distention. Upon palpation, an apparent wave on the abdominal surface can be shown. Still, no associated pain was exhibited in diseased cats, which is always difficult to be distinguished from female cats in pregnancy. Furthermore, abdominal masses, such as mesenteric lymph nodes swelling and organ-omentum adhesion, can also be detected during palpitation, which may hint at FIP differential diagnosis. The location of effusions is varied, including abdominal, pleural, and pericardial cavities. The color of them is typically straightforward, mucinous, and yellow. In the terminus of the disease, icterus may even be performed (Pedersen, 2009; Sykes, 2013). Besides, the mortality rate of FIP-diseased cats can achieve 90% through experimental infection (Hök, 1993), again strengthening the importance of the research on FIP. Interestingly, effusions in FIP cats were indicated to develop in the early stage of the disease and even shown before dry form FIP development (Pedersen, 2009), which meant that effusions might provide an essential point for further studies on FIPV infection (Gao et al., 2023; Tekes and Thiel, 2016),

1.2.3 Diagnosis of feline infectious peritonitis

1.2.3.1 Overview

First, the clinical symptoms of FIP were evaluated. Wet-form and dry-form FIP can develop uveitis and signs related to the central nervous system. In wet-form FIP patients,

doi:10.6342/NTU202301829

the apparent abdomen swelling caused by effusions has to be differentially diagnosed from other causes to lead to abdominal swelling, such as pregnancy in female cats. However, more examinations are needed to confirm FIP based on histology, biochemical, and molecular biology, though they were pointed out to be conducted more confidently on dead cats (Giori et al., 2011; Parodi et al., 1993). About lived cats, blood, effusions, cerebrospinal fluid (CSF), and aqueous humor of FIP-suspected cats can be collected to be examined by general laboratory tests, anti-FCoV antibodies (Abs) detection, immune-complex detection, FCoV antigen detection in macrophages through immunostaining, and RT-PCR as well, which can also detect mutations in FCoV sequence (Felten and Hartmann, 2019). Among the sample types mentioned above, blood and effusions are more common for FIP laboratory diagnosis, and we will focus on how to diagnose FIPV in these two kinds of samples.

1.2.3.2 Diagnosis of FIPV infection from blood

In blood analysis, biomedical characteristics, such as anemia, microcytosis, band neutrophilia, and thrombocytopenia, can commonly develop in FIP-diseased cats. Among them, lymphopenia was found to be correlated with wet-form FIP (Felten and Hartmann, 2019). Also, serum biochemistry tests can present abnormalities. The A/G ratio, which represents the comparison between the serum albumin and globulin level, was

doi:10.6342/NTU202301829

demonstrated to be one of the conspicuous features (Stenske, 2005). FIP can be ruled in more confidently since the A/G ratio is lower than 0.4. Nevertheless, if the value is higher than 0.6 to 0.8, the probability of developing FIP is lower, and FIP can be ruled out (Jeffery et al., 2012; Norris et al., 2005). The serum amyloid A (SAA), alpha-1-acid glycoprotein (AGP), and haptoglobin in blood serum also hint at FIP analysis. The level of them can be enhanced by FIPV infection dramatically (Hazuchova et al., 2017; Paltrinieri et al., 2007; Yuki et al., 2020). However, AGP also increases in cats with tumors or other inflammatory conditions, indicating that only the negative result in the AGP test can be used to rule out FIP (Felten and Hartmann, 2019). Interestingly, FIPV can also be detected in blood using RT-PCR with primers targeted at a fragment from the 3'-UTR of FCoV. However, the result can't be differentiated from FECV, CCoV, or other alphacoronavirus sequences. One report also pointed out that FECV can infect macrophage or monocytes as well, though they cannot replicate in these kinds of cells and lead to low titer, which cause a low sensitivity of this test. The sensitivity of FIPV detection using RT-PCR is around 56% to 75%, but the specificity is higher with the range from 75% to 88%, and even 100% in one paper (Herrewegh et al., 1997; Simons et al., 2005). The result shows that RT-PCR to detect FIPV may need to be conducted with other tests to validate the outcome, such as ELISA to measure the titer of anti-FCoV

doi:10.6342/NTU202301829

antibodies or immunostaining to investigate the antigen of FIPV in effusions (Addie et al., 2015; Gao et al., 2023; Tammer et al., 1995).

1.2.3.3 Diagnosis of FIPV infection from effusions

The viral titer of FIPV was indicated to be higher in effusions than in blood (Pedersen et al., 2015), which provides a better site for FIPV detection. Ascites, pleural effusions, and pericardial effusions are reported to be general types of effusions existing in wet-form FIP (Riemer et al., 2016). To measure these kinds of samples, the cytology needed to be conducted first, which may find specific cell morphology features from other diseases, such as tumors or other bacterial infections, to make the differential diagnosis (Felten and Hartmann, 2019; Giori et al., 2011; Stranieri et al., 2018). In addition to cytology, the Rivalta test and the total nucleated cell number (ΔTNC) analysis are also used to investigate FIPV infection in effusions. The Rivalta test is used in exudate detection with an excellent specificity of up to 91% to even 100%, which is a suitable method to rule out FIP. However, the sensitivity of it is only 66% to 81% due to the high level of inflammatory mediators caused by other factors (Berti-Bock et al., 1979; Felten and Hartmann, 2019; Fischer et al., 2012; Stenske, 2005). The total nucleated cell number (ΔTNC) analysis was reported to be conducted by an automatic hematology analyzer (Sysmex XT-2000iV, Sysmex Europe, Norderstedt, Denmark). If the cut-off value was

doi:10.6342/NTU202301829

set at 2.5 to 3.4, the test's specificity could also achieve 100% to rule out FIP (Giordano et al., 2015; Stranieri et al., 2017b). Besides, the immunostaining test can detect the FIPV antigen in samples through the enzyme- or fluorescein-conjugated antibody binding to the antigen in the cytoplasm of target cells, which may present the positive coloring signal in the result (Felten and Hartmann, 2019). Based on the test's target, the staining process method can differ. If the sample is from tissues of the diseased cats, the immunohistochemistry (IHC) test may be a suitable choice (Walter et al., 1989). If the sample originated from cells, such as macrophages and monocytes, the immunofluorescence assay (IFA) could provide a result more confidently (Addie et al., 2009). Though IHC is pointed out to be the gold standard to diagnose FIP with high sensitivity and specificity, which can reach 100% for each, in many reports, it can continuously be operated post-mortem and provide a limit to perform this test (Addie et al., 2004; Giori et al., 2011; Kipar et al., 1998; Kipar and Meli, 2014; Pedersen, 2009; Rissi, 2018; Tammer et al., 1995). Instead, IFA can resolve this problem and detect FIPV in the effusions from lived cats. The sensitivity and specificity remain high, with 95% and 100% for each from one report (Paltrinieri et al., 1999), which is a better and more convenient method for FIPV detection, though the non-specific binding to the structure of macrophages or other pathogens may sometimes influence the result (Felten et al., 2017; Litster et al., 2013). Furthermore, IFA is suggested to be finished within 24 hours

doi:10.6342/NTU202301829

after the samples are collected because the IFA sensitivity may decrease as the time interval between sample collection and IFA analysis increases. The storage time of the sample is recommended not to exceed two days at 4°C or room temperature. RT-PCR can also be conducted to investigate FIPV in effusions as well. Like the IFA, the specificity of it can reach 100% (Doenges et al., 2017; Longstaff et al., 2017), though the sensitivity was varied, and only 40% in one report using 71 samples to conduct the test (Stranieri et al., 2017a), which reveal that RT-PCR needs to be undertaken with other methods, such as IFA, to detect FIPV in effusions more confidently.

1.2.4 Host immune response during feline infectious peritonitis

The clinical forms of FIP were indicated to be determined by the immune status of the diseased cats during the early infection period. Wet-form FIP can be induced if the humoral but not cellular immune response is activated. Instead, dry-form FIP always occurs with the intense initiation of cellular immunity but weak humoral immunity, which also prevents the development of the clinical symptoms in diseased cats (Pedersen, 2009, 2014a). During the FIPV infection, monocytes and macrophages are targeted and activated to express cytokines and other immune-related molecules. The level of cytokines, such as Tumor necrosis factor-α (TNF-α) and IL-1β, are enhanced. Some adhesion molecules, including CD18 and CD11b, on monocytes are also highly presented

doi:10.6342/NTU202301829

to facilitate monocytes passing through the endothelial cells more easily for further immune responses against pathogens (Kiss et al., 2004; Malbon et al., 2020; Regan et al., 2009; Takano et al., 2009). Besides, in wet-form FIP cats, the level of matrix metalloproteinase-9 and vascular endothelial growth factor (VEGF) was reported to be higher, which may increase the permeability of the vascular barrier and lead to effusions formation in body cavities of FIP cats (Kipar et al., 2005; Kipar and Meli, 2014; Takano et al., 2011a). Furthermore, oxidative stress was also mentioned during virus infection to impair the immune response against the pathogen (Ciliberti et al., 2020). As the cat was infected with FIPV, two antioxidants in serum, total antioxidant capacity (TAC) and paraoxonase-1 (PON-1), were revealed to decrease, which might be used as biomarkers for FIP diagnosis (Tecles et al., 2015). As FIP is a systemic disease, the cytokine expression in different organs is also measured. The transcription level of IL-1β, IL-6, and TNF-α was demonstrated to be higher in hepatic and myocardial cells of FIP cats which were consistent with the result from IHC staining (Malbon et al., 2019). Also, due to neurologic signs in FIP cats, cytokine profiling in brain tissue was conducted. The result showed that the transcription level of IL-18 was significantly higher in brain samples from systemic FIP cats (Foley et al., 2003). Although several papers discussed the cytokines and oxidative stress factors in blood serum, liver, and other FIP-targeted

doi:10.6342/NTU202301829

organs, biomarkers in effusions were seldom mentioned, which needs more examinations to explain the unclear part of the immune-mediators in FIP cats.

1.3 Antibody-dependent enhancement

Antibody-dependent enhancement (ADE) is a phenomenon in which specific antibodies enhance the virus infection to form an immune complex with the antigen and accelerate the entry into the host cells and replication through the Fc gamma receptors (Wen et al., 2020). ADE has been chiefly mentioned in dengue virus infection. The clinical sign, such as dengue hemorrhagic fever (DHF), is a classic example of ADE occurrence during the second dengue virus infection. ADE can also influence vaccine development due to the danger of previously elicited antibodies to enhance the infection (Halstead, 1988; Halstead and O'Rourke, 1977; Huisman et al., 2009). In contrast to the *in vivo* ADE evidence of dengue virus infection, ADE of feline coronavirus infection was proved only by *in vitro* experiments (Hohdatsu et al., 1998; Takano et al., 2008b).

Interestingly, ADE was pointed out to be presented in both biotypes of FCoV, FECV and FIPV infection; however, the FIPV titer could be enhanced more significantly (Hohdatsu et al., 1998; Takano et al., 2017). One study even demonstrated that FIPV ADE could be exhibited well as the antibody and challenge strain of the virus were from the same genotypes (Takano et al., 2008b). Epitopes susceptible to ADE were

doi:10.6342/NTU202301829

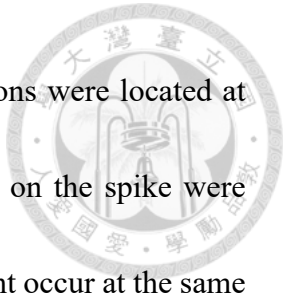

investigated. Several linear immunodominant antibody-binding regions were located at the nucleocapsid and spike S2 of FIPV. Among them, the epitopes on the spike were indicated to be responsible for neutralization and ADE, and they might occur at the same site. In addition, FIPV-infected cells, such as monocytes, were also revealed to be evaded from antibody-dependent complement-mediated lysis (ADCML), which was indicated to be a route correlated with the infection enhancement phenomenon (Cornelissen et al., 2009; Satoh et al., 2011; Takano et al., 2011b).

Furthermore, as to the antibody titer responsible for ADE elicitation, anti-spike sub- or non-neutralizing antibodies are more likely to enhance virus infection (Perlman and Dandekar, 2005). A neutralizing mouse-derived anti-FCoV spike monoclonal antibody (mAb) named 6-4-2 (Hohdatsu et al., 1991) was also developed to prove the hypothesis of FIPV ADE by several *in vitro* tests (Hu et al., 2017; Takano et al., 2017). About the receptor engaged in the procedure of FIPV ADE, instead of fAPN, which is the common receptor for FCoV infection, the Fc gamma receptor on monocytes and macrophages for the Fc part of IgG was also found to play an essential role like the dengue virus (Gao et al., 2022). Though many papers have studied ADE for a long time, the actual position of ADE is still being determined, even though no article mentioned the ADE in FIPV effusions, which needs more experiments to realize this mysterious phenomenon.

doi:10.6342/NTU202301829

1.4 SARS-CoV-2 and its relationship with cats

These years, the coronavirus disease 2019 (COVID-19) pandemic has influenced our life a lot, which is caused by another coronavirus from the betacoronavirus genus, named type 2 Severe Acute Respiratory Syndrome Coronavirus (SARS-CoV-2) (Adil et al., 2021). In addition to human patients, several animal cases have been reported. The affected animal species include cats, dogs, ferrets (Shi et al., 2020), lions, tigers (Mahdy et al., 2020), and minks (Oude Munnink et al., 2021). Regarding companion animals, pet cats are revealed to be more permissive to COVID-19 infection than dogs, which may result from the high similarity between the receptor of SARS-CoV-2, human ACE2, and feline ACE2. Domestic cats infected with SARS-CoV-2 can exhibit mild gastrointestinal and respiratory symptoms, including vomiting, diarrhea, inappetence, coughing, and shallow breathing. However, the infected dogs can't show any clinical signs but may shed a low load of SARS-CoV-2 through nasal and oral routes (Lin et al., 2021; Mahdy et al., 2020; Shi et al., 2020). Furthermore, the domestic cat cases were found to be related to contact with the cat owner, the COVID-19 patient, which might prove the human-to-cat pathway of the viral transmission (Kannekens-Jager et al., 2022). Besides, several reports from different countries demonstrated SARS-CoV-2 seroconversion in cats (Bessière et al., 2022; Dileepan et al., 2021; Patterson et al., 2020). As to the high prevalence of FCoV infection in domestic cats, the probability that cats are simultaneously infected by SARS-

doi:10.6342/NTU202301829

CoV-2 and FCoV can be higher. Also, the cross-reactivity between these two kinds of coronaviruses in one cat's body becomes an interesting issue to be addressed, and more examination is needed to investigate.

1.5 Cross-reactivity between SARS-CoV-2 and FIPV

The structure of SARS-CoV-2 is similar to FCoV, which also consists of four main structural proteins: S, M, N, and E. The S protein can also be divided into two subunits, S1 and S2, with the same function of viral binding, fusion, and entry (Wang et al., 2020). According to the probability of co-infection of FCoV and SARS-CoV-2 in one cat (El-Tholoth et al., 2023), the cross-reactivity between these two viruses must be investigated. Previous data from our lab revealed that effusion samples from post-COVID-19 pandemic cats could detect the spike S2 and N of SARS-CoV-2 using western blot. Also, the ELISA test conducted with feline effusions and receptor binding domain (RBD) of SARS-CoV-2 spike expressed from Expi293T cell showed that part of the cat's effusion could mildly react with SARS-CoV-2 RBD, which was also consistent with another paper mentioned that antibodies elicited from both genotype I and II FCoV can cross-react with SARS-CoV-2 RBD (Yamamoto et al., 2023).

Furthermore, based on the conserved sequence of N protein in coronavirus, one previous member from our lab investigated the antigenicity between FCoV and SARS-

doi:10.6342/NTU202301829

CoV-2 as well (陳耀云, 2022). The result showed that clinical sera of FCoV-infected cats could detect the N protein of SARS-CoV-2 with a strong positive signal, which indicated the high cross-reactivity between these two viruses. Also, the bilateral cross-antigenicity was proved using clinical anti-SARS-CoV-2 human sera and N protein of FCoV by western blot, though the intensity of the positive signal was low. Accordingly, the above result demonstrates the cross-reactivity between FCoV and SARS-CoV-2. As the FIPV ADE can be caused by non-neutralizing antibodies, antibodies against SARS-CoV-2, which can bind to FCoV and be elicited from FIPV-infected cats, may potentially threaten to induce such phenomenon. And this also plays an integral part in the cross-reactivity investigation, which may provide some clues for the influence of SARS-CoV-2 during FIPV infections.

1.6 Aim of this study

As the report mentioned, the pathogenesis of FIPV and the immune response against it was still controversial. The current phylogenetic status of genotype I FCoV is changing and needs surveillance. Besides, previous papers did not mention the cytokine biomarker and ADE phenomenon in FIP cat effusions. Due to the recent COVID-19 pandemic and its influence on cats, the cross-reactivity between FIPV and SARS-CoV-2 also deserves more attention when both viruses simultaneously exist in one cat. In this study, we aimed

doi:10.6342/NTU202301829

to enhance our understanding of FIP pathogenesis by characterizing the virus, cytokines, and antibodies from FIP-diseased effusions, which is still a mysterious feature of FIP, and apply the antibodies to reveal the potential cross-reactivity between FIPV and SARS-CoV-2.

doi:10.6342/NTU202301829

Chapter 2 Materials and methods

2.1 Clinical feline effusion samples collection and processing

From January 2022 to March 2023, 138 FIP-suspected feline effusion samples were collected mainly from animal hospitals located in northern Taiwan. The sample types included ascites, pleural effusion, broncho-alveolar lavage, and pericardial fluid, and their quantity was 74, 61, 2, and 1, respectively. The age of the patient cats also varied, ranging from 3 months to 18 years old. At first, after the sample was refrigerated and transported to the lab, the sample data, including the age, breed, gender, and blood A/G ratio of the patient cat, were recorded for signalments analysis.

For the examination, 300 μl of the effusion sample was taken out to extract RNA for FCoV sequence detection by RT-PCR, and another 10 μl was used to count the cell quantity at 5 μm and 7 μm gate by TC20 automated cell counter (Bio-Rad, Hercules, CA). After the original cell concentration was confirmed, the volume of the medium, Dulbecco's Modified Eagle Medium (DMEM) (Gibco, MT) supplemented with 2% Fetal bovine serum (FBS) (Gibco), 100 units penicillin, 100 μg streptomycin and 250 μg amphotericin B (P/S/A) (Sigma-Aldrich, Burlington, MA), to resuspend the cell with a diameter of 7 μm to a concentration from 2×10^9 to 5×10^9 cells per liter, could be estimated. To get good-quality cells, debris in the effusion fluid was removed first. Then the sample was centrifuged at 500× g, 4°C for 10 minutes to pellet the cells. After

doi:10.6342/NTU202301829

centrifugation, the supernatant was saved for FCoV genotyping, IgG purification, and cytokine profiling tests. Next, cell pellets were resuspended with 10 ml DMEM supplemented with 2% FBS and 1× P/S/A, then centrifuged at 500× g, 4°C for 10 minutes to wash out impurities. If the original sample color was too red and cloudy to be measured, red blood cell (RBC) lysis was carried out after removing the supernatant. In this part, RBC could be lysed with eBioscience 1× RBC Lysis Buffer (Invitrogen, Carlsbad, CA) by gently mixing 1 ml of that with cell pellets and then standing still at room temperature (RT) for 5 minutes. After that, compared with the cell mixture, 10 times the volume of DMEM was added to stop the activity of the lysis buffer. Like the washing step mentioned above, the mixture was centrifuged at 500× g, 4°C for 10 minutes. After washing and pelleting the targeted cells, the supernatant was removed again. And the estimated volume of DMEM was added to resuspend the cells. In addition, the mixture's cell concentration was rechecked at 5 μm and 7 μm gate by TC20 automated cell counter (Bio-Rad). At the same time, cytospin materials were prepared and assembled, including metal cups, carrying platforms, slide racks, cell tunnel bricks (Double Eagle Enterprise Co., New Taipei City, Taiwan), 26 × 76 mm slides (HICLIN, Taipei, Taiwan), 26 × 76 mm filtered papers (ADVANTEC®, Tokyo, Japan), and 25 mm typical rubber bands. Next, 400 μl of resuspended cell solution was added to the top of assembled cell tunnel bricks and centrifuged at 1000× g, 4°C for 10 minutes. After the cytospin, the cell's morphology and

doi:10.6342/NTU202301829

quantity were checked under optical inverted microscopes (Olympus, Tokyo, Japan). Finally, the cell slides were marked with the sample number and the fixation solution's name.

Additionally, the cells also needed to be fixed for further assays. Two fixation solutions were used, which were 80% acetone, mixed with 100% acetone (Merck, Darmstadt, Germany) and DDW, and 10% neutral buffered formalin (Burnett, Illinois, Chicago). In the 80% acetone fixation protocol, the cell slide was covered with 300 μl of acetone, then stood at -20°C for 15 minutes. After that, wash buffer, composed of 1× phosphate-buffered saline (PBS) (Omics Bio, New Taipei City, Taiwan) and 0.05% Tween 20 (Sigma-Aldrich), was used for washing the acetone solution—besides, about 10% formalin fixation. Cell slides must also be covered with 300 μl formalin at room temperature (RT) for 15 minutes. After that, the formalin solution was washed out with wash buffer at RT for 5 minutes. In addition, 300 μl 1% Triton X-100 (Sigma-Aldrich) would subsequently be added to the top of the cells and incubated at RT for 10 minutes. In the end, the cell slides were finished with washing by wash buffer at RT for 5 minutes and conducted in indirect immunofluorescence assay (IFA).

2.2 Indirect immunofluorescence assay

doi:10.6342/NTU202301829

At first, the cells needed to be blocked with 300 μl 10% goat serum, composed of 90% wash buffer and 10% goat serum (Jackson ImmunoResearch, Philadelphia, PA) as blocking buffer, at RT for 30 minutes. During the blocking period, the primary and secondary antibodies were prepared. The primary antibody was composed of mouse-derived anti-FCoV N mAb (Bio-Rad) with a 400-fold dilution by wash buffer. And the secondary antibody was also diluted in 400-folds from FITC-conjugated AffiniPure Goat Anti-Mouse IgG (H+L) (Jackson ImmunoResearch) with wash buffer. After the blocking step, the blocking buffer needed to be drained off, and 300 μl prepared primary antibody would directly cover the cells to incubate at RT for 45 minutes as the primary antibody step. Next, after the incubation, wash buffer was used to wash out the antibody at RT for 5 minutes 3 times. Subsequently, 300 μl prepared secondary antibody was added to the cells and incubated at RT for 30 minutes. Also, at the end of the step, the secondary antibody must be washed out by wash buffer at RT for 5 minutes 3 times. Finally, the cell nuclei were stained with DAPI mounting medium (VECTASHIELD, Newark, CA), which would overlay the cells, then be covered with 24 × 32 mm microscopic cover glasses (WillCo Wells, Amsterdam, Netherlands) and fixed with seal solution (CIS-Bio, Codolet, France). Finally, the slides were stored at 4°C and avoided lights.

After that, the stained cell slides were checked under the fluorescence microscope (Olympus) equipped with a manual operating system, OLYMPUS cellSens Dimension

doi:10.6342/NTU202301829

(Olympus), and a fluorescence light source machine (Olympus). Before the investigation of the cell slides, the burner status of the fluorescence light source was switched to 100, and the field of view was adjusted to 400-fold magnification. During the observation of the slides, macrophages were the target cells, and their morphology was checked first by the phase contrast channel. Next, the anti-FCoV N protein-positive FITC signal was found in the cytoplasm of macrophages by the FITC channel. Finally, the DAPI counterstained nuclei image detected by the DAPI channel was overlaid with FITC signal results. If most macrophages in the field of view were found with complete morphology and a clear FITC signal in the cytoplasm without non-specific binding on other types of cells, like neutrophils and lymphocytes, the IFA result of the sample was recognized as positive.

2.3 Nucleic acid extraction and RT-PCR

A 177-base sequence fragment from the 3'-untranslated regions gene of FIPV was amplified using two-step RT-PCR with primers mentioned in **Table 1** (Herrewegh et al., 1995). PetNAD Nucleic Acid Co-Prep Kit (GeneReach Biotechnology Corp., Taichung, Taiwan) was used for nuclei acid extraction. The protocol of cDNA reverse transcription followed M-MLV reverse transcription kit (Invitrogen). 4 μl 5× First-strand buffer, 2 μl 0.1M DTT, 1 μl 10 mM dNTP, 1 μl 50 μM Random Hexamer, 1 μl (200 units) M-MLV

doi:10.6342/NTU202301829

reverse transcriptase, and 21 μl extracted nucleic acid (RNA), were mixed at 37°C for 1 hour, 72°C for 15 minutes, and 94°C for 5 minutes. Next, for 1st step PCR, 22.5 μl Nuclease-Free ddH_2O (Invitrogen), 3 μl 10× reaction buffer, 1 μl 2.5 mM dNTP, 0.5 μl p205 primer (**Table 1**), 0.5 μl p211 primer (**Table 1**), 0.5 μl RBC Taq DNA polymerase (RBC bioscience, New Taipei City, Taiwan) and 2 μl cDNA template were mixed. The initial denaturation was at 94°C for 3 minutes. Then the amplification of cDNA used 40 cycles of 94°C for 15 seconds (denaturation), 57°C for 15 seconds (primer annealing), and 72°C for 15 minutes (extension). The sequence of cDNA was finally extended at 72°C for 5 minutes. For 2nd step PCR, 22.5 μl Nuclease-Free ddH_2O (Invitrogen), 3 μl 10× reaction buffer, 1 μl 2.5 mM dNTP, 0.5 μl p204 primer (**Table 1**), 0.5 μl p276 primer (**Table 1**), 0.5 μl Taq DNA polymerase and 2 μl 1st step PCR result products were mixed. The initial denaturation was at 94°C for 3 minutes. Then the amplification of cDNA used 35 cycles of 94°C for 15 seconds (denaturation), 57°C for 15 seconds (primer annealing), and 72°C for 15 minutes (extension). The cDNA sequence was finally extended at 72°C for 5 minutes. The result was confirmed with electrophoresis.

2.4 FCoV genotyping, sequencing, and phylogenetic analysis

The method of FCoV genotyping followed the protocol mentioned in the previous paper (Addie et al., 2003). 360-base and 218-base fragments from the spike sequence of

doi:10.6342/NTU202301829

FCoV were amplified using 2-step RT-PCR with primers mentioned in **Table 1** for FCoV type 1 and type 2 genotyping, respectively. Viral Nucleic Acid Extraction Kit II (Geneaid, New Taipei City, Taiwan) was used for nucleic acid extraction. For cDNA synthesis, M-MLV reverse transcription kit (Invitrogen) was used. 10 μl extracted nucleic acid (RNA) was mixed with 1 μl 10 μM Iubs primer or 1 μl 100 μM Randomized hexamer at 65°C for 5 minutes to denature the RNA template. Next, 4 μl 5× First Strand Buffer, 2 μl 0.1M DTT, 1 μl 10 mM dNTP (RBC), and 1 μl RNase OUT (Invitrogen) were added to the mixture and mixed at 32°C for 2 minutes. After that, cDNA synthesis was finished with 1 μl M-MLV added to the mixture and mixed at 37°C for 1 hour, 72°C for 15 minutes, and 94°C for 5 minutes. For 1st step PCR, 14.3 μl nuclease-Free ddH_2O (Invitrogen), 5 μl GoTaq 5× Buffer, 2 μl GoTaq $MgCl_2$, 0.5 μl 10 mM dNTP (RBC), 0.5 μl Iubs primer (**Table 1**), 0.5 μl Iffs primer (type 1) or Icfs primer (type 2) (**Table 1**), 0.2 μl GoTaq DNA polymerase (Promega, Madison, Wisconsin), and 2 μl cDNA template were mixed. The cDNA template was initially denatured at 95°C for 2 minutes. Subsequent amplification followed 40 cycles of 95°C for 30 seconds, 50°C for 30 seconds, and 72°C for 1 minute. And the reaction was finished at 72°C, 5 minutes for the final extension. For 2nd step PCR, 14.3 μl Nuclease-Free ddH_2O (Invitrogen), 5 μl GoTaq 5× Buffer, 2 μl GoTaq $MgCl_2$, 0.5 μl 10 mM dNTP (RBC), 0.5 μl nIubs primer (**Table 1**), 0.5 μl nIffles primer (type 1) or nIcfs primer (type 2) (**Table 1**), 0.2 μl GoTaq DNA polymerase (Promega, Madison,

doi:10.6342/NTU202301829

Wisconsin), and 2 μl 1st step result products were mixed. Also, the first denaturation was conducted at 95°C for 2 minutes. Then the cDNA template was amplified using 35 cycles of 95°C for 30 seconds, 50°C for 30 seconds, and 72°C for 30 seconds. And the final extension was finished at 72°C for 5 minutes. The result was confirmed with electrophoresis.

The FCoV genotyping products were processed for sequencing by GENOMICS bioscience & technology corporation (New Taipei City, Taiwan). Sanger sequencing was conducted, and the result was analyzed by Applied Biosystems 3730XL system (Thermo Fisher Scientific, Waltham, MA) with paired forward and reverse primers to ensure the sequence in two directions. After that, the chromatogram of the sequences was carefully checked using FinchTV (Geospiza. Seattle, WA) to find the appropriate exhibition and extract the consensus sequence from two directions. The sequences were submitted to the NCBI GenBank and obtained accession numbers OR141609 to OR141645 (**Table 2**). These sequences were aligned using the Clustal W method by CLC Main Workbench 20 (Qiagen, Hilden, Germany). The neighbor-joining phylogenetic trees were constructed with 1000 bootstrap replications using MegaX software. The bootstrap value was indicated reliable as it was higher than 50%.

2.5 Enzyme-linked immunosorbent assay (ELISA)

doi:10.6342/NTU202301829

Indirect ELISA was performed for the cross-antigenicity test between FCoV and SARS-CoV-2. At first, the targeted antigen, FCoV NTU156 strain whole virion (100 μl/well), needed to be coated at the 96 well plates (Thermo Fisher Scientific) using coating buffer (15 mM Na_2CO_3 (Sigma-Aldrich) and 35 mM $NaHCO_3$ (YAKURI PURE CHEMICALS, Osaka, Japan) in ddH_2O) with a concentration of 1 μg/ml at 4°C overnight. On the next day, coated wells were washed three times using PBST (250 μl/well), which was prepared with 0.05% Tween 80 (Merck) in 1× PBS (Omics Bio). The blocking step was conducted using the blocking buffer (200 μl/well), 5% Difco skim milk (BD, Franklin Lakes, NJ) in PBST, at RT for 30 minutes. After blocking, 1000-fold diluted rabbit-derived anti-SARS-CoV-2 spike subunit-S1 and S2, N (Sino Biological, Beijing, China), and M protein (ProSci, Poway, CA) polyclonal antibody (pAb) or 50-fold diluted, followed by serial 2-fold dilution, COVID-19 convalescent human serum kindly provided by National Taiwan University Hospital as the primary antibody, (100 μl/well) was directly added to the coated wells and incubated at RT for 1 hour. PBST (250 μl/well) washing five times followed the primary antibody step. Subsequently, 2000-fold diluted goat-derived anti-rabbit or anti-human HRP (Jackson ImmunoResearch) as the secondary antibody (100 μl/well) could be added to the wells and incubated at RT for 1 hour. Also, after the secondary antibody step, PBST washing (250 μl/well) needed to be conducted. At the end of the test, TMB peroxidase substrate (Seracare, Milford, MA) (100 μl/well)

doi:10.6342/NTU202301829

was used for the labeled enzyme conversion at RT for 10 minutes, and the reaction would directly be ceased using stop solution (1M H_2SO_4) (Honeywell, Charlotte, NC) (100 μl/well). And the final OD value was read at 450 nm using SYNERGY H1 microplate reader (BioTek, Winooski, VT).

2.6 Western blot (WB)

WB was performed for the purified feline IgG confirmation, IgG antigenicity test against FCoV, and cross-reactivity, two-way cross-antigenicity test between FCoV and SARS-CoV-2. First, the SDS-PAGE electrophoresis was conducted with the antigen, such as purified feline IgG for feline IgG confirmation, FCoV NTU156 strain whole virion for IgG antigenicity and cross-reactivity test, or SARS-CoV-2 Spike S1, S2 subunit (Sino biological), RBD, NTD (from our lab), complete N and three fragments of N protein kindly provided by professor Shih-Chung Chang at National Taiwan University for two-way cross-antigenicity test, with specific concentration for each test. And the gel was constructed using the 10% TGX Stain-Free FastCast Acrylamide Kit (Bio-Rad) following the protocol mentioned in the commercial data sheet. Before the antigen was loaded in the SDS-PAGE gel, it needed to be processed by 6× protein loading buffer (Omics Bio) or T-Pro Laemmli Reagent (non-reducing 4×) (T-Pro Biotechnology, New Taipei City, Taiwan). If the sample was processed by 6× protein loading buffer, the mixture must also

doi:10.6342/NTU202301829

be incubated at 98°C for 5 minutes. The SDS-PAGE electrophoresis cells and the power supply system (Bio-Rad) were prepared during the sample incubation. Then the TGS Tris-Glycine SDS running buffer (Omics Bio) would fill the gel box to test for leaks. Next, the processed sample mixture was loaded in the SDS-PAGE gel, and electrophoresis was conducted at 100 V for 10 minutes, then 180 V for 30 minutes. After the electrophoresis, the protein on the gel was transferred to the nitrocellulose (NC) membrane (PerkinElmer, Waltham, MA) using Western Transfer Buffer (Omics Bio) at 400 mA for 60 minutes.

The transferred membrane was subsequently blocked using the 5% Difco skim milk (BD) in wash buffer at RT for 30 minutes with gentle rocking. The wash buffer comprised 0.05% Tween 20 (Sigma-Aldrich) and 1× PBS (Omics Bio). During the blocking step, the primary antibody, such as goat anti-feline IgG HRP (Bethyl Laboratories, Montgomery, TX) for feline IgG confirmation (no secondary antibody for this test), four purified feline IgG samples for IgG antigenicity and two-way cross-antigenicity test, or rabbit-derived anti-SARS-CoV-2 S1, S2, N (Sino Biological), M protein (ProSci) pAb and COVID-19 convalescent human serum kindly provided by Dr. Sui-Yuan Chang National Taiwan University for cross-reactivity test, was prepared with varying dilution factor in the blocking buffer. After the blocking step finished, the primary antibody was directly added to the membrane and incubated at 4°C overnight or at RT for 1 hour with gentle rocking, and three times washing using wash buffer at RT for 5 minutes with gentle

doi:10.6342/NTU202301829

rocking followed the primary antibody incubation. Next, the prepared secondary antibody, such as goat-derived anti-feline IgG HRP (Bethyl Laboratories) for IgG antigenicity and two-way cross-antigenicity test, goat-derived anti-rabbit or anti-human HRP (Jackson ImmunoResearch) for cross-reactivity test, 2000-fold diluted in blocking buffer was incubated with the membrane at RT for 1 hour with gentle rocking followed by three times washing as well. The ECL reagent substrate (Bio-Rad) was added to the membrane, and the chemiluminescence signal was developed using the imaging system (ChemiDoc XRS+, Bio-Rad). The software Image Lab was used to quantitate the signal.

2.7 Feline cytokine levels measurement

DuoSet Feline TNF-α ELISA kit and DuoSet Feline IL-6 ELISA kit (R&D systems, Minneapolis, MN) were used for feline TNF-α and IL-6 level profiling in FIP-positive and FIP-negative cat's effusion samples. The FIP-negative cat's effusion samples must be tested negative using RT-PCR and IFA simultaneously. First, the capture antibody diluted with 1× PBS (Omics Bio) to the working concentration was coated on the 96-well ELISA plate (Thermo Fisher Scientific) (100 μl/well) at RT overnight. On the next day, the reagent diluent was prepared with 1% Bovine serum albumin (Sigma-Aldrich) diluted in 1× PBS (Omics Bio) and passed through 0.22 μm filter (Pall Corporation, Port Washington, NY) to remove the bacteria and impurities in it. The detection antibody and

doi:10.6342/NTU202301829

Streptavidin-HRP of the kit were also diluted to the working concentration with the reagent diluent before use.

Before the sample was conducted into the test, it needed to be centrifuged at 3000× g for 10 minutes to spin down the impurities and harvest the supernatant for further experiments. About the coated 96 ELISA plate, the coating solution was removed by inverting the plate and blotting it against clean paper towels. Subsequently, PBST (400 µl/well), which was prepared with 0.05% Tween 80 (Merck) in 1× PBS (Omics Bio), was used to wash the coated well three times. After each washing step, PBST must be obliterated by inverting and blotting the plate several times. Next, the prepared reagent diluent was used as the blocking buffer to block the coated wells by adding 300 µl to each well and incubating at RT for a minimum of 1 hour. The sample and standards of each kit were also diluted in reagent diluent during the blocking incubation. After that, the washing-inverting step was repeated three times, followed by diluted samples and assay standards (100 µl/well) and incubating at RT for 2 hours.

Also, the washing-inverting step would repeat three times to wash out the remaining samples. Then, the diluted detection antibody (100 µl/well) was added to each coated well and incubated at RT for 2 hours, followed by three washing-inverting steps. To detect the positive signal from the detection antibody, the diluted Streptavidin-HRP reagent (100 µl/well) was added to each well and incubated at RT for 20 minutes followed by the

doi:10.6342/NTU202301829

addition of TMB peroxidase substrate (Seracare) (100 µl/well) and also incubated at RT for 10 minutes. After the incubation, the reaction needed to be ceased by adding 50 µl stop solution (1M H_2SO_4) (Honeywell) to each well and avoiding light. Finally, the luminescence signal was determined and read at the wavelength 450 nm using the SYNERGY H1 microplate reader (BioTek). Besides, the value from wavelength 450 nm should also be corrected by subtracting the value read at the wavelength 540 nm or 570 nm. Finally, the value of the samples needed to be substituted in the formula converted from the standard curve to have the actual concentration.

2.8 Feline effusion IgG purification

Pierce protein A column kit (Thermo Fisher Scientific) was used for feline effusion IgG purification. The storage volume of FIP-positive samples included in this part must be at least 5 ml. First, IgG was purified from the samples. Before the sample was loaded into the protein A column, it needed to be sonicated at the amplitude of 3 for 3 seconds using the ultrasound sonication machine (Qsonica, Newtown, CT) to loosen the effusion protein and let the sample pass through the column more smoothly. About the protein A column, the storage solution was poured off first, and equilibration needed to be conducted with 5 ml supplemented binding buffer draining through the column. Next, 5 ml of the sonicated effusion sample was applied into the equilibrated column and allowed

doi:10.6342/NTU202301829

to pass through it, followed by washing with 15 ml binding buffer. The flow-through solution needed to be collected. Afterward, IgG, bonded with the protein A resin, was eluted using supplemented elution buffer. And each separate 1 ml fraction of the eluate was collected to measure the concentration of antibodies in it using the nanodrop spectrophotometer (Thermo Fisher Scientific) with a wavelength of 280 nm. After the absorbance of the fraction was almost equal to that of neutralized elution buffer, the fraction collection could be stopped. And the column was regenerated by washing it with 10 ml of elution buffer. For storage, 5 ml of the solution containing 0.02% sodium azide was used to pass through the column, and the cap could be replaced when 2 ml of the solution remained above the top disc. The column was stored upright at 4°C. And the collected fractions would also need to be ensured the purity of IgG using SDS-PAGE, which protocol was mentioned before. Then the fraction with great purity and concentration would subsequently be desalted. For desalting, the supplemented desalting column was conducted with the size-chromatography method. And filtered 1× PBS (Omics Bio) was used as desalting buffer. First, the storage solution in the column was poured off, followed by equilibration with 10 ml desalting buffer draining through the column. Subsequently, 1.25 ml of the IgG sample was applied to the column, and 1 ml of the first fraction and following fractions with each volume of 0.5 ml were collected. Then the absorbance of each fraction was measured using the nanodrop spectrophotometer

doi:10.6342/NTU202301829

(Thermo Fisher Scientific) with a wavelength of 280 nm. When the absorbance of the fraction was almost equal to that of the desalting buffer, the fraction collection could be stopped. Finally, the column was washed with 15 ml desalting buffer, and an additional solution with 0.02% sodium azide in the buffer was applied to the column and then stopped at the time when 2 ml of the solution remained above the resin gel to store the column at 4°C. Furthermore, the desalted IgG samples also needed to be applied to the FCoV Ab test kit (Bioguard, New Taipei City, Taiwan) and SDS-PAGE to confirm their purity, and the samples with high purity and concentration were mixed for IgG concentration determination using Pierce BCA Protein Assay Kit (Thermo Fisher Scientific) and further experiments.

2.9 Cell and virus cultures

The fcwf-4 cell line, originating from feline macrophages, was purchased from the American Type Culture Collection (ATCC, Manassas, VA). And the cells were maintained in the Dulbecco's Modified Eagle Medium (DMEM) (Gibco) supplemented with 10% Fetal bovine serum (FBS) (Gibco) and 1% P/S/A (Sigma-Aldrich) and incubated at 37°C with 5% CO_2. The sub-culture frequency of the cell was twice a week. Type II FIPV, FCoV/NTU156/P/2007 (NTU156) (Lin et al., 2009a), originated from the pleural effusions of wet-form FIP cats, was kindly provided by Professor Ling-Ling

doi:10.6342/NTU202301829

Chueh at National Taiwan University. And the virus was propagated and titrated in Fcwf-4. The virus stock with known titer was stocked at -80°C freezer.

2.10 Viral titer determination and plaque assay

The viral titer was determined using plaque assay in this project. First, 2×10^5 of Fcwf-4 cells were seeded in the 12-well plate (Corning Incorporation, Corning, NY) with media mentioned in the cell culture section at 37°C for one day. Before the experiment, the virus was 10-fold serially diluted with DMEM (Gibco), supplemented with 2% FBS (Gibco) and 1% P/S/A (Sigma-Aldrich). After that, the media of the cells was removed, followed by washing the cell surface with filtered 1× PBS (Omics Bio). Next, the diluted virus was directly applied to the cells and incubated at 37°C for 1 hour. Subsequently, the virus solution was removed and rewashed with PBS. 1 ml of the mixture with 1.8% methylcellulose (Sigma-Aldrich) in DMEM (2% FBS) was added to each well and incubated at 37°C for two days. After the incubation, the cells were fixed using 10% formalin (Burnett) at RT for 1 hour and stained using 1% crystal violet (Sigma-Aldrich) at RT for 10 minutes. Once the plate was dried, the plaques in each well were counted to determine the plaque forming unit (PFU) per ml of each sample using the formula (Count of plaques × Dilution factor)/[Volume of diluted virus (ml/well)].

doi:10.6342/NTU202301829

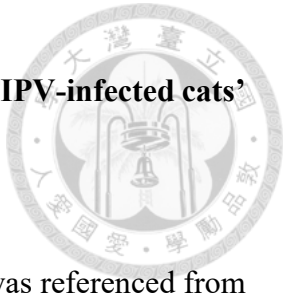

2.11 FIPV ADE assay and neutralizing test of purified IgG from FIPV-infected cats' effusions

The method of *in vitro* FIPV ADE phenomenon establishment was referenced from the previous paper (Hu et al., 2017). Fcwf-4 cells and FIPV NTU156 were used to investigate the varying ADE level elicited from different kinds of antibodies, including four purified feline IgG samples, rabbit-derived anti-SARS-CoV-2 S1, S2, N (Sino Biological), M protein (ProSci) pAb, or COVID-19 convalescent human serum kindly provided by National Taiwan University. Once the mAb 6-4-2, kindly provided by Dr. Tomomi Takano and Dr. Tsutomu Hohdatsu at Kitasato University, Japan, was added, the FIPV infection was enhanced through the Fc receptor on monocytes or macrophages but not fAPN on other feline cells (Takano et al., 2008a). The mAb 6-4-2 addition group was conducted as the positive control, and the FIPV-only group was as the negative control. To prepare the FIPV ADE model, FIPV suspension (Multiplicity of infection: 0.0035) and diluted antibody solution were mixed in a 1:1 ratio at 4°C for 1 hour to form the antigen-antibody (Ag-Ab) complex first. Next, the Ag-Ab complex solution was added to the Fcwf-4 cells, which were seeded with 2×10^5 cells per well on a 12-well plate (Corning) one day before and incubated at 37°C for 3 hours. After that, the mixture was removed, followed by three times washing using 1× PBS (Omics Bio). Each well was directly added with the maintaining DMEM (2% FBS) and incubated at 37°C for two

doi:10.6342/NTU202301829

days. Finally, each well's supernatant was harvested using the plaque assay to determine the viral titer. And the value was converted to ADE (%) to be standardized using the formula (titer of sample-titer of NC)/(titer of PC-titer of NC)*100%.

Regarding the neutralizing test, at first, the Fcwf-4 cells were coated at the 96-well plate with the quantity of 6×10^4/well at 37°C overnight. After that, 0.1 ml of the FIPV NTU156 strain (MOI 0.0003) was incubated with 4 purified IgG samples of 8 different concentrations, from 500 ng/0.1 ml to 1.95 ng/0.1 ml, in equal volume at 37°C for 1 hour. The mAb 6-4-2 was used as the positive control. Subsequently, 0.1 ml of each virus-antibody mixture was added to the cells at 37°C for 3 days. After the incubation, the cytopathic effect (CPE) in each well was observed. And the neutralizing titer was recorded.

2.12 Antigenic analysis of anti-FCoV S and N protein IgG in each purified IgG sample.

Western blot needed to be conducted for this analysis. The non-reducing antigen, including HEK 293T cell expressed spike protein of UU4 genotype I FCoV, kindly provided by Professor Yen-Chen Chang at National Taiwan University, for anti-FCoV S IgG analysis and *E. coli* expressed FCoV N protein from our lab for anti-FCoV N IgG analysis, was conducted for SDS-PAGE electrophoresis with specific concentration first.

doi:10.6342/NTU202301829

Transferring method followed the western blot section. Mouse anti-FCoV S mAb YB4F02, kindly provided by Professor Yen-Chen Chang at National Taiwan University, for anti-FCoV S standard curve, mouse anti-FCoV N mAb (Bio-Rad) for anti-FCoV N standard curve, and four purified feline IgG samples were used as the primary antibody with specific concentration to be incubated with the transferred membrane at 4°C overnight. Following the washing step, goat-derived anti-mouse IgG HRP (Jackson ImmunoResearch) for each standard curve and goat-derived anti-feline IgG HRP (Bethyl Laboratories) for four tested IgG samples were incubated with the membrane as the secondary antibody at RT for 1 hour. After washing, ECL reagent substrate (Bio-Rad) was used to express the positive signal. Subsequently, the positive band signal identity of each feline IgG sample group and standard curve were measured using the Image Lab software (Bio-Rad). Finally, the actual proportion of each kind of IgG in 4 purified feline IgG samples could be analyzed as the result value substituted into the calculated standard curve regression equation.

2.13 Statistical analysis

The data in this project was analyzed by Fisher's exact test and the unpaired t-test using Prism 9 software (GraphPad, San Diego, CA). When the p-value was < 0.05*, < 0.01**, or < 0.001***, the test result was considered significant.

doi:10.6342/NTU202301829

Chapter 3 Results

3.1 Sample collection and experimental design

In this study, effusions from FIP-suspected cats were collected for analysis (**Fig. 1**). After the cat was confirmed with FIPV infection from the effusions, the FIP-positive cases were included in the FIP epidemiology and risk factors analysis for the characteristics of FIP. Subsequently, FIPV, cytokines, and IgG in the effusions of FIP cats were used for FIP pathogenesis investigation, which was also based on the effusion samples. The current phylogenetic status was analyzed through FIPV gene sequencing. Cytokines were used for FIP cytokine profiling. IgG purified from the effusions was for FIPV ADE phenomenon examinations. Besides focusing on the ADE, antibodies against SARS-CoV-2 were also included in the FIPV infection enhancement test to measure the cross-reactivity between these two viruses. Also, the cross-antigenicity between FIPV and SARS-CoV-2 was examined using structural proteins of SARS-CoV-2 and IgG from FIP-positive cat effusions. Finally, we hope to discover more about the pathogenesis of FIP through the effusion samples to provide valuable insights for future FIPV studies.

3.2 FIP cases confirmed by IFA and RT-PCR

The FIP-positive effusion samples were confirmed using 2-step RT-PCR and IFA simultaneously. The nested RT-PCR for FCoV infection diagnosis had been documented

doi:10.6342/NTU202301829

in a previous report (Herrewegh et al., 1995) and was conducted in this project. The electrophoresis result showed that the target fragment of the reaction was 177 bp long. And this fragment was indicated to be at the 3'-UTR of FCoV (**Fig. 2A**), a highly conserved region (Ouyang et al., 2022). The IFA images in **Fig. 2B** showed the positive signal from the targeted FCoV N protein within the macrophage from feline body effusion samples. The IFA result needed to be confirmed positive considering several factors, including that the infected cells were in complete morphology and the signal was located at the correct area, the cytoplasm of macrophages, to avoid non-specific binding. As the sample tested positive in these two methods, the cats with effusions can be recognized as FIP-positive cases.

3.3 Characteristics of FIP cases

After the FIP-suspected samples were examined using the two methods mentioned above, the positive rate was calculated and found to be 33% in this project (**Fig. 3A**). **Fig. 3B** showed that the effusion samples from FIP-suspected cats were collected mainly from northern Taiwan. The number of the sample was the highest in Taipei with 90. Also, most FIP cases were distributed in the counties of the north, especially in Taipei. The signalments, such as sex, breed, age, and the blood A/G ratio level of diseased cats, were studied. We can find that many of the samples were from male, mixed-breed cats with

doi:10.6342/NTU202301829

age equal to or lower than 2 y/o and a blood A/G ratio higher than 0.4. The positive rate was also higher in these groups, except for the group of cats with a greater A/G ratio (**Table 3**). Besides, the cat breed from purebred groups was investigated, and it found that ten breeds of cats were recorded, including American shorthair, British shorthair, Chinchilla, Persian, Maine, Ragdoll, Munchkin, Bengal, Scottish fold, and Himalayan. The highest positive rate was in the Persian cat group, with 67%. However, the sample size of them was only three. It could not be statistically analyzed (**Fig. 4A**). The unpaired t-test and Fisher ‘s exact test were applied to each factor analysis to further examine potential risk factors. **Fig. 4B** revealed that the A/G ratio was significantly lower in FIP-positive cats. The odds ratio of each signalment measurement was also analyzed, demonstrating that only cats with age equal to or lower than 2 y/o and A/G ratio equal to or lower than 0.4 significantly correlated with FIPV infection (**Fig. 4C**).

3.4 FIPV genotyping and phylogenetic analysis

3.4.1 The proportion of genotype I and genotype II FIPV collected in this study

After analyzing the characteristics of FIP cases in Taiwan, we focus on the molecular characterization of FIPV in cat effusion samples. The nested RT-PCR conducted in this part successfully recognized the genotype of FCoV in samples collected in this study (**Fig. 5A**). FCoV in 36 of 46 FIP-positive effusion samples was successfully sequenced. Most

doi:10.6342/NTU202301829

of the cases were infected with type I FCoV (35/36, 97.2%), and only 1 case was co-infected with type I and II FCoV (1/36, 2.8%) (**Fig. 5B**). The 110 nucleotides (nt) sequence and its translated 36 amino acids (a.a.) sequence from each genotyping RT-PCR result product were studied. And the sequences from genotype I and genotype II FCoV were analyzed separately.

3.4.2 Phylogenetic analysis of genotype I FIPV sequences

The genotype I FIPV nucleotide phylogenetic tree was constructed with 36 partial spike nucleotide sequences of genotype I FCoV obtained in this study, 20 reference sequences from previous reports, and five sequences from other alphacoronaviruses, including Transmissible gastroenteritis virus (TGEV), Canine coronavirus (CCoV), Chinese ferret badger coronavirus (CFBCoV), and Raccoon dog coronavirus (Raccoon dog CoV) (**Table 2**). The sequence identity among strains obtained in this study ranged from 80% to 100%. As these sequences were compared with previous reports from Taiwan and other countries, the identity also varied, ranging from 80.91% to 98.18%. Furthermore, the sequences of genotype I FCoV were found to be greatly different from those of other alphacoronaviruses. The identity among them ranged from 53.64% to 60% (**Fig. 5C**).

doi:10.6342/NTU202301829

As for the protein sequences, the alignment of the translated FCoV a.a. sequence from this study and other reports showed that 25% (9/36) of them were silent mutations, and the remaining 27 sequences had 1 to 4 a.a. changes. The identity of them ranges from 83.33% to 100%. Regarding the comparison between the genotype I FCoV and other alphacoronaviruses, the identity ranges from 47.22% to 55.56% (**Fig. 5E**). The result revealed that the spike of genotype I FCoV still undergoes mutations and evolution.

3.4.3 Phylogenetic analysis of genotype II FIPV sequences

On the other hand, the phylogenetic tree built with the genotype II FCoV nucleotide sequences collected from this study, previous reports, and from other alphacoronaviruses (**Table 2**) reveals that the characteristics of the genotype II FCoV partial spike in Taiwan remained conserved. As the only nucleotide sequence (NTUCL120) obtained in this study was compared to other sequences from previous papers in Taiwan, the identity was high and up to 100%. However, as NTUCL120 was compared to sequences from other countries, the identity became mildly lower but remained higher than 90%. Furthermore, NTUCL120 was compared with the sequences of other alphacoronaviruses, such as CCoV, raccoon dog CoV, CFBCoV, and TGEV. Surprisingly, the identity among them ranged from 97.27% (TGEV) to 99.09% (CCoV), which represented the close relationship between type II FCoV and other alphacoronaviruses (**Fig. 5D**).

doi:10.6342/NTU202301829

Alignment of the a.a. sequences translated from these nucleotide sequences also showed a highly conserved condition, and the identity among them was between 97.22% to 100%. Only two genotype II FCoV sequences, 08K-609 (Korea) strain and DF-2 (Hungary) strain, had one a.a. mutation, and the other sequences were the same as NTUCL120 (**Fig. 5F**).

3.5 Cytokine profiling of FIPV positive and negative effusion samples

Cytokine level measurement was targeted at feline TNF-α and IL-6 in the effusions using the feline cytokine ELISA kit mentioned in Material and Methods. The volume of 16 of 46 FIP-positive and 28 of 92 FIP-negative effusion samples was sufficient for cytokine examination, which needed to remain higher than 200 μl after utilizing part of their stock for RT-PCR and IFA to detect FIPV at the first step. As to the result from the TNF-α level measurement, though there was no significant difference, the mean level of the FIP-negative group was higher than that of the FIP-positive group. And we could find that TNF-α wasn't detected in most of the FIP-positive effusion samples (**Fig. 6A**). Also, the mean level of IL-6 in FIP-positive cats was almost the same as that of the FIP-negative group (**Fig. 6B**).

doi:10.6342/NTU202301829

3.6 IgG purification: Sample selection, elution, desalting, and FCoV binding confirmation

3.6.1 IgG purification: the successful example

4 FIP-positive effusion samples were selected for IgG purification because of their sufficient remaining volume of higher than 5 ml after other necessary tests were finished with them first. Subsequently, IgG was purified from these samples using the protein A column, followed by the desalting step to ensure that the IgG samples could be used in cell culture level tests. The procedure is depicted in **Fig. 7A**, and the product collected from every step was investigated for IgG purity using SDS-PAGE to check only IgG heavy chain and light chain bands shown in one lane. And their locations were about 55 kDa and 25 kDa, respectively (**Fig. 7B**). These purified IgG samples were then applied in the BCA assay to measure the actual concentration, which was shown in **Fig. 7C**. Besides, to validate the purity of the IgG products, which needed to be free of antigen-antibody complex (Ag-Ab complex) formed by FIPV and FIPV-specific IgG, and reduce the influence on the result of further FIPV ADE examination, the RT-PCR detecting FIPV 3'-UTR fragment was also used in this part. The result showed that FIPV was not detected in the purified IgG samples, which confirmed that only IgG was obtained from the clinical effusions (**Fig. 7D**).

doi:10.6342/NTU202301829

3.6.2 The examination of the binding ability of purified IgG against FCoV

After successfully purifying IgG from 4 clinical effusion samples, these IgG products were subsequently applied to the FCoV antibody detection kit to measure the binding ability to FCoV. The varying positive signal from the kit showed that specific IgG against FCoV existed in the purified IgG result products (**Fig. 8A**). Furthermore, the antigenicity test against FCoV, which was conducted with genotype II FIPV NTU156 strain whole virion and 4 IgG samples, were examined. The concentration of the primary antibodies, the four IgG samples, was 1000 ng/ml. The secondary antibody was goat-derived anti-cat IgG HRP (Bethyl Laboratories) with a 2000-fold dilution. Other western blot steps followed the procedure mentioned in Material and Methods. The result found that all IgG samples could bind to the N protein of FCoV, but only half had reactivity with the FCoV M protein. Surprisingly, none of the IgG samples could detect the S protein of the virus. But the previous results could still prove these antibody samples' binding ability toward FCoV (**Fig. 8B**).

3.7 FIPV ADE establishment and the assay with IgG from FIP cats' clinical effusions

3.7.1 Successful FIPV ADE establishment

In addition to phylogenetic analysis and cytokine profiling, the FIPV antibody-dependent enhancement (ADE) phenomenon was also investigated due to its unclear

doi:10.6342/NTU202301829

information. IgG purified from the 4 FIP-positive effusion samples was conducted in this section to realize the ADE occurrence in effusions of FIP-diseased cats. First, the titer of the virus stock (FIPV NTU156 strain) used in this study was determined using plaque assay, which had the result of 8.4×10^5 pfu/ml that was calculated from the average number of plaques in two 10^{-4} wells (**Fig. 9**). Next, FIPV ADE model was established according to the method mentioned in a previous report (Hohdatsu et al., 1991). **Fig. 10A** showed the experimental flow conducted with FIPV NTU156 strain as antigen, and mAb 6-4-2 as an antibody, which was kindly provided by Dr. Tomomi Takano and Dr. Tsutomu Hohdatsu at Kitasato University, Japan, in Fcwf-4 cell monolayers. After following the procedure in **Fig.10A,** we would have the result that the viral titer of the mAb 6-4-2 adding group was significantly (**, $p < 0.01$) higher than that of the virus-only group with a ten times viral titer enhancement (**Fig. 10B**), which might provide a model for further FIPV ADE tests with different kinds of antibodies.

3.7.2 FIPV ADE assay with IgG purified from 4 FIP-positive cats and neutralizing test of these IgG samples

After establishing the FIPV ADE test model, IgG from 4 clinical samples was introduced, which was examined with four concentrations, 10000, 1000, 100, and 10 ng/ml. **Fig. 11** showed that FIPV infection was mildly enhanced with IgG from all 4

doi:10.6342/NTU202301829

different FIP patient's effusions. And the result even showed that IgG from cat #1 could increase by 20% of the FIPV infection. Though the infection enhancement from the samples was not as significant as from the confirmed mAb, the result could also provide evidence that the ADE phenomenon was actually in FIP-positive cats and their effusions.

The IgG from 4 FIP cat effusions was also examined to determine whether they could neutralize *in vitro* FIPV infection. The result revealed that the neutralization titer of all 4 IgG samples was lower than 2-fold, and they were recognized as non-neutralizing antibodies (data not shown).

3.7.3 Antigenic analysis of cat effusion IgG

To understand the proportion of IgG against different FCoV structural proteins in each purified antibody sample, we conducted a western blot to measure their level. **Fig. 12A** showed that the level of anti-FCoV S IgG was varying, with the highest level within IgG from cat #3 compared to the other 3 cases. In addition, we also investigated the proportion of anti-FCoV N IgG in each IgG sample. Instead, the level of anti-FCoV N protein IgG in most purified IgG samples was almost the same, exclusive of the lower signal found in the IgG sample of cat #4 (**Fig. 12B**). Subsequently, the actual level of anti-FCoV S and N protein IgG in 1000 ng of each IgG sample was calculated through the regression formula analyzed from the standard curve intensity presented in (**Fig. 12A**)

doi:10.6342/NTU202301829

and (**Fig. 12B**) to account for the proportion of them. The principal antibody type in each IgG sample was revealed to be the anti-FCoV N IgG. However, the ratio of anti-FCoV S IgG was much lower in part of the IgG samples and was even only 0.03% in the cat #4 IgG sample. Other kinds of IgG were not discussed in this section and needed more experiments to realize the actual contents of it (**Fig. 12C**).

3.8 Cross-reactivity between FCoV and SARS-CoV-2

3.8.1 Cross-antigenicity test with FCoV whole virion and anti-SARS-CoV-2 spike S1 and S2, N, and M protein pAb

According to the susceptibility of cats to SARS-CoV-2, which caused the current COVID-19 pandemic, and the evidence of co-infection with FIPV and SARS-CoV-2 in one cat (El-Tholoth et al., 2023), the potential cross-reactivity between these two viruses needed to be investigated to reveal whether SARS-CoV-2 could influence the pathogenesis of FIPV infection. First, the cross-antigenicity test was conducted using rabbit-derived anti-SARS-CoV-2 spike S1 and S2, N (Sino Biological), and M protein (ProSci) pAb and FIPV NTU156 whole virion by ELISA and western blot. In these tests, the primary antibodies were rabbit-derived pAb mentioned before, which were started with a 50-fold dilution followed by further seven times serial diluted by two folds in ELISA and diluted in 1000 folds in western blot. The secondary antibody was anti-human

doi:10.6342/NTU202301829

IgG HRP (Jackson ImmunoResearch), diluted in 2000 folds. Other steps followed the ELISA and western blot procedure mentioned in Material and Methods. **Fig. 13A** showed that only rabbit-derived anti-SARS-CoV-2 N protein pAb could detect FCoV with the OD 450 nm value close to 1.5 when the antibody was diluted in 50 folds. Also, **Fig. 13B** demonstrated that only rabbit-derived pAb against SARS-CoV-2 N protein could bind to the N protein of FCoV with the positive signal band (50 kDa) shown on the lane. And these results revealed that cross-antigenicity might only exist within the N protein of these two viruses.

3.8.2 FIPV ADE assay with anti-SARS-CoV-2 spike S1 and S2, N, and M protein pAb

After confirming the cross-antigenicity between FIPV and SARS-CoV-2, we also wondered whether the cross-reactivity between them would influence the pathogenesis of FIPV infection and even enhance it, which was called the FIPV ADE phenomenon. Also, rabbit-derived pAb against spike S1, S2, N, and M protein, diluted in 10, 40, 160, and 640 folds, were used to evaluate the ability to enhance FIPV infection. Even though the cross-reactivity between the N protein of FCoV and pAb against SARS-CoV-2 was confirmed, the FIPV ADE phenomenon was not observed after these rabbit-derived pAb

doi:10.6342/NTU202301829

incubated with FIPV to infect Fcwf-4 monolayers. We could find that the result ADE% of each pAb group maintained at 0 with no apparent fluctuating (**Fig. 14**).

3.8.3 Cross-antigenicity test with FCoV whole virion and human COVID-19 convalescent serum

To further investigate the cross-antigenicity between FIPV and SARS-CoV-2, eight human COVID-19 convalescent serum samples, which were kindly provided by National Taiwan University, were conducted in ELISA and western blot to evaluate the titer of these samples against FCoV and the actual reactivity sites on the virus. In this part, the primary antibodies were human COVID-19 convalescent serum samples, which were also started with a 50-fold dilution followed by further seven times serial two folds dilution in ELISA and diluted in 1000 folds in western blot. The secondary antibody was anti-human IgG HRP (Jackson ImmunoResearch), treated with a 2000-fold dilution. Other steps followed the ELISA and western blot procedure mentioned previously. Besides, data obtained from ELISA was subsequently converted to the viral titer using the sigmoidal dose-response model to standardize the result value from each sample.

Interestingly, 5 of 8 human serum samples were found to react with FCoV with the titer of antibody against FCoV higher than the limit of detection (**Fig. 15A**). In the result of western blot (either reducing or non-reducing condition), 2 of 8 human serum samples

doi:10.6342/NTU202301829

were observed to bind to the S protein S1 subunit (115 kDa) (de Haan et al., 2008) of FCoV, and only one could react with the FCoV N protein (**Fig. 15B**). Besides, the alignment of the S1 subunit a.a. sequence was created using sequences from the FCoV NTU156 strain (Accession number: ACS44218) and the SARS-CoV-2 Wuhan strain (Accession number: YP_009724390). The identity of the S1 between these two viruses was 18.98% (data not shown). The data mentioned above revealed that cross-antigenicity existed between FIPV and SARS-CoV-2, despite the low identity between these two viruses. And we would focus on the serum samples from human #3 and human #5, which could react with the S1 of the spike, for further discussion.

3.8.4 FIPV ADE assay with human COVID-19 convalescent serum

In the case of the advanced result from the cross-antigenicity test between FIPV and human samples, the FIPV ADE model was also conducted with these two materials to reveal the potential influence of human anti-SARS-CoV-2 pAb samples. Before these serum samples were used, the inactivation was performed at 56°C for 30 minutes. And they were also diluted in 10, 40, 160, and 160 folds before they were incubated with FIPV to form the immune complex. **Fig. 16A** showed that the ADE% of most samples consistently maintained close to 0%. However, some were lower, indicating that the pAb from most human serum samples could not enhance the FIPV infection and even mildly

doi:10.6342/NTU202301829

hindered it. Surprisingly, the serum from human #1 elevated the FIPV infection by 35% at the 10-fold dilution. This revealed that the pAb in this sample might interact with the live FIPV virus and elicit the ADE phenomenon. We also examined the human #1 serum in the FIPV ADE test model in triplicate to validate the result. Also, we observed the ADE phenomenon that occurred during FIPV infection in the serum 10-fold dilution group. Though the ADE level was not as elicited from the confirmed mAb 6-4-2, it might deserve more attention about the potential hazard of the antibodies against SARS-CoV-2 toward the FIP-diseased cats (**Fig. 16B**).

3.8.5 Two-way cross-antigenicity test with IgG purified from FIP-positive cat's effusions and structural proteins from SARS-CoV-2

3.8.5.1 IgG purified from FIP-positive cat's effusions and SARS-CoV-2 spike

Besides, to further investigate the cross-antigenicity between FIPV and SARS-CoV-2 and prove this condition in a two-way direction, we also used the IgG purified from clinical FIP effusions and different SARS-CoV-2 structural proteins to conduct western blot. About the cross-reactivity test between the spike of SARS-CoV-2, which is the vital pathogenic factor during the virus-cell binding, and FIP feline IgG, the result showed that the IgG from all four cats was able to react with the spike S2 of SARS-CoV-2 with varying intensity of the positive signal. However, no positive bands were detected after

doi:10.6342/NTU202301829

the IgG samples were incubated with the spike S1 subunit. Besides, two functional domains, receptor binding domain (RBD) and amino-terminal domain (NTD), of the spike were also tested for antigenicity with IgG from FIP cats. The result demonstrated that none of these IgG samples could bind to these two kinds of proteins with no positive bands on each lane (**Fig. 17A**). Besides, to understand the similarity of the S2 between FCoV and SARS-CoV-2, the alignment of the S2 subunit a.a. sequence was also constructed using sequences from the FCoV NTU156 strain (Accession number: ACS44218) and the SARS-CoV-2 Wuhan strain (Accession number: YP_009724390). The identity of the S2 between these two viruses was 33.74% (data not shown).

3.8.5.2 IgG purified from FIP-positive cat's effusions and SARS-CoV-2 nucleocapsid protein

In addition to the spike protein, the N protein of SARS-CoV-2, which was indicated to be more conserved than other structural proteins, was also included in this test. The result revealed that the complete N protein and its three fragments could react with the four IgG samples. Among them, IgG from cat #1 was found to detect the N protein better, and the N protein NTD fragment might be the more conserved region for antibodies detection with three of four strong signal bands expressed from the N protein NTD lanes, which demonstrated the significant cross-reactivity between the IgG against FIPV and

doi:10.6342/NTU202301829

SARS-CoV-2 N protein (**Fig. 17B**). According to the results from previous experiments and this section, the two-way cross-reactivity between FIPV and SARS-CoV-2 was confirmed, which proved the close relationship among them. However, they were from a different genus.

doi:10.6342/NTU202301829

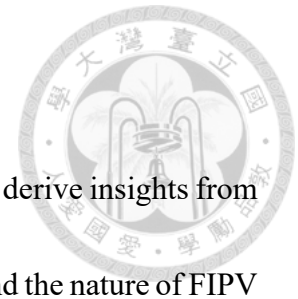

Chapter 4 Discussion

Upon completion of experiments in this project, we were able to derive insights from the clinical samples, specifically effusions from FIP cats, to understand the nature of FIPV infection better. The recent positive rate of FIPV infection in Taiwan detected from RT-PCR and IFA simultaneously in effusion samples of FIP-suspected cats was 33%. Compared to two reports analyzed in Taiwan, the positive rate of FIP cases declined year by year, from 58% (2020) to 38% (2022, this study). The bias within the sample sources might cause this, but it needed to be noticed that FIPV infection still prevailed over cats in Taiwan. Also, the positive rate of FIP in other countries fluctuates, and the gap range among them may be up to 70% (Benetka et al., 2004; Yin et al., 2021) with different kinds of detection methods, including IHC, ICC, IFA, and RT-PCR. Due to their low sensitivity or specificity, some of these methods might be used in pairs. For example, the sensitivity of RT-PCR and IFA to detect FIPV was indicated to be low and only close to 70% (Felten and Hartmann, 2019), so we confirmed the positive samples by both of them to increase the confidence of the detection.

Among the FIP-positive cases in this project, characteristics such as age (≤ 2 y/o) and blood A/G ratio (≤ 0.4) were indicated to be the risk factors correlated to the FIPV infection, which was consistent with what has been mentioned in reports from other countries (Foley et al., 1997; Pedersen, 2009; Rohrbach et al., 2001). And this may

doi:10.6342/NTU202301829

provide some suggestions for the vet to suspect FIP when the diseased cats with these signalments. Importantly, all these signalments of concern needed to be considered with the clinical exhibition of the cats.

As for the analysis of the FIP disease itself, we would start from the clinical feline effusion samples and focus on three materials within it to study the phylogenetic status (FIPV), cytokine profiling (cytokine), and the ADE phenomenon (antibodies) of FIPV infection.

The phylogenetic analysis with the sequence from the FCoV 3'-terminal spike of successfully sequenced samples revealed a high diversity in the genotype I FIPV spike. Instead, the genotype II FCoV phylogenetic tree demonstrated a highly conserved condition of the collected sequences in Taiwan. Also, sequences from these FIP-positive cases were compared to those from other countries. A high level of heterogenicity was also presented in the genotype I FCoV spike. However, the genotype II FCoV spike did not change a lot.

Furthermore, the relatively conserved genotype II FCoV sequences were also similar to the sequence from other related viruses belonging to the genus Alphacoronavirus, subgenus Tegacovirus, including TGEV, CCoV, CFBCoV, and Raccoon dog CoV. However, these sequences were vastly different from genotype I FCoV sequences. In case of a high diversity within the genotype I FCoV spike, the potential mutating motif, which

doi:10.6342/NTU202301829

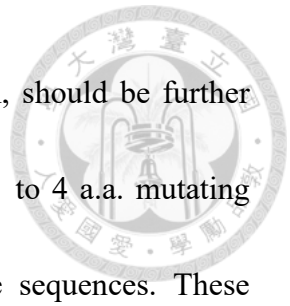

may influence the virulence and lead to cross-species transmission, should be further investigated and monitored. In the alignment result of this study, 1 to 4 a.a. mutating residues were found within 27 obtained genotype I FCoV spike sequences. These locations might also provide clues for the FIPV spike structure and function examination, especially the targeted site of the genotyping RT-PCR used in this study, the spike S2 subunit heptad repeat-2 subdomain, which is responsible for the viral fusion during FCoV infection. However, due to the relatively high conserved condition within the genotype II spike sequence among the samples from Taiwan and the close relationship with other common tegacoviruses, the potential cross-reactivity among coronaviruses from different species should be concerned, which may affect the efficiency of the clinical detection tools, such as the FCoV antibody detection kit, and even lead to cross-reactivity between FIPV and other viruses. Therefore, the sequence comparison analysis and further antigenicity tests should be conducted for more information.

The cytokine level in the effusions from this study was measured to realize more about immune mediators during FIPV infection through the feline TNF-α and IL-6 ELISA kits. The result from the TNF-α measurement was below expectations, which demonstrated that the level of it was higher in the FIP-free group. Also, unfortunately, the result from the IL-6 level examination revealed that the mean level of IL-6 was almost the same in both FIP-positive and FIP-free groups. The result did not correspond to the

doi:10.6342/NTU202301829

high TNF-α and IL-6 levels in other systemic organs of FIP-diseased cats, such as the liver, heart, and brain, mentioned in previous papers (Foley et al., 2003; Malbon et al., 2019). This may be related to several factors. For example, all of the samples collected in this study were diseased cats' effusions, which may be originated from various diseases. Some aged patients with probable cancer disease or other inflammation causes may also have a higher concentration of TNF-α, which can be the limit of this cross-sectional project.

Furthermore, the sensitivity of the methods, including IFA and RT-PCR, used in this project was low, and this might be the potential influence on the positive sample collection. Though we could not obtain the potential FIP biomarker, IL-6, and TNF-α level, detected from the feline effusions, the result could provide some information about the cytokine profile during FIPV infection, which indicated that further *in vivo* tests should be considered. The condition of cytokine distribution in different organs and even in effusions also needed to be compared to various diseases. Surprisingly, one study discussing the relationship between antibodies against SARS-CoV-2 and cytokines revealed that the anti-SARS-CoV-2 N protein antibodies might elevate the production of IL-6 in COVID-19 human patient alveoli through *in vitro* tests (Nakayama et al., 2022), which could be the reference for further FIP biomarker evaluation since the titer of anti-FCoV N antibodies was also high in FIP-diseased cats. The different detection methods,

doi:10.6342/NTU202301829

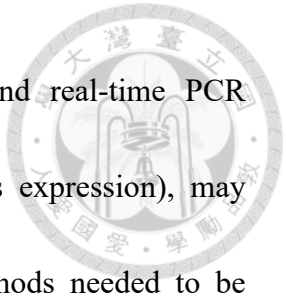

such as ELISA (measurement of the cytokine protein level) and real-time PCR (evaluation of the transcriptional condition of the cytokine genes expression), may influence the result as well, which indicated that these both methods needed to be conducted in pairs to find out the cytokine profile of the diseased cats more confidently.

Furthermore, the IgG antibodies within the effusions were purified to investigate the ADE phenomenon during FIPV infection. Antibody-dependent enhancement (ADE), a mysterious immunopathological phenomenon that may affect the vaccine development of the disease, has been studied for several years. However, the actual procedure of it still needed to be clarified. Some reports indicated that the virus, IgG, and Fc receptors on immune cells formed the ADE during the coronavirus infection. And both neutralizing and non-neutralizing antibodies were found to be responsible for this horrible condition (Lee et al., 2020). Therefore, in this project, we focused on the antibody and used different kinds of it to test its ability to FIPV infection enhancement. Among the used antibodies, the anti-FCoV S protein neutralizing mAb 6-4-2 was confirmed to increase the efficiency of FIPV infection and used as the positive control of this ADE evaluation test. In addition to mAb 6-4-2, other non-neutralizing antibodies against FCoV M protein were reported as the infection enhancement reagent (Hohdatsu et al., 1991). As to the previous pandemic disease, SARS-CoV infection, the antibodies against the SARS-CoV N protein were also found the association with severe clinical symptoms, which might be corresponded with

doi:10.6342/NTU202301829

the ADE (Leung et al., 2004) and indicate that the investigation of ADE phenomenon could not only focus on the antibody against the important pathogenic factor, the spike protein, and anti-other structural proteins antibodies might also be considered. Using IgG purified from clinical samples in our project in the established FIPV ADE test model showed that IgG from all four clinical FIP samples could also mildly enhance the infection. However, the level of the phenomenon, which was calculated from the standardized ADE percentage (ADE%) formula, caused by them was not as that of the mAb 6-4-2 group. Besides, we found that IgG from all four clinical FIP patients were non-neutralizing antibodies. Furthermore, the varying concentration of anti-FCoV S antibodies was not found to be correlated to the level of FIPV ADE. Though the anti-FCoV N IgG accounted for the most in each IgG sample, it may not be responsible for ADE and just corresponded to the evidence that the N protein of coronavirus was produced the most among different kinds of structural proteins, which is responsible for the virus replication (McBride et al., 2014). These results revealed that the non-neutralizing antibodies might also enhance the FIPV infection, consistent with the previous papers' results. They proved that ADE existed within the effusions of the FIP cats, which may be correlated to more severe clinical signs such as the rapid aggravation of the disease. Besides, the FIPV was revealed to infect more efficiently in the modified

doi:10.6342/NTU202301829

Fcwf-4 cell line, Fcwf-4 CU, which was established at Cornell University (O'Brien et al., 2018). The FIPV ADE test model might be applied in Fcwf-4 CU to reveal a better result.

According to the recent COVID-19 pandemic cross-species cat infection cases and the evidence of the co-infection of FIPV and SARS-CoV-2 in one cat, the cross-reactivity between these two viruses was investigated to evaluate the influence of SARS-CoV-2 on FIPV infection. The result from our study showed that anti-SARS-CoV-2 N protein pAb could react with the N protein of FCoV. FIPV ADE was not observed after the cells were incubated with the antibody and FIPV. Human COVID-19 convalescent serum samples were also applied in the cross-reactivity experiments and FIPV ADE test model to further investigate the phenomenon. The result showed that 5 of the serum samples presented the antibody titer against FCoV by ELISA. The N protein and the S protein S1 subunit of FCoV were detected by part of these serum samples. Surprisingly, the human #1 serum, one of the samples able to react with FCoV by ELISA, could enhance the FIPV infection by 35%, and this result was even validated in triplicate. This might provide evidence of the cross-reactivity between these two viruses and emphasize the potential hazard of enhancing the FIPV infection as the cats were simultaneously infected with FIPV and SARS-CoV-2. However, the western blot results (either reducing or non-reducing condition) showed that the human #1 serum could not detect any structural proteins of FCoV, and this might be due to different conformation of the antigens under ELISA and

doi:10.6342/NTU202301829

western blot. Besides, antibodies against CCoV and HCoV 229E in human (Vlasova et al., 2022) may affect the result as well, which may be related to the potential cross-reactivity with FCoV (Horzinek et al., 1982), but needed more experiments to realize it. Besides, the epitope of the antibody enhancing the infection was investigated in a previous study using different monoclonal antibodies (Takano et al., 2008b). And this information could also be used to be compared with the sequence of SARS-CoV-2, which may provide some clues for the evaluation of the FIPV ADE phenomenon.

In addition, we used IgG purified from clinical FIP patients to detect different structural proteins on SARS-CoV-2 in this study. The bilateral cross-antigenicity was still found at the SARS-CoV-2 spike S2 subunit and all fragments of N protein using western blot. Another result from our lab found that feline FIP effusions could also detect the spike RBD using ELISA. And this again proved the close relationship between these two viruses. Besides, one report even indicated that serum from both genotype FCoV-infected cats could react with spike RBD of SARS-CoV-2, which may be implicated in the progression of vaccine development against pan-coronavirus (Yamamoto et al., 2023). In addition to realizing the disease itself, vaccine development may also become the target for our cross-reactivity study.

According to a previous study from our lab discussing the comparison of N protein from four groups of coronaviruses, the N protein a.a. sequence identity between FCoV

doi:10.6342/NTU202301829

and SARS-CoV-2 was 30.88%. The identity of the N protein NTD from these two viruses was even up to 75% (陳耀云, 2022), which provided evidence that the bilateral cross-reactivity showed on the N protein of FCoV and SARS-CoV-2 and even on the N protein NTD. Besides, our results revealed that human COVID-19 convalescent serum could bind to the FCoV S protein S1 subunit, and IgG from FIP cat's effusions was able to detect the SARS-CoV-2 S protein S2 subunit. Regarding the potential cross-reactivity on the S protein between FCoV and SARS-CoV-2, alignment of the FCoV and SARS-CoV-2 S protein a.a. sequence was created. The identity of the S1 and S2 subunit between these two viruses was 18.98% and 33.74%, respectively. The identity value was consistent with the fact that the S protein S2 subunit of coronavirus was more conserved than S1 subunit (Shah et al., 2021). As the S protein S1 subunit may have a higher probability of mutating to enhance the virulence or the susceptibility to the host, the difference between distinct coronaviruses may be significant. But the antigen conformation under different assays may influence the epitope exhibition. Besides, some unknown antibodies in human serum may also affect the result and be the cause of the ADE phenomenon during FIPV infection, which needs further discussion.

Additionally, a strong cross-reaction was shown as the IgG from FIP cats' effusions was incubated with the SARS-CoV-2 S protein S2 subunit. But anti-SARS-CoV-2 pAb could not detect the FCoV S protein S2 subunit, which may also be influenced by the

doi:10.6342/NTU202301829

conformation of the protein. Though the identity of the S2 subunit between these two viruses was only 30.88%, according to the higher identity of S2 than S1 subunit between FCoV and SARS-CoV-2 the SARS-CoV-2 S protein 3-D conformation was more likely to exhibit potential epitopes for anti-FCoV antibodies. The result demonstrated that the cross-reactivity between these two viruses may need more attention.

In this study, we examined the characteristics and pathogenesis of FIP, focusing on the FIP cases, FIPV, cytokine, and IgG in feline effusions. The potential cross-reactivity was found through the established FIPV ADE test model with the virus isolated from effusions. Besides, the IgG purified from the effusions also detected the structural proteins of SARS-CoV-2. These two results indicated that effusions might be an excellent specimen for FIP and virus cross-reactivity investigation. Also, the phylogenetic analysis demonstrated the mutating condition within genotype I FIPV spike protein, which needed to be monitored continuously. Some characteristics, such as the age and the blood A/G ratio, could provide suggestions for FIP diagnosis, though they are considered with the clinical symptoms of the diseased cats. TNF-α and IL-6, the potential biomarkers in FIP cats, should be investigated in further *in vivo* tests. Other cytokines also needed to be studied to realize more about the immune mediators during FIPV infection.

Last but not least, the cross-reactivity between FIPV and SARS-CoV-2 has been demonstrated, more further experiments should be conducted to validate the result. And

doi:10.6342/NTU202301829

coronavirus in other genera could also be included in the cross-reactivity test to establish a pan-coronavirus panel, which might be the reference for future vaccine development and provide some clues for the horrible ADE phenomenon. Ultimately, this study is the first to report *in vitro* ADE phenomenon elicited from FIP-diseased cats' effusions IgG and discovered potential cross-reactivity between FCoV and SARS-CoV-2, providing valuable insights for future FIPV studies.

doi:10.6342/NTU202301829

Chapter 5 Figures and tables

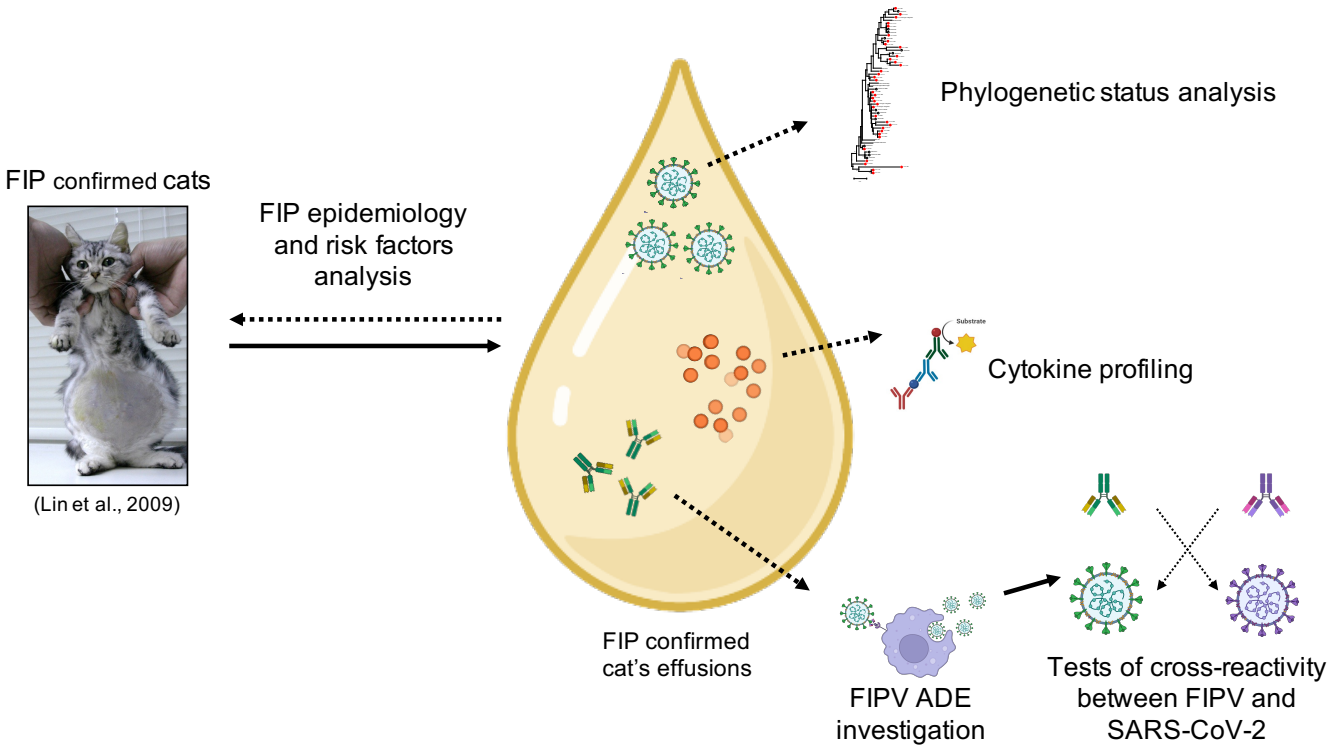

Figure 1. Experimental design in this study.

This study could be divided into two parts, the analysis of the FIP patient characteristics (epidemiology and risk factors) and the investigation of the FIP disease itself (virus, cytokines, and antibodies), focusing on the effusion sample acquired from FIP-suspected cats. The figure was depicted using BioRender (Toronto, Canada).

doi:10.6342/NTU202301829

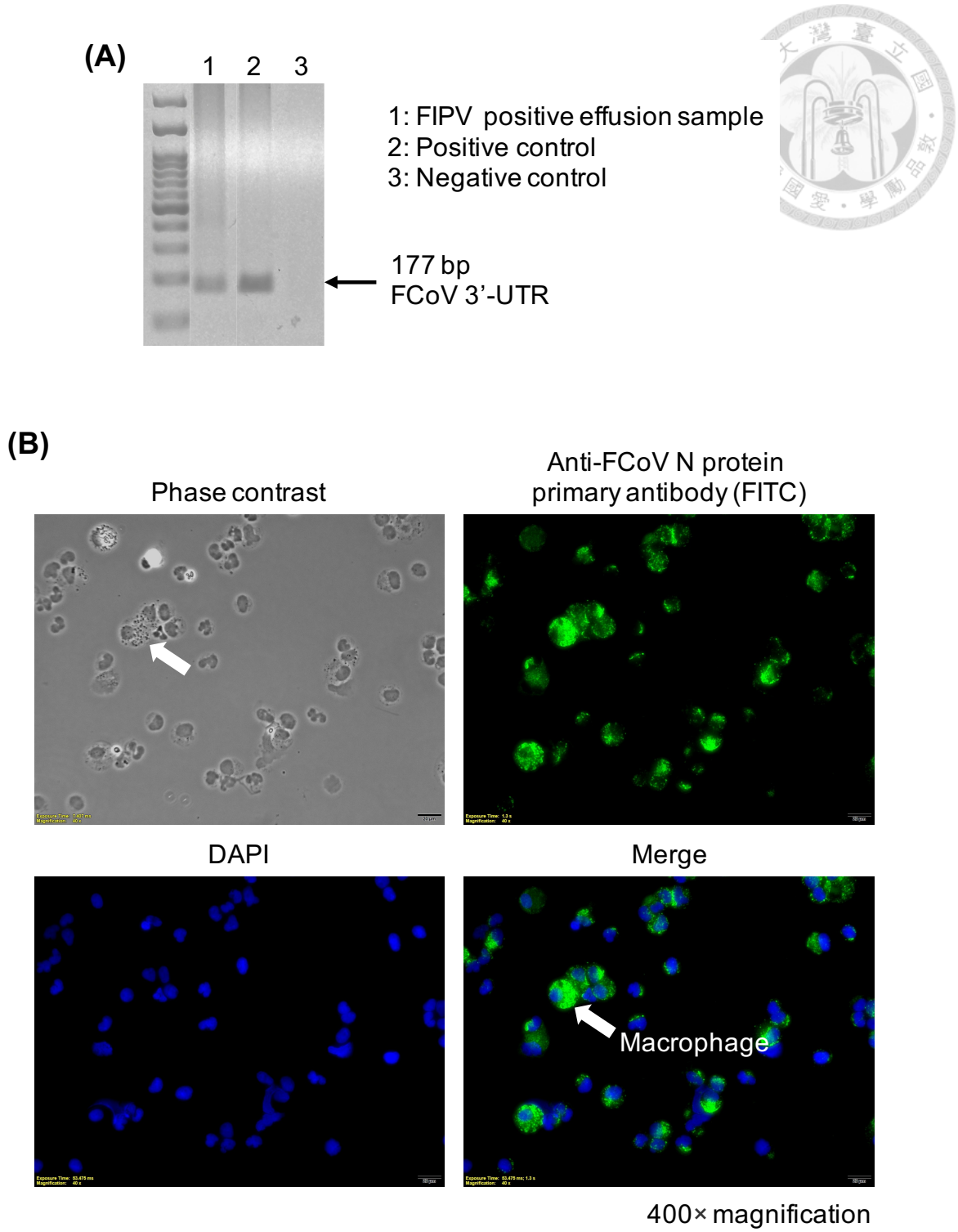

Figure 2. FIP-positive sample confirmation with both RT-PCR and IFA.

(A) The FCoV detection RT-PCR targeted site was at 3'UTR of FCoV with 177 bp. The result figure was processed to be an inverted image. And the positive bands were changed

doi:10.6342/NTU202301829

from white to black. (B) FCoV was also confirmed in macrophages using IFA with mouse-derived anti-FCoV N protein primary mAb following the protocol mentioned in the Material and Methods, and the field of view was 400× magnification. (A)(B) The FIP-suspected cat's effusion samples needed to be confirmed FIPV positive using these two methods simultaneously.

doi:10.6342/NTU202301829

(A)

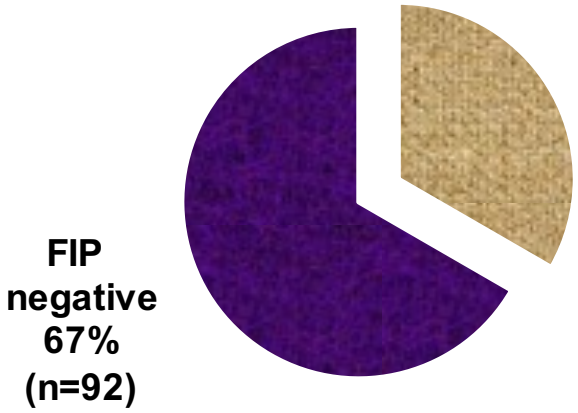

(B)

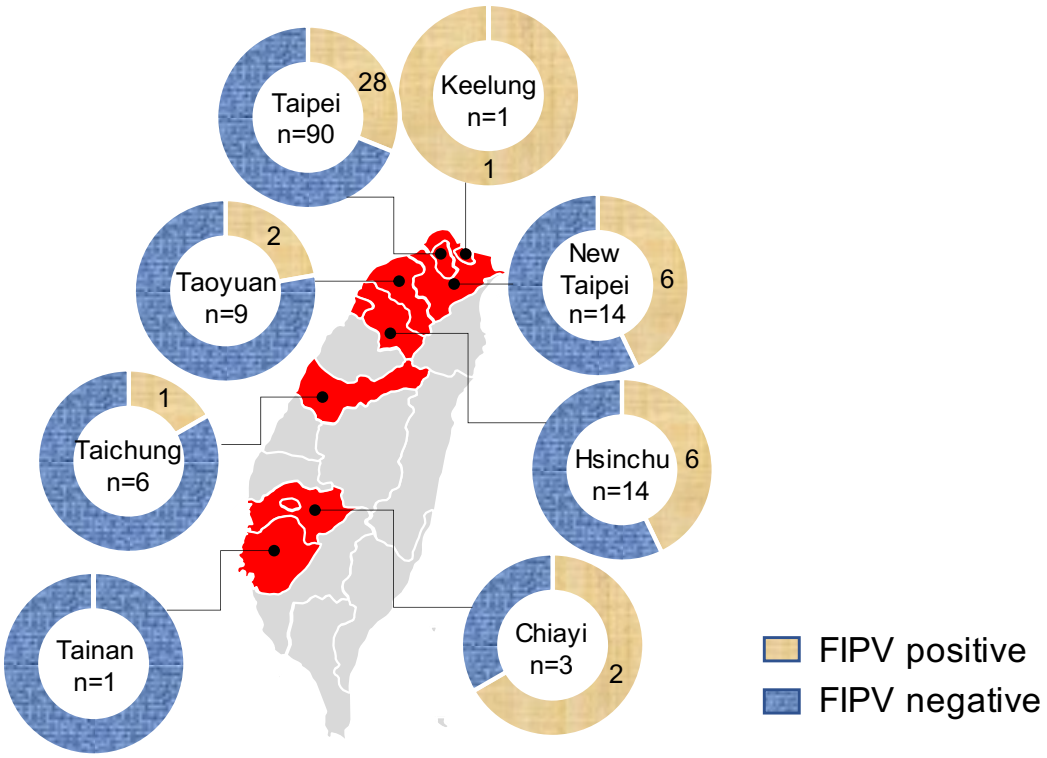

doi:10.6342/NTU202301829

Figure 3. FIP positive rate and geographical distribution

(A) The FIP-positive samples proportion was depicted as the light part of the pie chart with the legend mentioning the percentage and sample size beside it. The dark part of the pie chart represents the FIP-negative samples proportion. (B) The red parts of the Taiwan map represented the counties having FIP-positive cases with the sample size, county name mentioned in the circle, and the number of FIP-positive cases marked on the light part of the circle, which depicted the proportion of these FIP-positive cases in each region. The dark purple side of the ring represented the FIP-negative ratio of the samples collected from that county.

doi:10.6342/NTU202301829

(A)

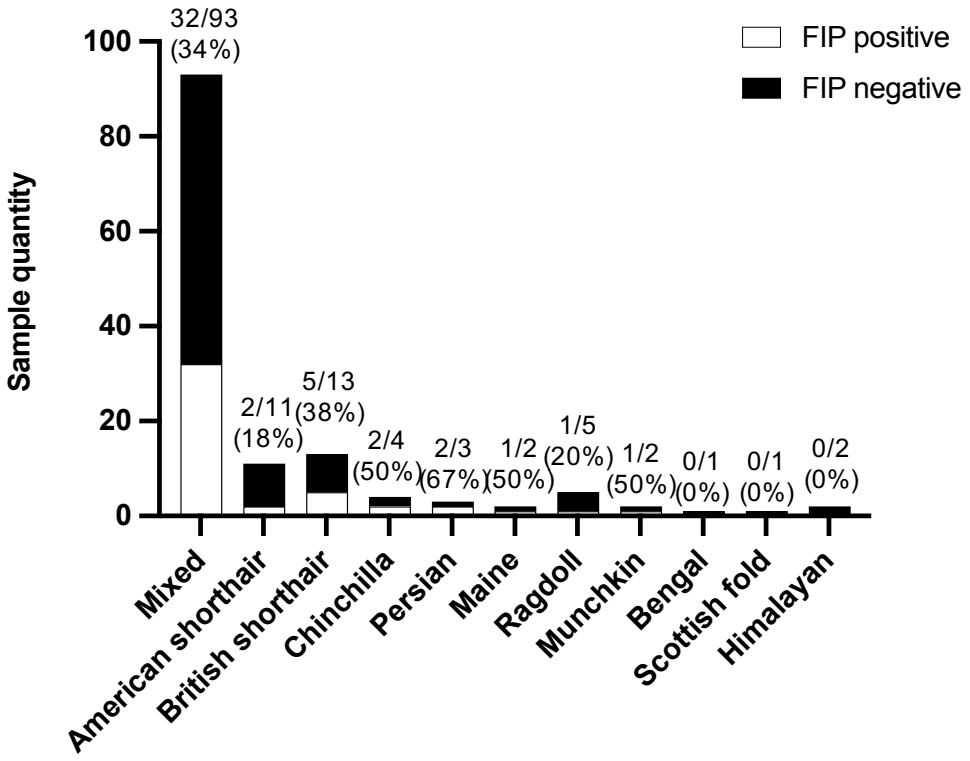

(B)

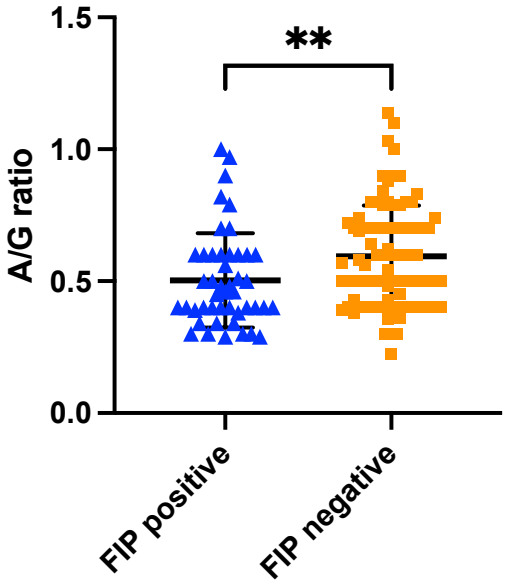

doi:10.6342/NTU202301829

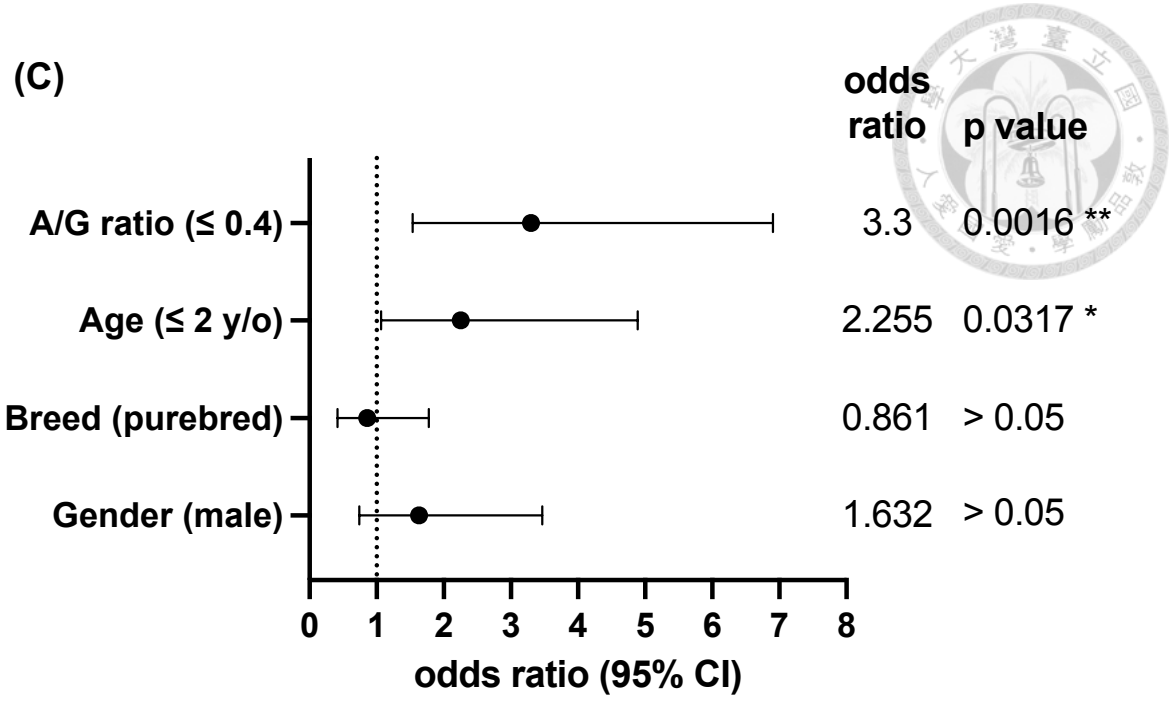

Figure 4. FIP risk factors analysis.

(A) The breed of cats included in this project was recorded with a positive rate above each column. X-axis showed groups of mixed cats and different cat breeds recorded from the inspection sheet. Y-axis demonstrated the sample size of each group, with the dark-white proportion representing the FIP negative-positive ratio among the samples in the group. (B) The A/G ratio value analysis. Blue triangle dots (n=46) showed the A/G ratio value of each FIP-positive case. Orange square dots (n=90) represented the A/G ratio value of each FIP-negative case. The level between the FIP-positive and -negative groups were compared by a two-tailed unpaired t-test (**, $P < 0.01$). Data were shown as the mean ± SD. (FIP positive cases, n=46. FIP negative cases, n=90) (C) Odds ratio of four signalment titles was calculated with legends mentioning odds ratio mean and p-value.

doi:10.6342/NTU202301829

Data represented the mean ± 95% CI. And the two groups in one title were compared by Fisher's exact test (*, P < 0.05. **, P < 0.01).

doi:10.6342/NTU202301829

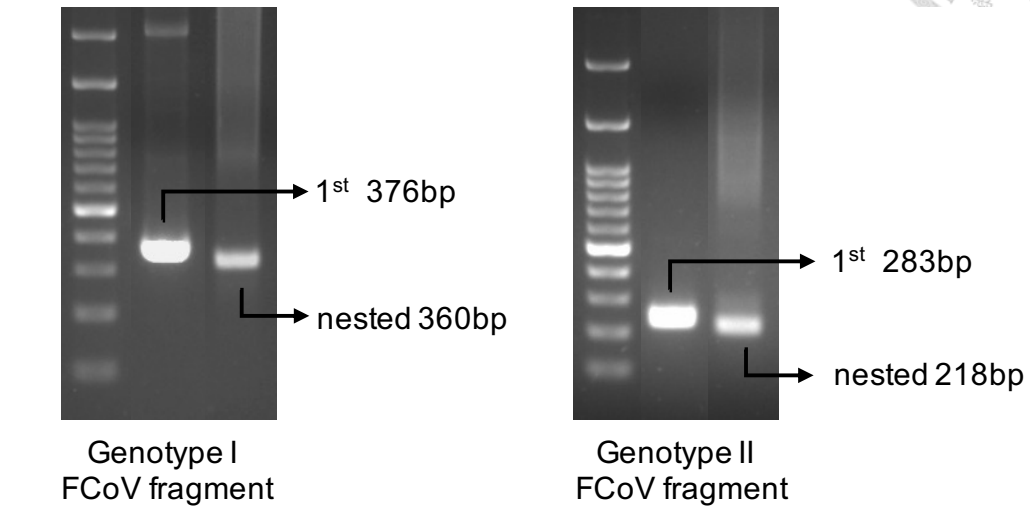

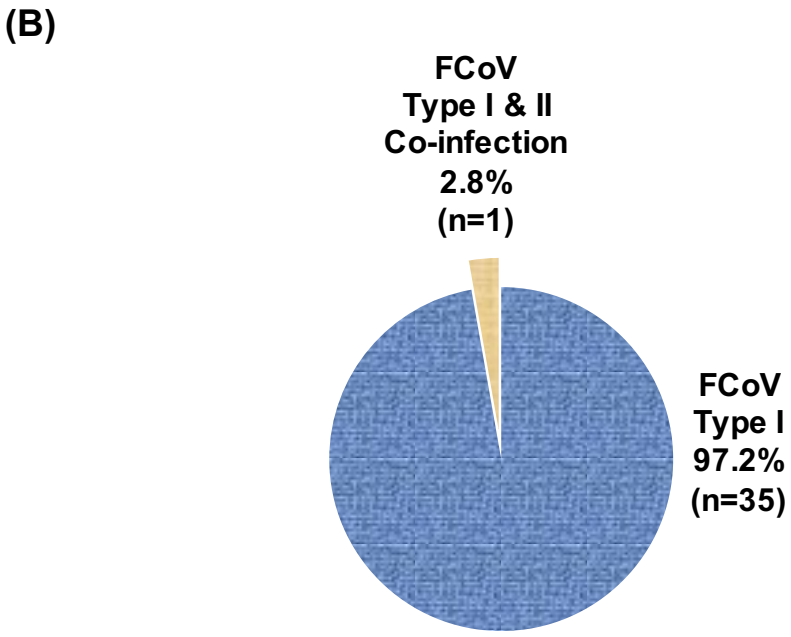

doi:10.6342/NTU202301829

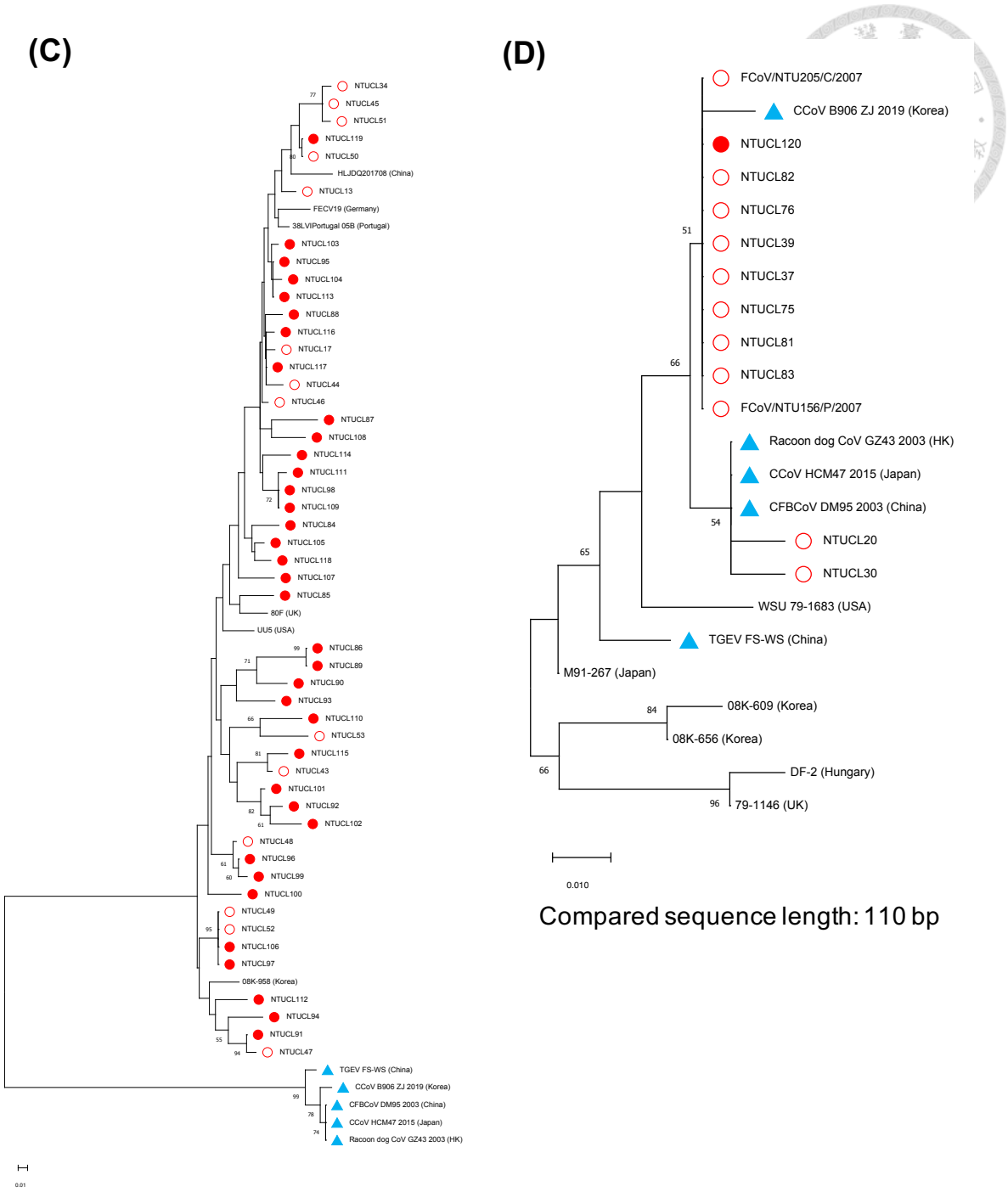

Compared sequence length: 110 bp

Compared sequence length: 110 bp

● FCoV sequences in this project

○ FCoV sequences from previous Taiwan reports

No marker FCoV sequences from other countries

▲ Sequences from other alphacoronavirus

doi:10.6342/NTU202301829

(E)

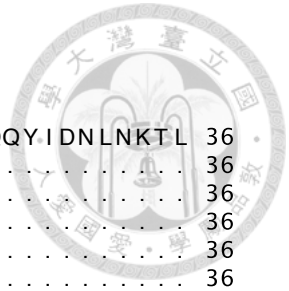

```
                                                  20
                                                  |
NTUCL13  KLNLTAEIDQLEQRADNLTNIAHELQQYIDNLNKTL 36
NTUCL17  ....................R.............. 36
NTUCL34  ........H..............................  36
NTUCL43  ............L.........Q.............. 36
NTUCL44  ....V.................................. 36
NTUCL45  ..................................... 36
NTUCL46  ..................................... 36
NTUCL47  ....................T.............. 36
NTUCL48  ..................................... 36
NTUCL49  ..................................... 36
NTUCL50  ..................................... 36
NTUCL51  ..................................... 36
NTUCL52  ..................................... 36
NTUCL53  ....................IM............I 36
*NTUCL84  ....................Q.............. 36
*NTUCL85  ....................T............I 36
*NTUCL86  ....................T.....E........ 36
*NTUCL87  ........H...K.....S............I 36
*NTUCL88  ..................................... 36
*NTUCL89  ....................T.....E........ 36
*NTUCL90  ....................T.............. 36
*NTUCL91  ....................T.............. 36
*NTUCL92  ....V.............A.............. 36
*NTUCL93  ....................T.............. 36
*NTUCL94  ..........K.......T...........N.. 36
*NTUCL95  ..................................... 36
*NTUCL96  ..................................... 36
*NTUCL97  ..................................... 36
*NTUCL98  ....................D............I 36
*NTUCL99  ........N............................. 36
*NTUCL100 ....................L.............. 36
*NTUCL101 ....................A.............. 36
*NTUCL102 ....V..N.........V.............. 36
*NTUCL103 ....................D.............. 36
*NTUCL104 ..................................... 36
*NTUCL105 ..........K.........D.............. 36
*NTUCL106 ..................................... 36
*NTUCL107 ..........Q.......I.............. 36
*NTUCL108 ....................D.............. 36
*NTUCL109 ....................D............I 36
*NTUCL110 ....................T....R......... 36
*NTUCL111 ....V................D............I 36
*NTUCL112 ............T.........L.............. 36
*NTUCL113 ..................................... 36
*NTUCL114 ....................G.............. 36
*NTUCL115 ............L.....I..Q.............. 36
*NTUCL116 ....................Y.............. 36
*NTUCL117 ..................................... 36
*NTUCL118 ..........K.........D.............. 36
*NTUCL119 ..................................... 36
UU5 (USA)  ..................................... 36
08K-958 (Korea)  ..................................... 36
80F (UK)  ..................................... 36
38LVIPortugal_05B (Portugal)  ..................................... 36
HLJDQ201708 (China)  ..................................... 36
FECV19 (Germany)  ........G.............D.............. 36
CFBCoV DM95 2003 (China)  Y...G..D..F.SEK.H.TTV..AIL...I.N.. 36
CCoV HCM47 2015 (Japan)  Y...G..D..F.SEK.H.TTV..AIL...I.N.. 36
Racoon dog CoV GZ43 2003 (HK)  Y...G..D..F.SEK.H.TTV..AIL...I.N.. 36
TGEV FS-WS (China)  Y...G..D..F.SEK.H.TTV..AIL...I.N.. 36
CCoV B906 ZJ 2019 (Korea)  Y...G..D..F.SEK.H.TTV..AIL...I.N.. 36
```


doi:10.6342/NTU202301829

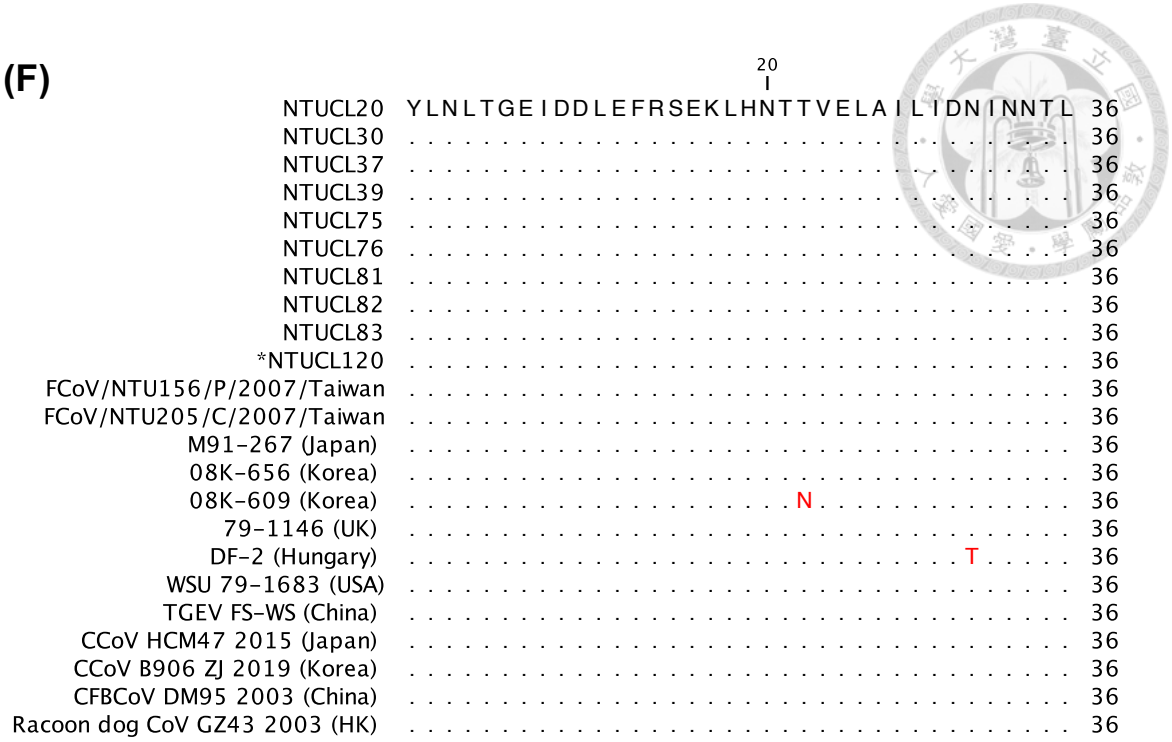

Figure 5. Phylogenetic analysis of genotype I and genotype II FCoV.

(A) The electrophoresis result was from the FCoV 2-step genotyping RT-PCR used in this project. The procedure and target sequence reference was from a previous report (Addie et al., 2003)**.** (B) The pie chart represented the distribution of the two genotypes of FCoV in these FIP-positive effusion samples with legends mentioning the percentage and the sample size. The light part showed the proportion of cases co-infected with type I and type II FCoV. The dark part showed the proportion of cases infected with type I FCoV. (C)(D) The neighbor-joining phylogenetic tree of genotype I FCoV (C) and genotype II FCoV (D) was constructed following the method mentioned in Material and Methods with the original tree demonstration (Scale length of each tree was 0.01). The 110 bp nucleotide sequence from each positive sample was compared. The red solid circle

doi:10.6342/NTU202301829

labeled sequences were acquired from the samples collected during this project. The red hollow circle marks the sequences reported from previous studies in Taiwan. Other sequences with no marker were sequences from other countries. Sequences with blue triangles are from other alphacoronaviruses. (E)(F) Alignment of amino acid sequences from genotype I (E) and genotype II (F) FCoV phylogenetic analysis. The translation started from the second nucleotide of the sequence on the positive strand. The different residues were colored red, and matching residues were as dots. Asterisk (*) marked title represented the sequence obtained in this study.

doi:10.6342/NTU202301829

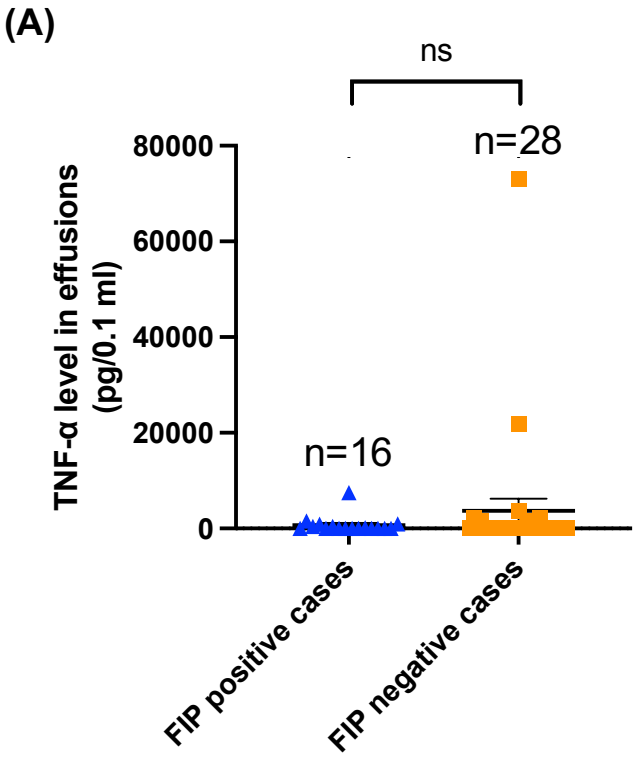

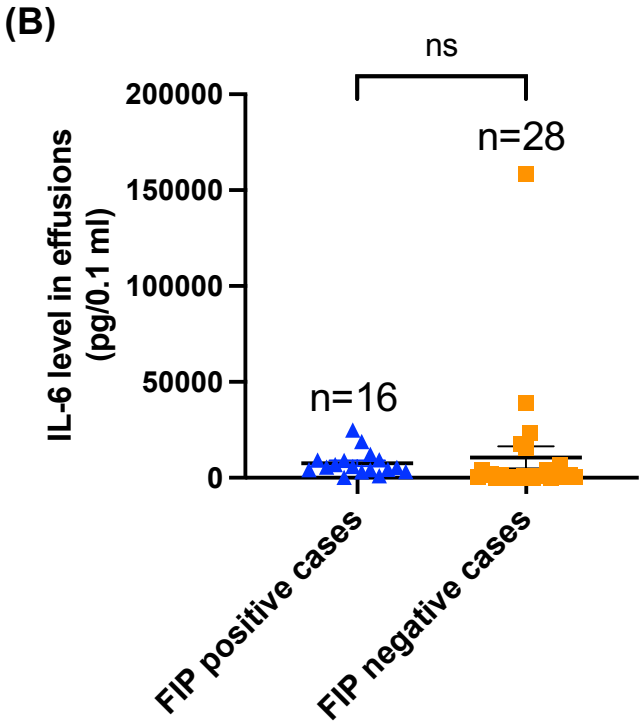

doi:10.6342/NTU202301829

Figure 6. Analysis of the level of TNF-α and IL-6 in FIP-positive effusion samples and FIP-negative samples.

The actual level of (A) TNF-α (n=16) and (B) IL-6 (n=28) in each sample was measured using the feline cytokine ELISA kit. X-axis represents the FIP positive effusion group and FIP negative effusion group. Y-axis represents the calculated level (ng/0.1 ml) of (A) TNF-α and (B) IL-6 in each sample. The data of the FIP-positive group and FIP-negative group represented the mean ± SEM. And the value of the two groups was compared by unpaired t-test.

doi:10.6342/NTU202301829

(A)

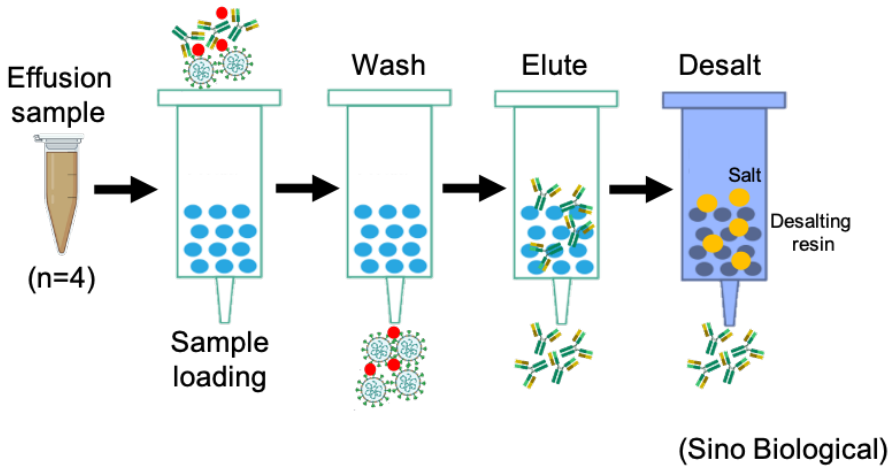

(Sino Biological)

(B)

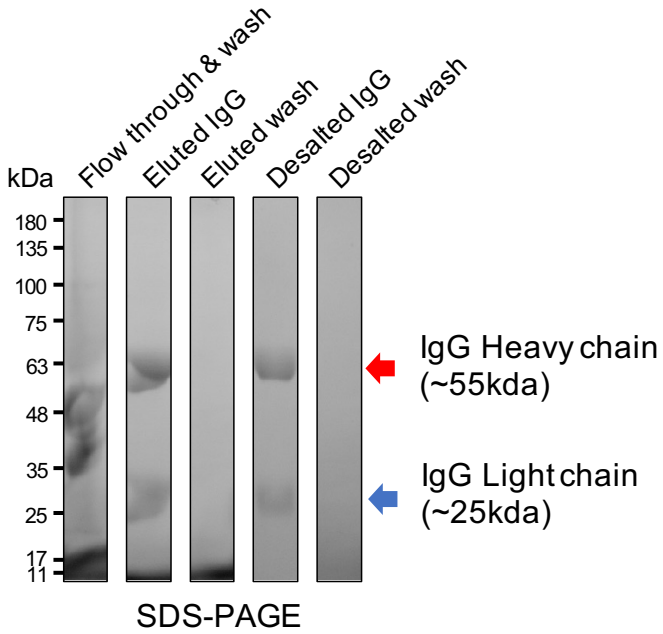

SDS-PAGE

doi:10.6342/NTU202301829

(C)

	Cat #1	Cat #2	Cat #3	Cat #4
Purified IgG concentration (ng/μl)	4417	146	1120	3100

(D)

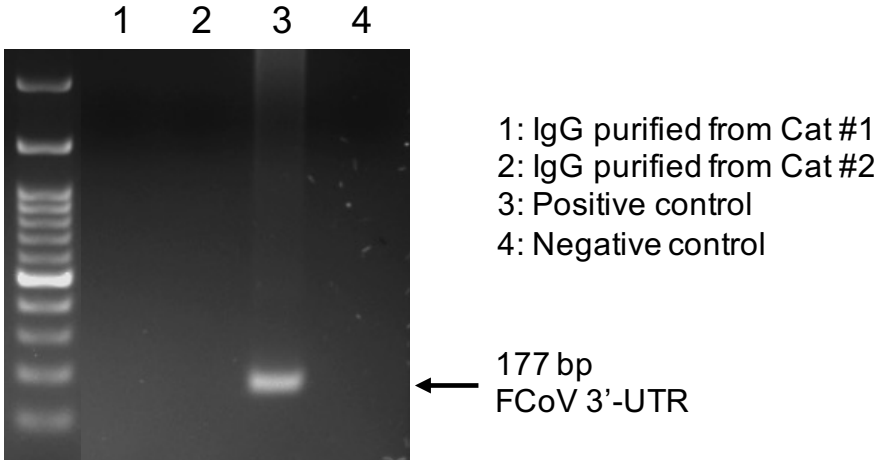

Figure 7. IgG purification from FIP suspected cat's effusion samples and IgG concentration determination.

(A) Cartoon flow chart of IgG purification procedure with a protein A column. 4 of 46 FIP-positive cat's effusion samples were selected because of their storage volume. IgG in them was purified following the method mentioned in Material and Methods. The white column represented the protein A column for IgG purification. The blue column represented the chromatography column for sample desalting. This figure was depicted and referenced by the Sino Biological Corporation. (B) The purity of IgG was ensured using SDS-PAGE following the method mentioned in Material and Methods. The sample

doi:10.6342/NTU202301829

in this experiment was processed by the reducing buffer. The molecular weight of the IgG heavy chain and light chain was 55 and 25 kDa for each. The IgG purification was finished by detecting IgG heavy chain and light chain simultaneously on SDS-PAGE. (C) The concentration of the IgG purified from each sample was determined using the BCA assay, and these data were used for sample volume calculation in further experiments. (D) Two purified IgG samples were selected to measure the existence of the Ag-Ab complex. 2-step RT-PCR was conducted following the methods mentioned in FIP-positive sample detection with the 177 bp target fragment at the 3'-UTR of FCoV. Ag-Ab complex, antigen-antibody complex. 3'-UTR, 3'-untranslated regions.

doi:10.6342/NTU202301829

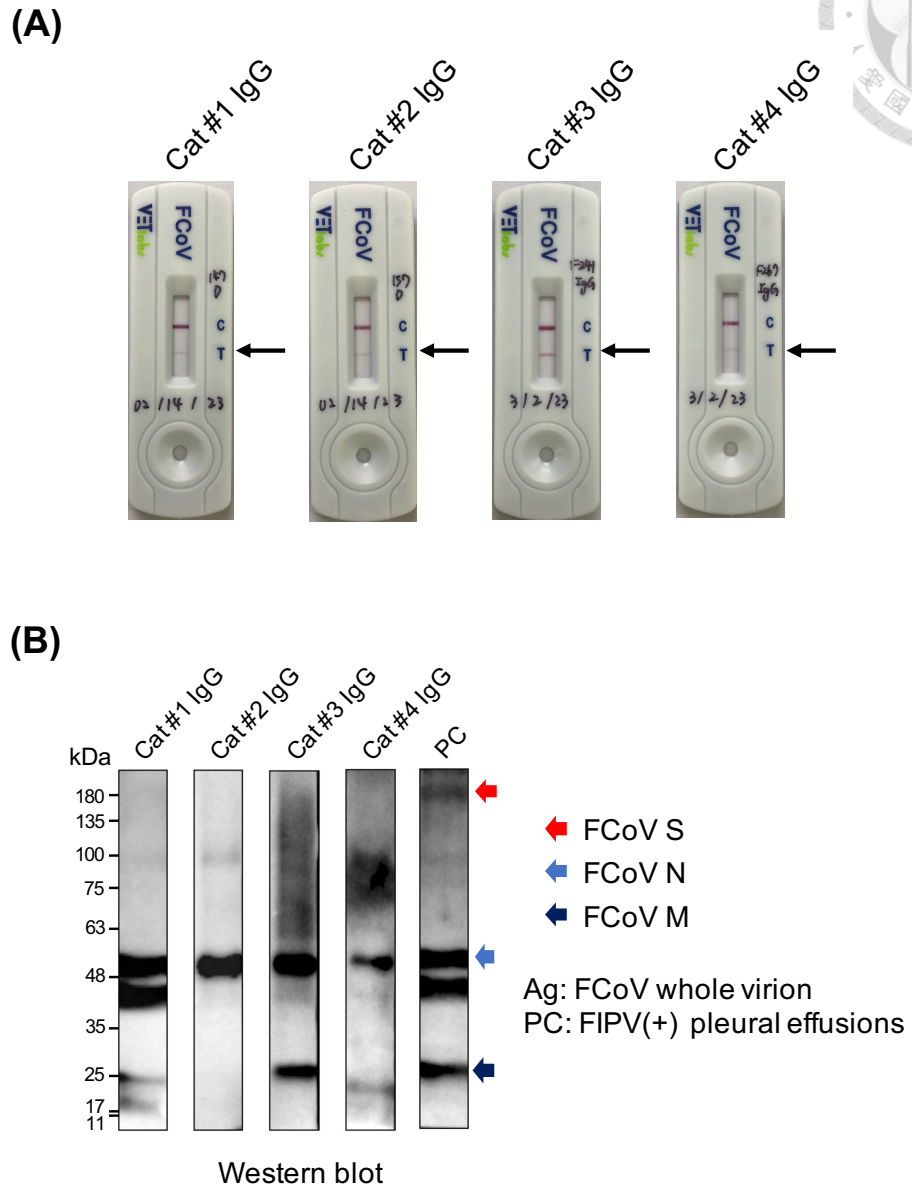

Figure 8. Detection of anti-FCoV IgG and antigenicity test against FCoV.

(A) IgG against FCoV in the IgG samples purified from four FIP-positive effusions was ensured using the FCoV detection kit following the commercial data sheet protocol. (B) The IgG from 4 samples was conducted in the antigenicity test against FCoV. The antigen in this test was FCoV whole virion processed by reducing buffer. The primary antibody

doi:10.6342/NTU202301829

was the purified IgG with a concentration of 1000 ng/ml and incubated at 4°C overnight. The secondary antibody was goat-derived anti-cat IgG labeled with HRP (Bethyl Laboratories) with the dilution in 2000 folds and incubated at RT for 1 hour. Other steps followed the Western blot section of Material and Methods. The red, blue, and dark purple arrows marked the location of the FCoV spike, nucleocapsid, and membrane protein, respectively.

doi:10.6342/NTU202301829

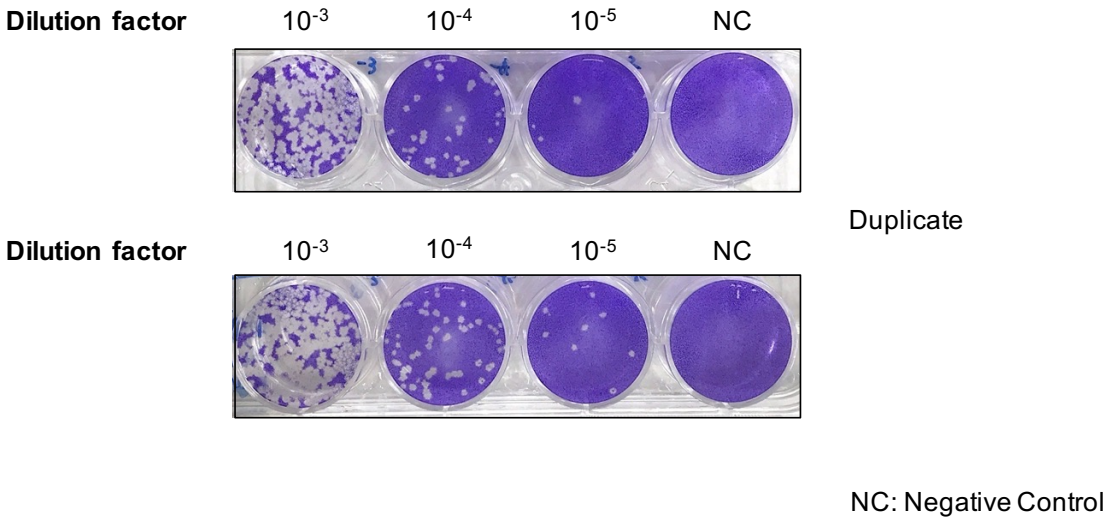

Figure 9. Virus titration using plaque assay.

Virus stock for this study was prepared with the FIPV NTU156 strain (accession number: EU513388). The stock titer was analyzed using plaque assay with three dilution factors and one negative control in duplicate. The final titer was calculated using the formula (Count of plaques × Dilution factor)/[Volume of diluted virus (ml/well)]. The average of the plaque number in two 10^{-4} wells was calculated and had the titer of 8.4×10^5 pfu/ml.

doi:10.6342/NTU202301829

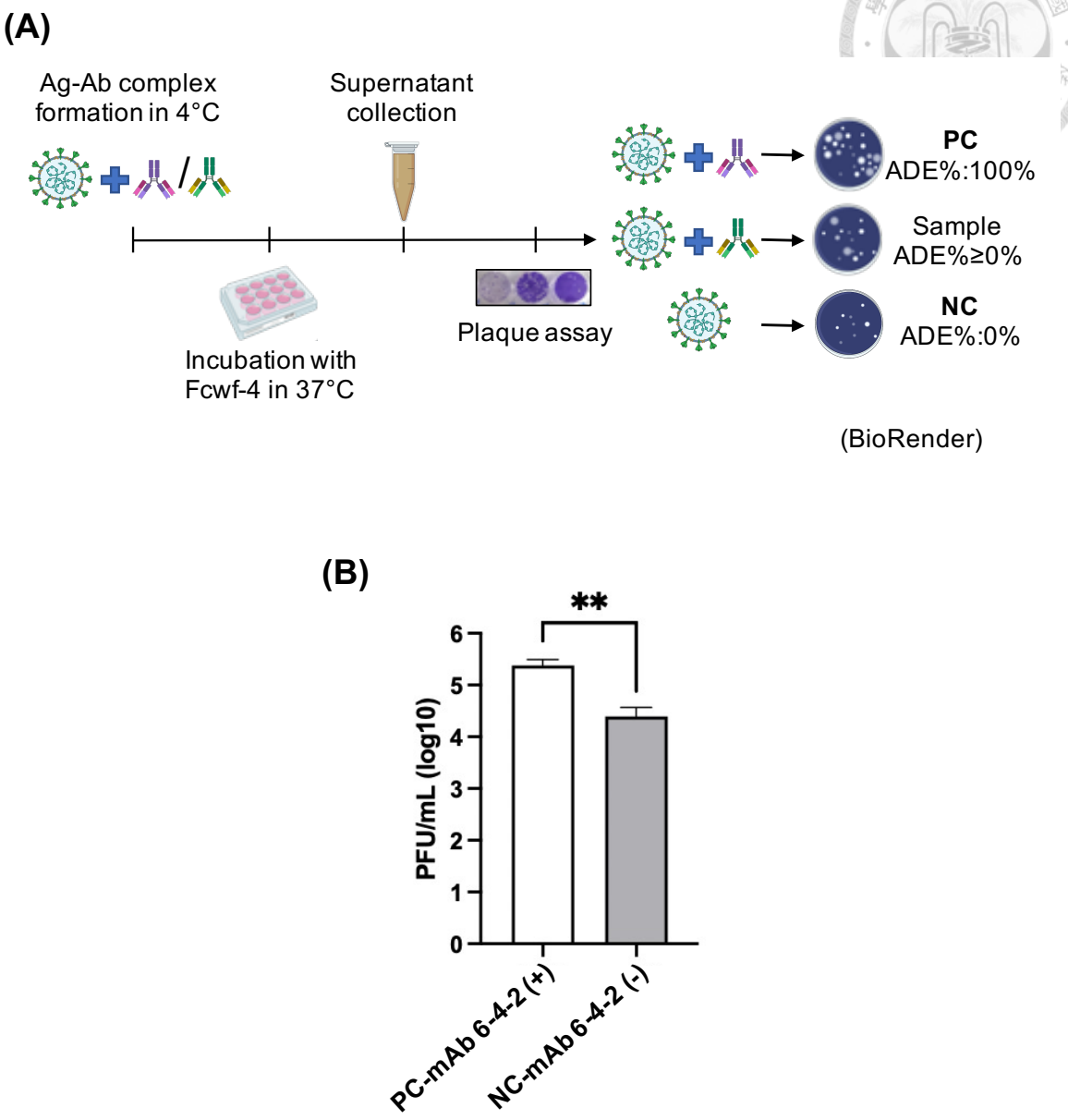

Figure 10. Feline infectious peritonitis virus (FIPV) antibody-dependent enhancement (ADE) *in vitro* phenomenon establishment.

(A) Flow chart of FIPV ADE establishment in Fcwf-4 culture with FIPV NTU156 and mAb 6-4-2 depicted using BioRender (Toronto, Canada). The formula (titer of sample-titer of NC)/(titer of PC-titer of NC)*100% was used for ADE% calculation to standardize

doi:10.6342/NTU202301829

the result value. (B) FIPV ADE establishment triplicate test was performed with FIPV infection (MOI 0.0035) and mAb 6-4-2 (10× diluted), and the viral titer of each test was statistically analyzed using the unpaired t-test (**, $P < 0.01$). Data were shown as the mean ± SD.

doi:10.6342/NTU202301829

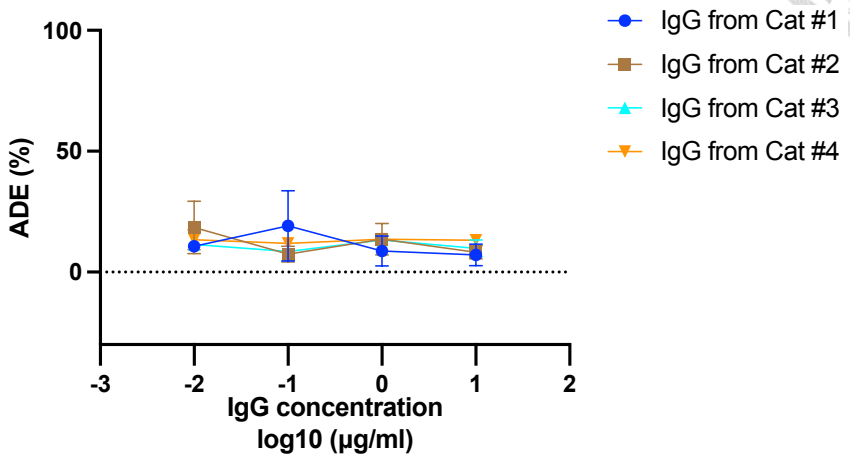

Figure 11. FIPV ADE investigation with purified IgG.

IgG purified from 4 FIP-positive effusion samples was conducted in the FIPV ADE experiment with four different kinds of concentrations, 10, 100, 1000, and 10000 ng/ml, to be mixed with FIPV solution (MOI 0.0035) in a 1:1 ratio. Other steps followed the FIPV ADE assay procedure of Material and Methods. X-axis represented the log10 value of each concentration of the IgG sample (ng/ml). Y-axis represented the FIPV ADE% elicited from each sample. Data were shown as the mean ± SEM with a triplicate test.

doi:10.6342/NTU202301829

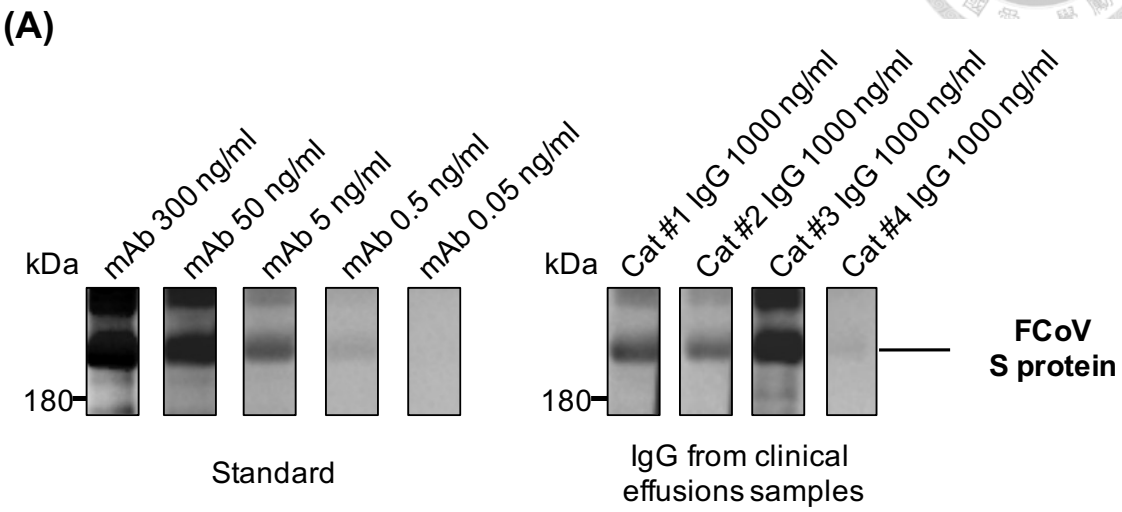

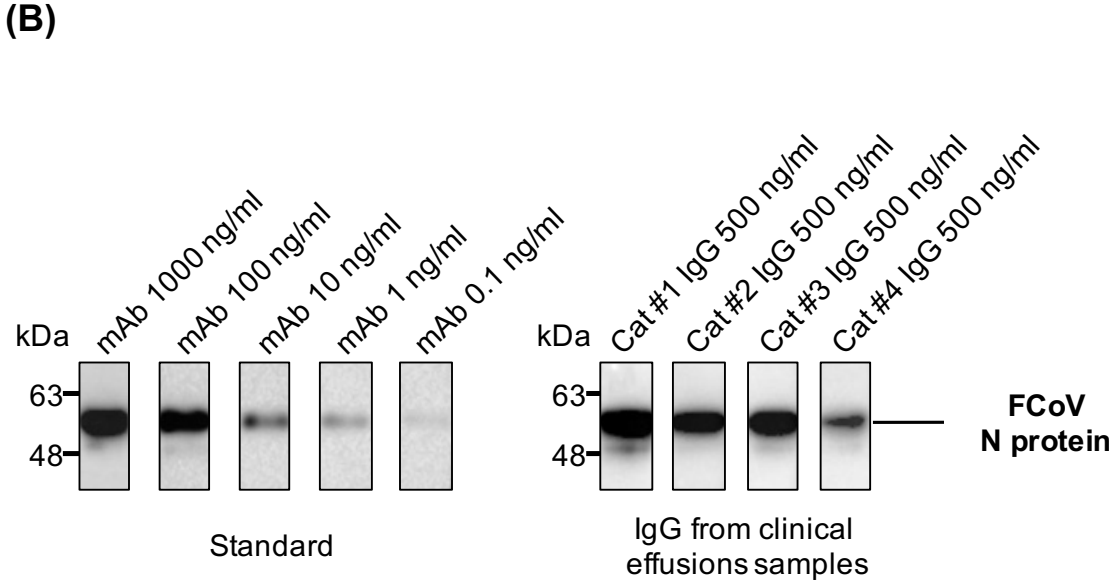

doi:10.6342/NTU202301829

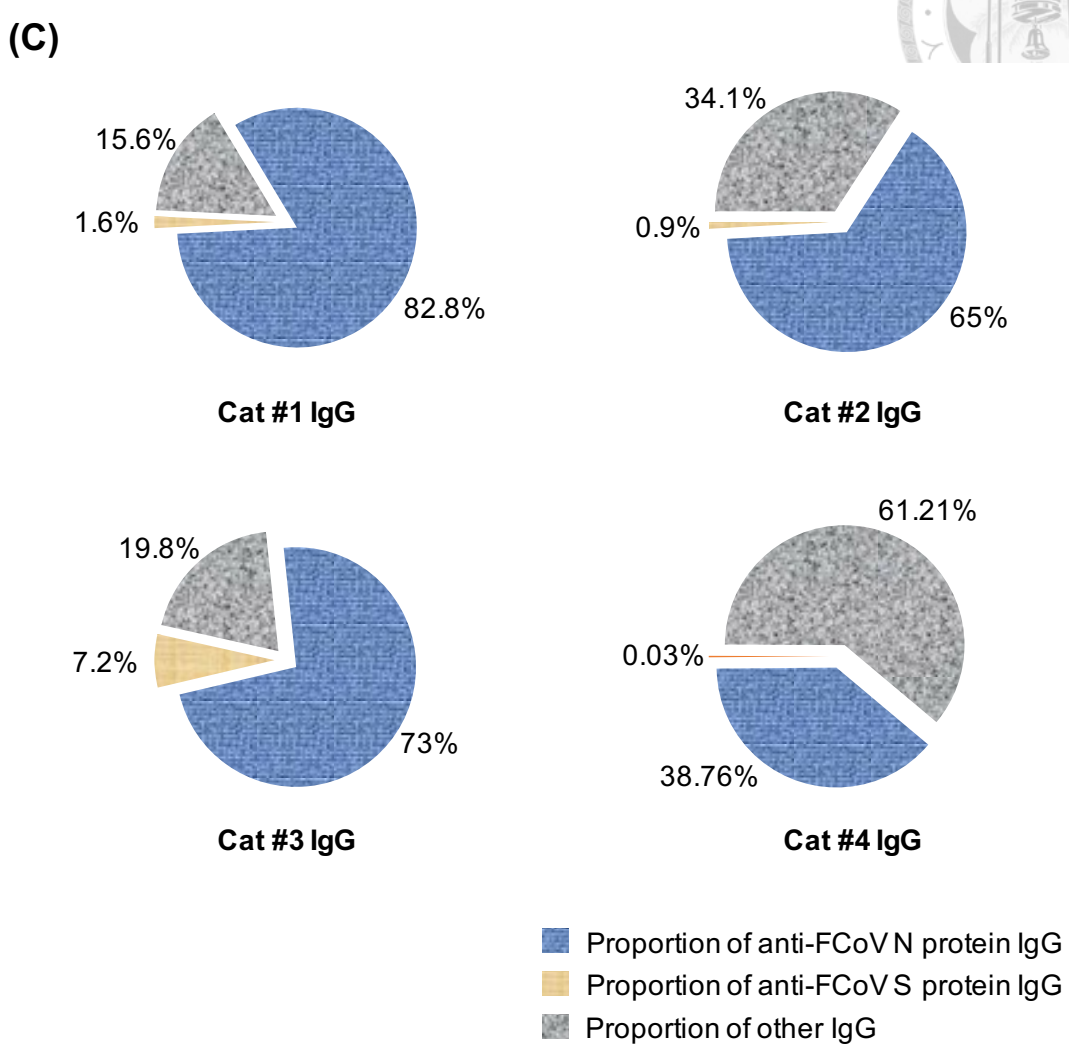

Figure 12. Proportion analysis of anti-FCoV S and N protein IgG in each purified IgG sample.

The antigenicity of IgG from 4 FIP-positive effusions was analyzed using western blot against FCoV (A) S and (B) N protein and (C) calculated for the proportion of different pAb in it. The antigen used for these two tests were (A) HEK 293T cell expressed spike protein (1000 ng/lane) and (B) *E. coli* expressed FCoV N protein (5000 ng/lane) from our

doi:10.6342/NTU202301829

lab. IgG from 4 samples was used as the primary antibody with the concentrations (A) 1000 ng/ml (anti-FCoV S) and (B) 500 ng/ml (anti-FCoV N). The secondary antibody was goat-derived anti-cat IgG labeled with HRP (Bethyl Laboratories) for IgG samples with a 5000-fold dilution (0.4 mg/ml). For the antibodies used in the standard curve, the primary antibody was (A) mouse anti-FCoV S mAb YB4F02 (anti-FCoV S), and (B) mouse anti-FCoV N mAb (Bio-Rad) (anti-FCoV N) with 10-fold serial dilutions. The secondary antibody was goat-derived anti-mouse IgG HRP (Jackson ImmunoResearch) with a 2000-fold dilution. The identity of each lane was used for the actual level calculation. (C) The proportion of anti-FCoV S and N protein IgG in each IgG sample was presented with a pie chart. The green part represented the proportion of anti-FCoV S protein IgG. The blue part represented the proportion of anti-FCoV N protein IgG. The gray part represented the proportion of other kinds of IgG in the samples.

doi:10.6342/NTU202301829

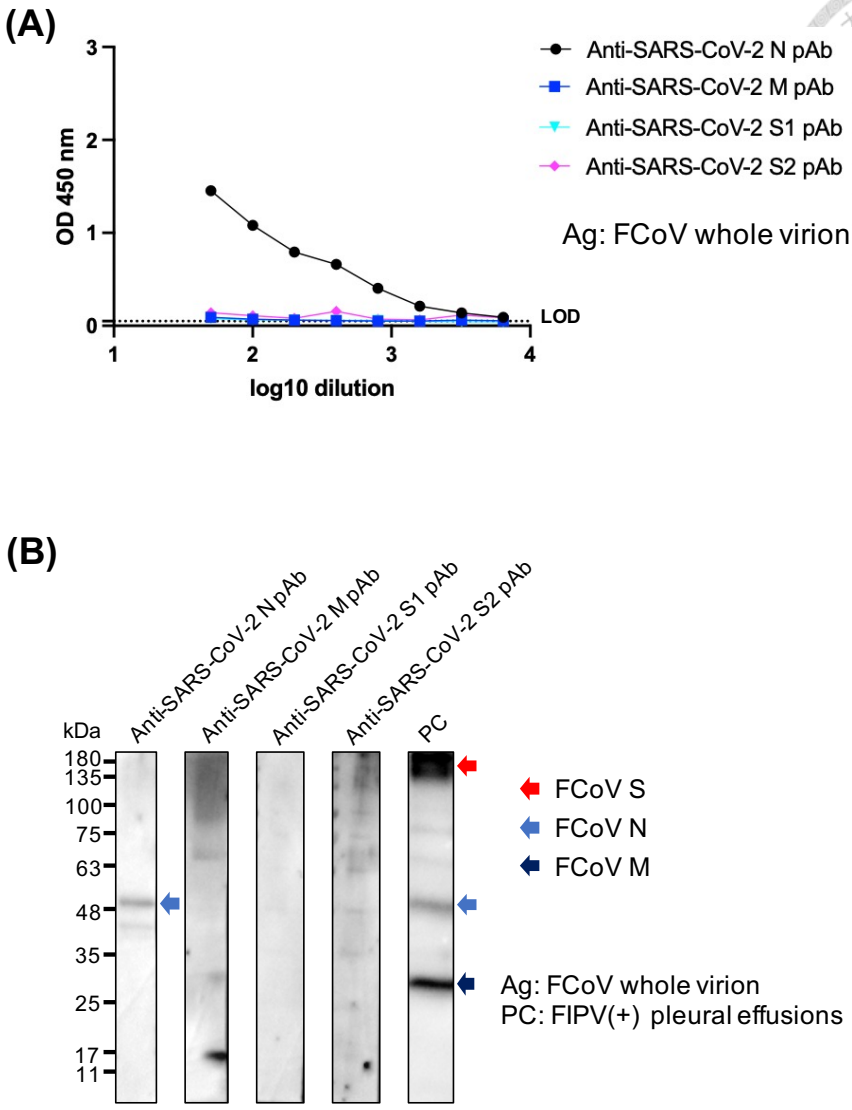

Figure 13. Investigation of the cross-reactivity between FCoV and SARS-CoV-2 using FCoV whole virion and rabbit-derived anti-SARS-CoV-2 N, M, S1, S2 protein polyclonal antibodies.

(A) ELISA was conducted with FIPV NTU156 strain whole virion and rabbit-derived anti-SARS-CoV-2 spike subunit-S1 and S2, N (Sino Biological), and M protein (ProSci) pAb. The primary antibody needed to be 50-fold diluted at first, then two-fold serial dilution was continued seven times to reveal the capability to bind to FCoV. The

doi:10.6342/NTU202301829

secondary antibody was goat anti-rabbit IgG HRP (Jackson ImmunoResearch) with a 2000-fold dilution. X-axis represented the log10 dilution factor of the antibodies. Y-axis represented the OD450 value detected from the HRP substrate reaction. (B) The anti-SARS-CoV-2 spike subunit S1 and S2, N (Sino Biological), and M protein (ProSci) pAb were conducted in the antigenicity test against FCoV using western blot. The antigen in this test was FCoV whole virion processed by reducing buffer. The primary antibody was the four kinds of pAb with a 1000-fold dilution and incubated at 4°C overnight. The secondary antibody was goat anti-rabbit IgG HRP (Jackson ImmunoResearch) with a 2000-fold dilution. Other steps followed the Western blot section of Material and Methods. The red, blue, and dark purple arrows marked the location of the FCoV spike, nucleocapsid, and membrane protein, respectively.

doi:10.6342/NTU202301829

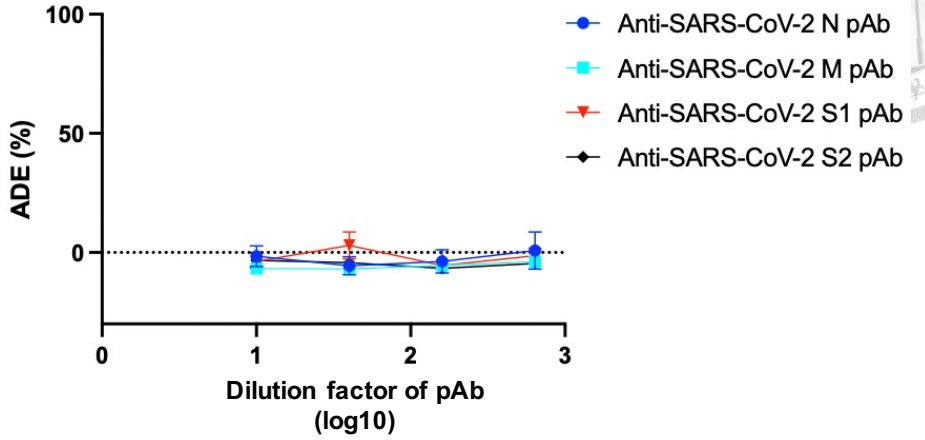

Figure 14. Investigation of the potential capability of antibodies against SARS-CoV-2 to enhance FIPV infection using anti-SARS-CoV-2 N, M, S1, S2 protein polyclonal antibodies in the FIPV ADE model.

Anti-SARS-CoV-2 spike subunit-S1 and S2, N (Sino Biological), and M protein (ProSci) pAb were conducted in the FIPV ADE test with four different dilution factors, 10-fold, 40-fold, 160-fold, and 640-fold to be mixed with FIPV solution (MOI 0.0035) in 1:1 ratio. Other steps followed the FIPV ADE assay section of Material and Methods. X-axis represented the log10 dilution factor value of each concentration of the pAb sample. Y-axis represented the FIPV ADE% elicited from each kind of pAb. Data were shown as the mean ± SD with a triplicate test.

doi:10.6342/NTU202301829

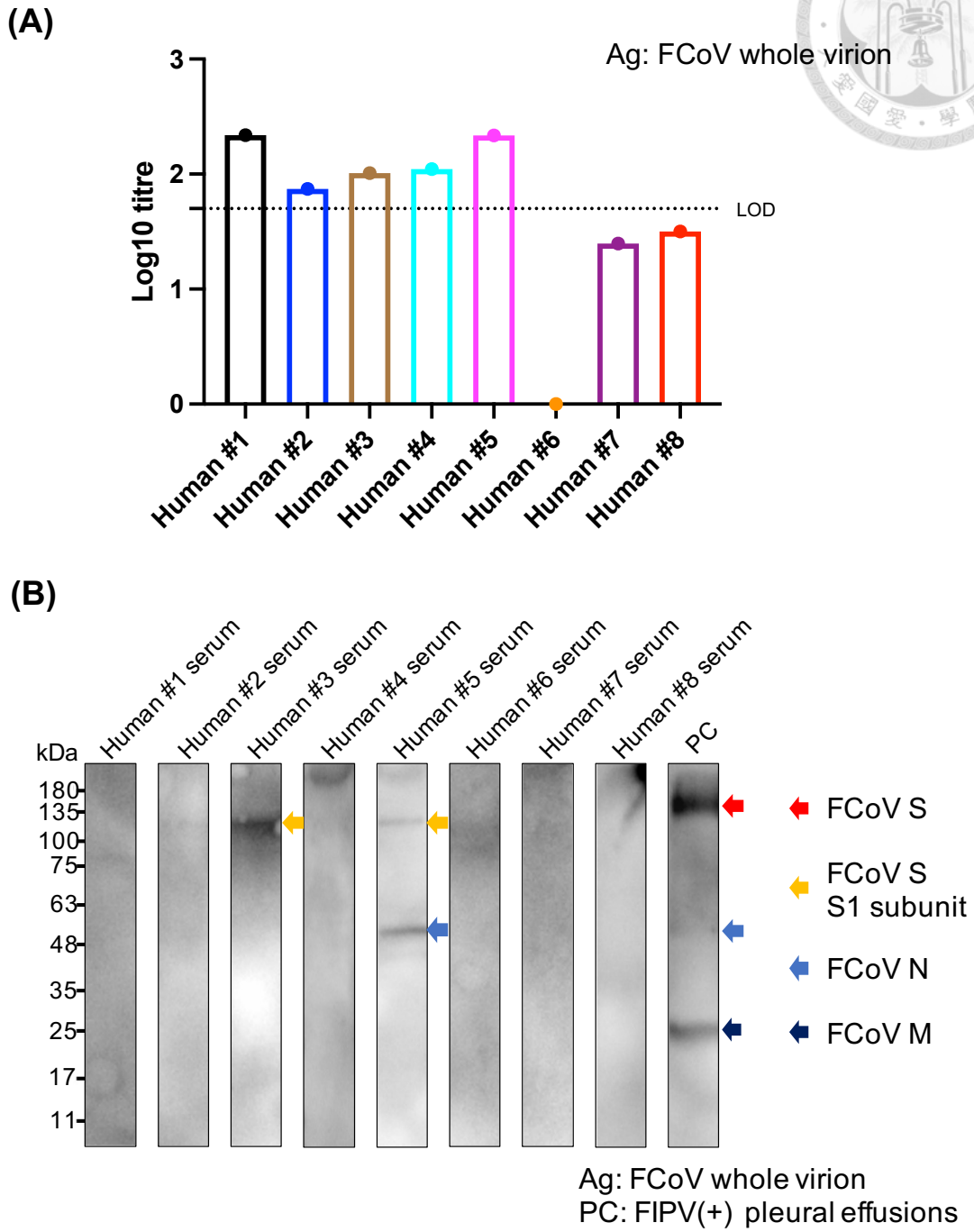

Figure 15. Investigation of the cross-reactivity between FCoV and SARS-CoV-2 using FCoV whole virion and human COVID-19 convalescent serum.

doi:10.6342/NTU202301829

(A) ELISA was conducted with FCoV whole virion and eight different COVID-19 human convalescent serum samples kindly provided by National Taiwan University Hospital. The primary antibody needed to be 50-fold diluted at first, then two-fold serial dilution was continued seven times to reveal the capability to bind to FCoV. The secondary antibody was goat anti-human IgG HRP (Jackson ImmunoResearch) with a 2000-fold dilution. Next, the data of each sample were analyzed using nonlinear regression with the sigmoidal dose-response model and a cut-off value of 0.5 to standardize the actual titer of each serum sample to be against FCoV. X-axis represented the log10 dilution factor of the antibodies. Y-axis represented the log10 titer of each serum sample against FCoV. (B) Eight human COVID-19 convalescent serum samples were conducted in the antigenicity test against FCoV. The antigen in this test was FCoV whole virion processed by reducing buffer. The primary antibody was the eight human COVID-19 convalescent serum samples with a 1000-fold dilution and incubated at 4°C overnight. The secondary antibody was goat anti-human IgG HRP (Jackson ImmunoResearch) with a 2000-fold dilution. Other steps followed the Western blot section of Material and Methods. The red, green, blue, and dark purple arrows marked the location of the FCoV spike, spike S1 subunit, nucleocapsid, and membrane protein, respectively.

doi:10.6342/NTU202301829

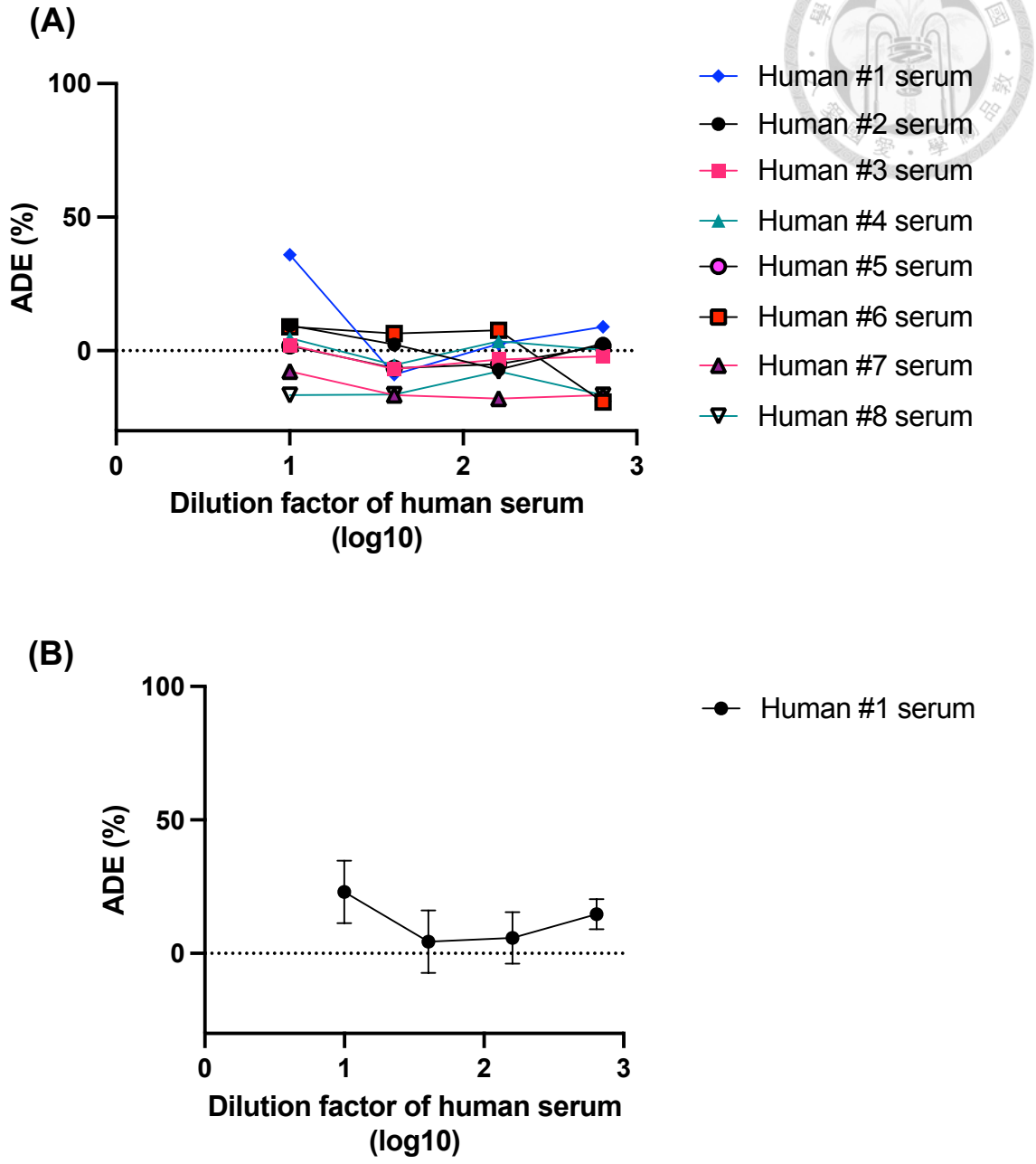

Figure 16. FIPV ADE investigation with human COVID-19 convalescent serum.

(A) Eight different inactivated human COVID-19 convalescent serum samples were conducted in the FIPV ADE test with four different dilution factors, 10-fold, 40-fold, 160-fold, and 640-fold to be mixed with FIPV solution (MOI 0.0035) in 1:1 ratio. Other steps followed the FIPV ADE assay section of Material and Methods. X-axis represented the

doi:10.6342/NTU202301829

log10 dilution factor value of each concentration of each human serum sample. Y-axis represented the FIPV ADE% elicited from each human serum sample. (B) The human #1 serum sample was conducted in the triplicate FIPV ADE test to ensure the FIPV ADE phenomenon elicited by the sample. The serum sample must also be diluted in four dilution factors, 10-fold, 40-fold, 160-fold, and 640-fold, to be mixed with FIPV solution (MOI 0.0035) in a 1:1 ratio. Other steps followed the FIPV ADE assay section of Material and Methods. X-axis represented the log10 dilution factor value of each concentration of the human #1 serum sample. Y-axis represented the FIPV ADE% elicited from the human #1 serum sample. Data were shown as the mean ± SD.

doi:10.6342/NTU202301829

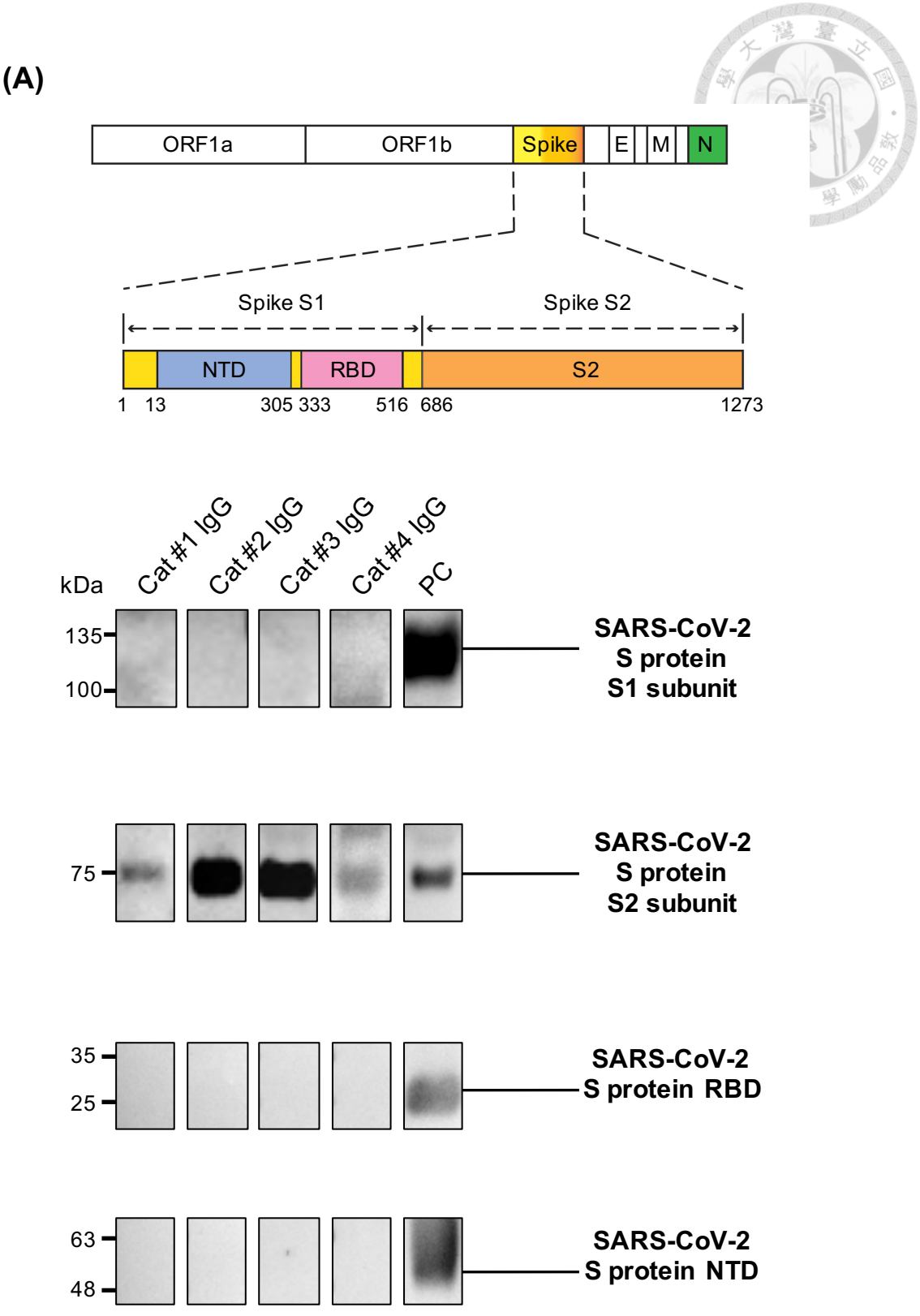

PC (S1, S2): Human COVID-19 convalescent serum
PC (RBD, NTD): rabbit-derived anti-SARS-CoV-2 spike S1 pAb

doi:10.6342/NTU202301829

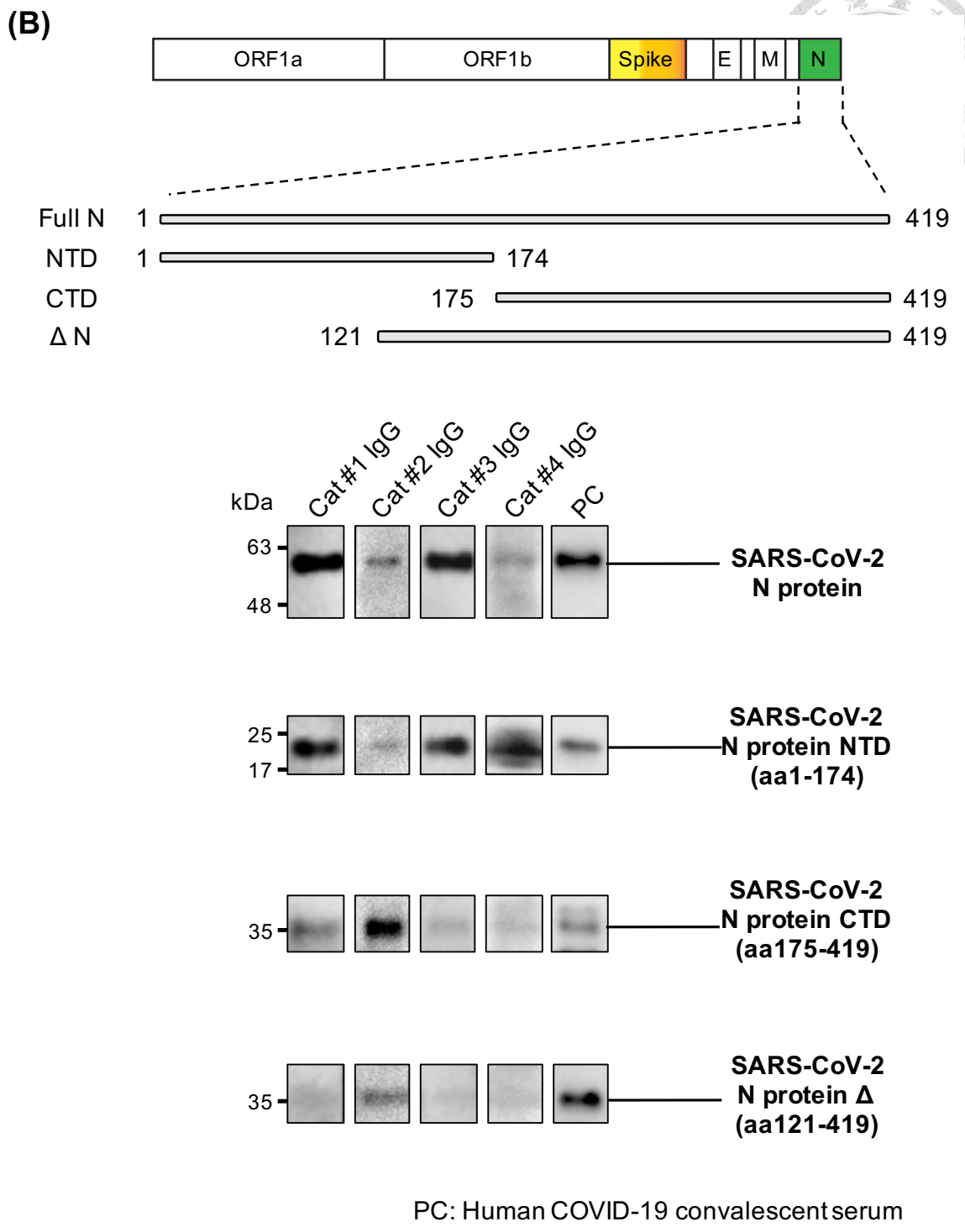

Figure 17. Investigation of the cross-reactivity between FCoV and SARS-CoV-2 using IgG purified from FIP cat's effusions and SARS-CoV-2 structural proteins.

doi:10.6342/NTU202301829

IgG from 4 FIP-positive effusion samples and SARS-CoV-2 proteins (non-reducing condition), including S1, S2 subunit (Sino biological), purified RBD, NTD of spike protein, purified complete N protein, and three fragments of N protein, were conducted to examine for the cross-reactivity between FIPV and SARS-CoV-2 using western blot. The concentration of IgG used for each test as primary antibody was 1000 ng/ml, and human COVID-19 convalescent serum, rabbit-derived anti-SARS-CoV-2 spike S1 pAb for PC was diluted in 1000-folds. The secondary antibody, goat-derived anti-cat IgG labeled with HRP (Bethyl Laboratories), was diluted in 2000-folds, so as the goat anti-human IgG labeled with HRP (Jackson ImmunoResearch) and goat-derived anti-rabbit IgG labeled with HRP (Jackson ImmunoResearch) for PC also as the secondary antibody. Other procedures of western blot followed the steps mentioned before. (A) The result from the cross-reactivity test between IgG against FIPV and fragments of SARS-CoV-2 spike protein. (B) The result from the cross-reactivity test between feline IgG and SARS-CoV-2 truncated nucleocapsid protein.

doi:10.6342/NTU202301829

Table 1. Primers used in this study.

Use	Step	Name	Sequence (5' to 3')	Sense	Result	Target site
FIPV detection	1st	P211	CACTAGATCCAGACGTTAGCTC	-	233 bp	FCoV 3'-UTR
		P205	GGCAACCCGATGTTTAAAACTGG	+		
	2nd	P204	GCTCTTCCATTGTTGGCTCGTC	-	177 bp	
		P276	CCGAGGAATTACTGGTCATCGCG	+		
FCoV genotyping (I)	1st	Iubs	CCACACATACCAAGGCC	-	376 bp	FCoV Spike S2
		Iffs	GTTTCAACCTAGAAAGCCTCAGAT	+		
	2nd	nIubs	CCAAGGCCATTTTACATA	-	360 bp	
		nIffles	CCTAGAAAGCCTCAGATGAGTG	+		
FCoV genotyping (II)	1st	Iubs	CCACACATACCAAGGCC	-	283 bp	
		Icfs	GCCTAGTATTATACCTGACTA	+		
	2nd	nIubs	CCAAGGCCATTTTACATA	-	218 bp	
		nIcfs	CAGACCAAACTGGACTGTAC	+		

doi:10.6342/NTU202301829

Table 2. Sequences examined in the FCoV phylogenetic analysis.

Virus strain	FCoV genotype	Host	Accession number	Location
NTUCL84	I	Feline	OR141609	Taiwan
NTUCL85	I	Feline	OR141610	Taiwan
NTUCL86	I	Feline	OR141611	Taiwan
NTUCL87	I	Feline	OR141612	Taiwan
NTUCL88	I	Feline	OR141613	Taiwan
NTUCL89	I	Feline	OR141614	Taiwan
NTUCL90	I	Feline	OR141615	Taiwan
NTUCL91	I	Feline	OR141616	Taiwan
NTUCL92	I	Feline	OR141617	Taiwan
NTUCL93	I	Feline	OR141618	Taiwan
NTUCL94	I	Feline	OR141619	Taiwan
NTUCL95	I	Feline	OR141620	Taiwan
NTUCL96	I	Feline	OR141621	Taiwan
NTUCL97	I	Feline	OR141622	Taiwan
NTUCL98	I	Feline	OR141623	Taiwan
NTUCL99	I	Feline	OR141624	Taiwan
NTUCL100	I	Feline	OR141625	Taiwan
NTUCL101	I	Feline	OR141626	Taiwan
NTUCL102	I	Feline	OR141627	Taiwan
NTUCL103	I	Feline	OR141628	Taiwan
NTUCL104	I	Feline	OR141629	Taiwan
NTUCL105	I	Feline	OR141630	Taiwan
NTUCL106	I	Feline	OR141631	Taiwan
NTUCL107	I	Feline	OR141632	Taiwan
NTUCL108	I	Feline	OR141633	Taiwan
NTUCL109	I	Feline	OR141634	Taiwan

doi:10.6342/NTU202301829

Virus strain	FCoV genotype	Host	Accession number	Location
NTUCL110	I	Feline	OR141635	Taiwan
NTUCL111	I	Feline	OR141636	Taiwan
NTUCL112	I	Feline	OR141637	Taiwan
NTUCL113	I	Feline	OR141638	Taiwan
NTUCL114	I	Feline	OR141639	Taiwan
NTUCL115	I	Feline	OR141640	Taiwan
NTUCL116	I	Feline	OR141641	Taiwan
NTUCL117	I	Feline	OR141642	Taiwan
NTUCL118	I	Feline	OR141643	Taiwan
NTUCL119	I	Feline	OR141644	Taiwan
NTUCL120	II	Feline	OR141645	Taiwan
NTUCL13	I	Feline	MK736789	Taiwan
NTUCL17	I	Feline	MK736792	Taiwan
NTUCL34	I	Feline	MK736801	Taiwan
NTUCL43	I	Feline	MW648553	Taiwan
NTUCL44	I	Feline	MW648554	Taiwan
NTUCL45	I	Feline	MW648555	Taiwan
NTUCL46	I	Feline	MW648556	Taiwan
NTUCL47	I	Feline	MW648557	Taiwan
NTUCL48	I	Feline	MW648558	Taiwan
NTUCL49	I	Feline	MW648559	Taiwan
NTUCL50	I	Feline	MW648560	Taiwan
NTUCL51	I	Feline	MW648561	Taiwan
NTUCL52	I	Feline	MW648562	Taiwan
NTUCL53	I	Feline	MW648563	Taiwan

doi:10.6342/NTU202301829

Virus strain	FCoV genotype	Host	Accession number	Location
08K-958	I	Feline	JN654404	Korea
80F	I	Feline	KP143511	United Kingdom
38LVIPortugal_05B	I	Feline	EU327731	Portugal
HLJDQ201708	I	Feline	MG892408	China
UU5	I	Feline	FJ938056	USA
FECV19	I	Feline	KJ665866	Germany
NTUCL20	II	Feline	MK736807	Taiwan
NTUCL30	II	Feline	MK736808	Taiwan
NTUCL37	II	Feline	MK736809	Taiwan
NTUCL39	II	Feline	MK736810	Taiwan
NTUCL75	II	Feline	MW656200	Taiwan
NTUCL76	II	Feline	MW656201	Taiwan
NTUCL81	II	Feline	MW656206	Taiwan
NTUCL82	II	Feline	MW656207	Taiwan
NTUCL83	II	Feline	MW656208	Taiwan
FCoV NTU156 P 2007 Taiwan	II	Feline	EU513388	Taiwan
FCoV NTU205 C 2007 Taiwan	II	Feline	EU513389	Taiwan
WSU 79-1683	II	Feline	JN634064	USA
DF-2	II	Feline	JQ408981	Hungary
08K-609	II	Feline	JN654412	Korea
08K-656	II	Feline	JN654413	Korea
79-1146	II	Feline	DQ010921	United Kingdom
M91-267	II	Feline	AB781788	Japan

doi:10.6342/NTU202301829

Virus strain	FCoV genotype	Host	Accession number	Location
CCoV HCM47 2015	-	Canine	LC190907	Japan
CCoV B906 ZJ 2019	-	Canine	MT114554	Korea
TGEV FS-WS	-	Swine	MK272773	China
CFBCoV DM95 2003	-	Chinese ferret badger	EF192156	China
Racoon dog CoV GZ43 2003	-	Racoon dog	EF192155	HK

Sequences of NTUCL84 to NTUCL120 were obtained in this study.

doi:10.6342/NTU202301829

Table 3. Case signalments data statistical analysis.

IFA and PCR	Gender		Breed		Age (y/o)		Blood A/G ratio*	
	M	**F**	**Pure breed**	**Mixed breed**	**≤ 2**	**> 2**	**≤ 0.4**	**> 0.4**
Positive (n=46)	33	13	14	32	31	15	26	20
Negative (n=92)	56	36	31	61	44	48	26	64
Total	89	49	45	93	75	63	52	84
Positive rate	37.1%	26.5%	31.1%	34.4%	41.3%	23.8%	50%	23.8%

* 2 missing values from FIP-negative cases

doi:10.6342/NTU202301829

Chapter 6 References

陳耀云, 2022. 四種不同型別冠狀病毒核殼蛋白的交叉抗原性探討. 國立臺灣大學, 台北市.

Addie, D., Belák, S., Boucraut-Baralon, C., Egberink, H., Frymus, T., Gruffydd-Jones, T., Hartmann, K., Hosie, M.J., Lloret, A., Lutz, H., Marsilio, F., Pennisi, M.G., Radford, A.D., Thiry, E., Truyen, U., Horzinek, M.C., 2009. Feline infectious peritonitis. ABCD guidelines on prevention and management. J Feline Med Surg 11, 594-604.

Addie, D.D., Covell-Ritchie, J., Jarrett, O., Fosbery, M., 2020. Rapid Resolution of Non-Effusive Feline Infectious Peritonitis Uveitis with an Oral Adenosine Nucleoside Analogue and Feline Interferon Omega. Viruses 12.

Addie, D.D., le Poder, S., Burr, P., Decaro, N., Graham, E., Hofmann-Lehmann, R., Jarrett, O., McDonald, M., Meli, M.L., 2015. Utility of feline coronavirus antibody tests. J Feline Med Surg 17, 152-162.

Addie, D.D., Paltrinieri, S., Pedersen, N.C., 2004. Recommendations from workshops of the second international feline coronavirus/feline infectious peritonitis symposium. J Feline Med Surg 6, 125-130.

Addie, D.D., Schaap, I.A.T., Nicolson, L., Jarrett, O., 2003. Persistence and transmission of natural type I feline coronavirus infection. J Gen Virol 84, 2735-2744.

Adil, M.T., Rahman, R., Whitelaw, D., Jain, V., Al-Taan, O., Rashid, F., Munasinghe, A., Jambulingam, P., 2021. SARS-CoV-2 and the pandemic of COVID-19. Postgrad Med J 97, 110-116.

Amer, A., Siti Suri, A., Abdul Rahman, O., Mohd, H.B., Faruku, B., Saeed, S., Tengku Azmi, T.I., 2012. Isolation and molecular characterization of type I and type II feline coronavirus in Malaysia. Virol J 9, 278.

Bank-Wolf, B.R., Stallkamp, I., Wiese, S., Moritz, A., Tekes, G., Thiel, H.J., 2014. Mutations of 3c and spike protein genes correlate with the occurrence of feline infectious peritonitis. Vet Microbiol 173, 177-188.

Bárcena, M., Oostergetel, G.T., Bartelink, W., Faas, F.G., Verkleij, A., Rottier, P.J., Koster, A.J., Bosch, B.J., 2009. Cryo-electron tomography of mouse hepatitis virus: Insights into the structure of the coronavirion. Proc Natl Acad Sci U S A 106, 582-587.

Benetka, V., Kübber-Heiss, A., Kolodziejek, J., Nowotny, N., Hofmann-Parisot, M., Möstl, K., 2004. Prevalence of feline coronavirus types I and II in cats with histopathologically verified feline infectious peritonitis. Vet Microbiol 99, 31-42.

Berti-Bock, G., Vial, F., Premuda, L., Rullière, R., 1979. [Exudates, transudates and the Rivalta reaction (1895). Current status and historical premises]. Minerva Med 70,

doi:10.6342/NTU202301829

3573-3580.

Bessière, P., Vergne, T., Battini, M., Brun, J., Averso, J., Joly, E., Guérin, J.L., Cadiergues, M.C., 2022. SARS-CoV-2 Infection in Companion Animals: Prospective Serological Survey and Risk Factor Analysis in France. Viruses 14.

Cham, T.C., Chang, Y.C., Tsai, P.S., Wu, C.H., Chen, H.W., Jeng, C.R., Pang, V.F., Chang, H.W., 2017. Determination of the cell tropism of serotype 1 feline infectious peritonitis virus using the spike affinity histochemistry in paraffin-embedded tissues. Microbiol Immunol 61, 318-327.

Chang, H.W., Egberink, H.F., Rottier, P.J., 2011. Sequence analysis of feline coronaviruses and the circulating virulent/avirulent theory. Emerg Infect Dis 17, 744-746.

Ciliberti, M.G., Albenzio, M., De Palo, P., Santillo, A., Caroprese, M., 2020. Nexus Between Immune Responses and Oxidative Stress: The Role of Dietary Hydrolyzed Lignin in ex vivo Bovine Peripheral Blood Mononuclear Cell Response. Front Vet Sci 7, 9.

Cornelissen, E., Dewerchin, H.L., Van Hamme, E., Nauwynck, H.J., 2009. Absence of antibody-dependent, complement-mediated lysis of feline infectious peritonitis virus-infected cells. Virus Res 144, 285-289.

De Groot, R.J., Andeweg, A.C., Horzinek, M.C., Spaan, W.J., 1988. Sequence analysis of the 3'-end of the feline coronavirus FIPV 79-1146 genome: comparison with the genome of porcine coronavirus TGEV reveals large insertions. Virology 167, 370-376.

de Haan, C.A., Haijema, B.J., Schellen, P., Wichgers Schreur, P., te Lintelo, E., Vennema, H., Rottier, P.J., 2008. Cleavage of group 1 coronavirus spike proteins: how furin cleavage is traded off against heparan sulfate binding upon cell culture adaptation. J Virol 82, 6078-6083.

Decaro, N., Mari, V., Lanave, G., Lorusso, E., Lucente, M.S., Desario, C., Colaianni, M.L., Elia, G., Ferringo, F., Alfano, F., Buonavoglia, C., 2021. Mutation analysis of the spike protein in Italian feline infectious peritonitis virus and feline enteric coronavirus sequences. Res Vet Sci 135, 15-19.

Desmarets, L.M., Vermeulen, B.L., Theuns, S., Conceição-Neto, N., Zeller, M., Roukaerts, I.D., Acar, D.D., Olyslaegers, D.A., Van Ranst, M., Matthijnssens, J., Nauwynck, H.J., 2016. Experimental feline enteric coronavirus infection reveals an aberrant infection pattern and shedding of mutants with impaired infectivity in enterocyte cultures. Sci Rep 6, 20022.

Dileepan, M., Di, D., Huang, Q., Ahmed, S., Heinrich, D., Ly, H., Liang, Y., 2021. Seroprevalence of SARS-CoV-2 (COVID-19) exposure in pet cats and dogs in Minnesota, USA. Virulence 12, 1597-1609.

doi:10.6342/NTU202301829

Doenges, S.J., Weber, K., Dorsch, R., Fux, R., Hartmann, K., 2017. Comparison of real-time reverse transcriptase polymerase chain reaction of peripheral blood mononuclear cells, serum and cell-free body cavity effusion for the diagnosis of feline infectious peritonitis. J Feline Med Surg 19, 344-350.

Dye, C., Siddell, S.G., 2005. Genomic RNA sequence of Feline coronavirus strain FIPV WSU-79/1146. J Gen Virol 86, 2249-2253.

El-Tholoth, M., Hussein, M., Mohammed, D., Al-Rasheedi, M., Al-Qubaisi, H., Al-Blooshi, A., Al-Ahbabi, M., Al-Dhaheri, Z., Al-Blooshi, K., Al-Herbawi, M., Abo Elfadl, E.A., Seboussi, R., 2023. Serological Investigation on the Presence of Feline Coronavirus (FCoV) and Severe Acute Respiratory Syndrome Coronavirus 2 (SARS-CoV-2) in Domestic Cats Living with COVID-19 Positive Owners in the UAE, 2022. Animals (Basel) 13.

Fehr, A.R., Perlman, S., 2015. Coronaviruses: an overview of their replication and pathogenesis. Methods Mol Biol 1282, 1-23.

Felten, S., Hartmann, K., 2019. Diagnosis of Feline Infectious Peritonitis: A Review of the Current Literature. Viruses 11.

Felten, S., Matiasek, K., Gruendl, S., Sangl, L., Wess, G., Hartmann, K., 2017. Investigation into the utility of an immunocytochemical assay in body cavity effusions for diagnosis of feline infectious peritonitis. J Feline Med Surg 19, 410-418.

Fischer, Y., Sauter-Louis, C., Hartmann, K., 2012. Diagnostic accuracy of the Rivalta test for feline infectious peritonitis. Vet Clin Pathol 41, 558-567.

Foley, J.E., Poland, A., Carlson, J., Pedersen, N.C., 1997. Risk factors for feline infectious peritonitis among cats in multiple-cat environments with endemic feline enteric coronavirus. J Am Vet Med Assoc 210, 1313-1318.

Foley, J.E., Rand, C., Leutenegger, C., 2003. Inflammation and changes in cytokine levels in neurological feline infectious peritonitis. J Feline Med Surg 5, 313-322.

Gao, Y.Y., Liang, X.Y., Wang, Q., Zhang, S., Zhao, H., Wang, K., Hu, G.X., Liu, W.J., Gao, F.S., 2022. Mind the feline coronavirus: Comparison with SARS-CoV-2. Gene 825, 146443.

Gao, Y.Y., Wang, Q., Liang, X.Y., Zhang, S., Bao, D., Zhao, H., Li, S.B., Wang, K., Hu, G.X., Gao, F.S., 2023. An updated review of feline coronavirus: mind the two biotypes. Virus Res 326, 199059.

Giordano, A., Stranieri, A., Rossi, G., Paltrinieri, S., 2015. High diagnostic accuracy of the Sysmex XT-2000iV delta total nucleated cells on effusions for feline infectious peritonitis. Vet Clin Pathol 44, 295-302.

Giori, L., Giordano, A., Giudice, C., Grieco, V., Paltrinieri, S., 2011. Performances of different diagnostic tests for feline infectious peritonitis in challenging clinical

doi:10.6342/NTU202301829

cases. J Small Anim Pract 52, 152-157.

Haijema, B.J., Rottier, P., de Groot, R.J., 2007. Feline coronaviruses: a tale of two-faced types. Coronaviruses: molecular and cellular biology. Caister Academic Press, Norfolk, United Kingdom, 183-203.

Haijema, B.J., Volders, H., Rottier, P.J., 2004. Live, attenuated coronavirus vaccines through the directed deletion of group-specific genes provide protection against feline infectious peritonitis. J Virol 78, 3863-3871.

Halstead, S.B., 1988. Pathogenesis of dengue: challenges to molecular biology. Science 239, 476-481.

Halstead, S.B., O'Rourke, E.J., 1977. Dengue viruses and mononuclear phagocytes. I. Infection enhancement by non-neutralizing antibody. J Exp Med 146, 201-217.

Hayashi, T., Goto, N., Takahashi, R., Fujiwara, K., 1977. Systemic vascular lesions in feline infectious peritonitis. Nihon Juigaku Zasshi 39, 365-377.

Hazuchova, K., Held, S., Neiger, R., 2017. Usefulness of acute phase proteins in differentiating between feline infectious peritonitis and other diseases in cats with body cavity effusions. J Feline Med Surg 19, 809-816.

Herrewegh, A.A., de Groot, R.J., Cepica, A., Egberink, H.F., Horzinek, M.C., Rottier, P.J., 1995. Detection of feline coronavirus RNA in feces, tissues, and body fluids of naturally infected cats by reverse transcriptase PCR. J Clin Microbiol 33, 684-689.

Herrewegh, A.A., Mähler, M., Hedrich, H.J., Haagmans, B.L., Egberink, H.F., Horzinek, M.C., Rottier, P.J., de Groot, R.J., 1997. Persistence and evolution of feline coronavirus in a closed cat-breeding colony. Virology 234, 349-363.

Herrewegh, A.A., Smeenk, I., Horzinek, M.C., Rottier, P.J., de Groot, R.J., 1998. Feline coronavirus type II strains 79-1683 and 79-1146 originate from a double recombination between feline coronavirus type I and canine coronavirus. J Virol 72, 4508-4514.

Hirschberger, J., Hartmann, K., Wilhelm, N., Frost, J., Lutz, H., Kraft, W., 1995. [Clinical symptoms and diagnosis of feline infectious peritonitis]. Tierarztl Prax 23, 92-99.

Hofmann-Lehmann, R., Fehr, D., Grob, M., Elgizoli, M., Packer, C., Martenson, J.S., O'Brien, S.J., Lutz, H., 1996. Prevalence of antibodies to feline parvovirus, calicivirus, herpesvirus, coronavirus, and immunodeficiency virus and of feline leukemia virus antigen and the interrelationship of these viral infections in free-ranging lions in east Africa. Clin Diagn Lab Immunol 3, 554-562.

Hohdatsu, T., Nakamura, M., Ishizuka, Y., Yamada, H., Koyama, H., 1991. A study on the mechanism of antibody-dependent enhancement of feline infectious peritonitis virus infection in feline macrophages by monoclonal antibodies. Arch Virol 120, 207-217.

Hohdatsu, T., Okada, S., Ishizuka, Y., Yamada, H., Koyama, H., 1992. The prevalence of

doi:10.6342/NTU202301829

types I and II feline coronavirus infections in cats. J Vet Med Sci 54, 557-562.

Hohdatsu, T., Yamada, M., Tominaga, R., Makino, K., Kida, K., Koyama, H., 1998. Antibody-dependent enhancement of feline infectious peritonitis virus infection in feline alveolar macrophages and human monocyte cell line U937 by serum of cats experimentally or naturally infected with feline coronavirus. J Vet Med Sci 60, 49-55.

Hök, K., 1993. Morbidity, mortality and coronavirus antigen in previously coronavirus free kittens placed in two catteries with feline infectious peritonitis. Acta Vet Scand 34, 203-210.

Horzinek, M.C., Lutz, H., Pedersen, N., 1982. Antigenic relationships among homologous structural polypeptides of porcine, feline, and canine coronaviruses. Infection and Immunity 37, 1148-1155.

Hu, C.J., Chang, W.S., Fang, Z.S., Chen, Y.T., Wang, W.L., Tsai, H.H., Chueh, L.L., Takano, T., Hohdatsu, T., Chen, H.W., 2017. Nanoparticulate vacuolar ATPase blocker exhibits potent host-targeted antiviral activity against feline coronavirus. Sci Rep 7, 13043.

Huisman, W., Martina, B.E., Rimmelzwaan, G.F., Gruters, R.A., Osterhaus, A.D., 2009. Vaccine-induced enhancement of viral infections. Vaccine 27, 505-512.

Jaimes, J.A., Whittaker, G.R., 2018. Feline coronavirus: Insights into viral pathogenesis based on the spike protein structure and function. Virology 517, 108-121.

Jeffery, U., Deitz, K., Hostetter, S., 2012. Positive predictive value of albumin: globulin ratio for feline infectious peritonitis in a mid-western referral hospital population. J Feline Med Surg 14, 903-905.

Kannekens-Jager, M.M., de Rooij, M.M.T., de Groot, Y., Biesbroeck, E., de Jong, M.K., Pijnacker, T., Smit, L.A.M., Schuurman, N., Broekhuizen-Stins, M.J., Zhao, S., Duim, B., Langelaar, M.F.M., Stegeman, A., Kooistra, H.S., Radstake, C., Egberink, H.F., Wagenaar, J.A., Broens, E.M., 2022. SARS-CoV-2 infection in dogs and cats is associated with contact to COVID-19-positive household members. Transbound Emerg Dis 69, 4034-4040.

Kennedy, M., Citino, S., McNabb, A.H., Moffatt, A.S., Gertz, K., Kania, S., 2002. Detection of feline coronavirus in captive Felidae in the USA. J Vet Diagn Invest 14, 520-522.

Kipar, A., Bellmann, S., Kremendahl, J., Köhler, K., Reinacher, M., 1998. Cellular composition, coronavirus antigen expression and production of specific antibodies in lesions in feline infectious peritonitis. Vet Immunol Immunopathol 65, 243-257.

Kipar, A., May, H., Menger, S., Weber, M., Leukert, W., Reinacher, M., 2005. Morphologic features and development of granulomatous vasculitis in feline

doi:10.6342/NTU202301829

infectious peritonitis. Vet Pathol 42, 321-330.

Kipar, A., Meli, M.L., 2014. Feline infectious peritonitis: still an enigma? Vet Pathol 51, 505-526.

Kiss, I., Kecskeméti, S., Tanyi, J., Klingeborn, B., Belák, S., 2000. Preliminary studies on feline coronavirus distribution in naturally and experimentally infected cats. Res Vet Sci 68, 237-242.

Kiss, I., Poland, A.M., Pedersen, N.C., 2004. Disease outcome and cytokine responses in cats immunized with an avirulent feline infectious peritonitis virus (FIPV)-UCD1 and challenge-exposed with virulent FIPV-UCD8. J Feline Med Surg 6, 89-97.

Kummrow, M., Meli, M.L., Haessig, M., Goenczi, E., Poland, A., Pedersen, N.C., Hofmann-Lehmann, R., Lutz, H., 2005. Feline coronavirus serotypes 1 and 2: seroprevalence and association with disease in Switzerland. Clin Diagn Lab Immunol 12, 1209-1215.

Le Poder, S., 2011. Feline and canine coronaviruses: common genetic and pathobiological features. Adv Virol 2011, 609465.

Lee, W.S., Wheatley, A.K., Kent, S.J., DeKosky, B.J., 2020. Antibody-dependent enhancement and SARS-CoV-2 vaccines and therapies. Nat Microbiol 5, 1185-1191.

Leung, D.T., Tam, F.C., Ma, C.H., Chan, P.K., Cheung, J.L., Niu, H., Tam, J.S., Lim, P.L., 2004. Antibody response of patients with severe acute respiratory syndrome (SARS) targets the viral nucleocapsid. J Infect Dis 190, 379-386.

Lin, C.-N., Su, B.-L., Wu, C.-W., Hsieh, L.-E., Chueh, L.-L., 2009a. Isolation and identification of a novel feline coronavirus from a kitten with naturally occurring feline infectious peritonitis in Taiwan. 臺灣獸醫學雜誌 35, 145-152.

Lin, C.N., Chan, K.R., Ooi, E.E., Chiou, M.T., Hoang, M., Hsueh, P.R., Ooi, P.T., 2021. Animal Coronavirus Diseases: Parallels with COVID-19 in Humans. Viruses 13.

Lin, C.N., Su, B.L., Wang, C.H., Hsieh, M.W., Chueh, T.J., Chueh, L.L., 2009b. Genetic diversity and correlation with feline infectious peritonitis of feline coronavirus type I and II: a 5-year study in Taiwan. Vet Microbiol 136, 233-239.

Litster, A.L., Pogranichniy, R., Lin, T.L., 2013. Diagnostic utility of a direct immunofluorescence test to detect feline coronavirus antigen in macrophages in effusive feline infectious peritonitis. Vet J 198, 362-366.

Longstaff, L., Porter, E., Crossley, V.J., Hayhow, S.E., Helps, C.R., Tasker, S., 2017. Feline coronavirus quantitative reverse transcriptase polymerase chain reaction on effusion samples in cats with and without feline infectious peritonitis. J Feline Med Surg 19, 240-245.

Luo, Y.C., Liu, I.L., Chen, Y.T., Chen, H.W., 2020. Detection of Feline Coronavirus in Feline Effusions by Immunofluorescence Staining and Reverse Transcription

doi:10.6342/NTU202301829

Polymerase Chain Reaction. Pathogens 9.

Mahdy, M.A.A., Younis, W., Ewaida, Z., 2020. An Overview of SARS-CoV-2 and Animal Infection. Front Vet Sci 7, 596391.

Malbon, A.J., Fonfara, S., Meli, M.L., Hahn, S., Egberink, H., Kipar, A., 2019. Feline Infectious Peritonitis as a Systemic Inflammatory Disease: Contribution of Liver and Heart to the Pathogenesis. Viruses 11.

Malbon, A.J., Michalopoulou, E., Meli, M.L., Barker, E.N., Tasker, S., Baptiste, K., Kipar, A., 2020. Colony Stimulating Factors in Early Feline Infectious Peritonitis Virus Infection of Monocytes and in End Stage Feline Infectious Peritonitis; A Combined In Vivo And In Vitro Approach. Pathogens 9.

McBride, R., van Zyl, M., Fielding, B.C., 2014. The coronavirus nucleocapsid is a multifunctional protein. Viruses 6, 2991-3018.

Nakayama, E.E., Kubota-Koketsu, R., Sasaki, T., Suzuki, K., Uno, K., Shimizu, J., Okamoto, T., Matsumoto, H., Matsuura, H., Hashimoto, S., Tanaka, T., Harada, H., Tomita, M., Kaneko, M., Yoshizaki, K., Shioda, T., 2022. Anti-nucleocapsid antibodies enhance the production of IL-6 induced by SARS-CoV-2 N protein. Sci Rep 12, 8108.

Norris, J.M., Bosward, K.L., White, J.D., Baral, R.M., Catt, M.J., Malik, R., 2005. Clinicopathological findings associated with feline infectious peritonitis in Sydney, Australia: 42 cases (1990-2002). Aust Vet J 83, 666-673.

O'Brien, A., Mettelman, R.C., Volk, A., André, N.M., Whittaker, G.R., Baker, S.C., 2018. Characterizing replication kinetics and plaque production of type I feline infectious peritonitis virus in three feline cell lines. Virology 525, 1-9.

Oude Munnink, B.B., Sikkema, R.S., Nieuwenhuijse, D.F., Molenaar, R.J., Munger, E., Molenkamp, R., van der Spek, A., Tolsma, P., Rietveld, A., Brouwer, M., Bouwmeester-Vincken, N., Harders, F., Hakze-van der Honing, R., Wegdam-Blans, M.C.A., Bouwstra, R.J., GeurtsvanKessel, C., van der Eijk, A.A., Velkers, F.C., Smit, L.A.M., Stegeman, A., van der Poel, W.H.M., Koopmans, M.P.G., 2021. Transmission of SARS-CoV-2 on mink farms between humans and mink and back to humans. Science 371, 172-177.

Ouyang, H., Liu, J., Yin, Y., Cao, S., Yan, R., Ren, Y., Zhou, D., Li, Q., Li, J., Liao, X., Ji, W., Du, B., Si, Y., Hu, C., 2022. Epidemiology and Comparative Analyses of the S Gene on Feline Coronavirus in Central China. Pathogens 11.

Paltrinieri, S., Giordano, A., Tranquillo, V., Guazzetti, S., 2007. Critical assessment of the diagnostic value of feline alpha1-acid glycoprotein for feline infectious peritonitis using the likelihood ratios approach. J Vet Diagn Invest 19, 266-272.

Paltrinieri, S., Parodi, M.C., Cammarata, G., 1999. In vivo diagnosis of feline infectious peritonitis by comparison of protein content, cytology, and direct

doi:10.6342/NTU202301829

immunofluorescence test on peritoneal and pleural effusions. J Vet Diagn Invest 11, 358-361.

Parodi, M.C., Cammarata, G., Paltrinieri, S., Lavazza, A., Ape, F., 1993. Using direct immunofluorescence to detect coronaviruses in peritoneal in peritoneal and pleural effusions. Journal of Small Animal Practice 34, 609-613.

Patterson, E.I., Elia, G., Grassi, A., Giordano, A., Desario, C., Medardo, M., Smith, S.L., Anderson, E.R., Prince, T., Patterson, G.T., Lorusso, E., Lucente, M.S., Lanave, G., Lauzi, S., Bonfanti, U., Stranieri, A., Martella, V., Basano, F.S., Barrs, V.R., Radford, A.D., Agrimi, U., Hughes, G.L., Paltrinieri, S., Decaro, N., 2020. Evidence of exposure to SARS-CoV-2 in cats and dogs from households in Italy. bioRxiv.

Paul-Murphy, J., Work, T., Hunter, D., McFie, E., Fjelline, D., 1994. Serologic survey and serum biochemical reference ranges of the free-ranging mountain lion (Felis concolor) in California. J Wildl Dis 30, 205-215.

Payne, S., 2017. Family coronaviridae. Viruses, 149.

Pedersen, N.C., 1987. Virologic and immunologic aspects of feline infectious peritonitis virus infection. Adv Exp Med Biol 218, 529-550.

Pedersen, N.C., 2009. A review of feline infectious peritonitis virus infection: 1963-2008. J Feline Med Surg 11, 225-258.

Pedersen, N.C., 2014a. An update on feline infectious peritonitis: diagnostics and therapeutics. Vet J 201, 133-141.

Pedersen, N.C., 2014b. An update on feline infectious peritonitis: virology and immunopathogenesis. Vet J 201, 123-132.

Pedersen, N.C., Boyle, J.F., Floyd, K., Fudge, A., Barker, J., 1981. An enteric coronavirus infection of cats and its relationship to feline infectious peritonitis. Am J Vet Res 42, 368-377.

Pedersen, N.C., Eckstrand, C., Liu, H., Leutenegger, C., Murphy, B., 2015. Levels of feline infectious peritonitis virus in blood, effusions, and various tissues and the role of lymphopenia in disease outcome following experimental infection. Vet Microbiol 175, 157-166.

Perlman, S., Dandekar, A.A., 2005. Immunopathogenesis of coronavirus infections: implications for SARS. Nat Rev Immunol 5, 917-927.

Perlman, S., Masters, P., Howley, P., Knipe, D., Whelan, S. 2020. Fields virology: emerging viruses (Wolters Kluwer Health/lippincott Williams & Wilkins Philadelphia, PA).

Poland, A.M., Vennema, H., Foley, J.E., Pedersen, N.C., 1996. Two related strains of feline infectious peritonitis virus isolated from immunocompromised cats infected with a feline enteric coronavirus. J Clin Microbiol 34, 3180-3184.

doi:10.6342/NTU202301829

Regan, A.D., Cohen, R.D., Whittaker, G.R., 2009. Activation of p38 MAPK by feline infectious peritonitis virus regulates pro-inflammatory cytokine production in primary blood-derived feline mononuclear cells. Virology 384, 135-143.

Regan, A.D., Ousterout, D.G., Whittaker, G.R., 2010. Feline lectin activity is critical for the cellular entry of feline infectious peritonitis virus. J Virol 84, 7917-7921.

Regan, A.D., Whittaker, G.R., 2008. Utilization of DC-SIGN for entry of feline coronaviruses into host cells. J Virol 82, 11992-11996.

Riemer, F., Kuehner, K.A., Ritz, S., Sauter-Louis, C., Hartmann, K., 2016. Clinical and laboratory features of cats with feline infectious peritonitis--a retrospective study of 231 confirmed cases (2000-2010). J Feline Med Surg 18, 348-356.

Rissi, D.R., 2018. A retrospective study of the neuropathology and diagnosis of naturally occurring feline infectious peritonitis. J Vet Diagn Invest 30, 392-399.

Rohrbach, B.W., Legendre, A.M., Baldwin, C.A., Lein, D.H., Reed, W.M., Wilson, R.B., 2001. Epidemiology of feline infectious peritonitis among cats examined at veterinary medical teaching hospitals. J Am Vet Med Assoc 218, 1111-1115.

Satoh, R., Furukawa, T., Kotake, M., Takano, T., Motokawa, K., Gemma, T., Watanabe, R., Arai, S., Hohdatsu, T., 2011. Screening and identification of T helper 1 and linear immunodominant antibody-binding epitopes in the spike 2 domain and the nucleocapsid protein of feline infectious peritonitis virus. Vaccine 29, 1791-1800.

Severance, E.G., Bossis, I., Dickerson, F.B., Stallings, C.R., Origoni, A.E., Sullens, A., Yolken, R.H., Viscidi, R.P., 2008. Development of a nucleocapsid-based human coronavirus immunoassay and estimates of individuals exposed to coronavirus in a U.S. metropolitan population. Clin Vaccine Immunol 15, 1805-1810.

Shah, P., Canziani, G.A., Carter, E.P., Chaiken, I., 2021. The Case for S2: The Potential Benefits of the S2 Subunit of the SARS-CoV-2 Spike Protein as an Immunogen in Fighting the COVID-19 Pandemic. Front Immunol 12, 637651.

Shi, J., Wen, Z., Zhong, G., Yang, H., Wang, C., Huang, B., Liu, R., He, X., Shuai, L., Sun, Z., Zhao, Y., Liu, P., Liang, L., Cui, P., Wang, J., Zhang, X., Guan, Y., Tan, W., Wu, G., Chen, H., Bu, Z., 2020. Susceptibility of ferrets, cats, dogs, and other domesticated animals to SARS-coronavirus 2. Science 368, 1016-1020.

Shiba, N., Maeda, K., Kato, H., Mochizuki, M., Iwata, H., 2007. Differentiation of feline coronavirus type I and II infections by virus neutralization test. Vet Microbiol 124, 348-352.

Simons, F.A., Vennema, H., Rofina, J.E., Pol, J.M., Horzinek, M.C., Rottier, P.J., Egberink, H.F., 2005. A mRNA PCR for the diagnosis of feline infectious peritonitis. J Virol Methods 124, 111-116.

Soma, T., Wada, M., Taharaguchi, S., Tajima, T., 2013. Detection of ascitic feline coronavirus RNA from cats with clinically suspected feline infectious peritonitis.

doi:10.6342/NTU202301829

J Vet Med Sci 75, 1389-1392.

Stenske, K., 2005. Comparison of different tests to diagnose feline infectious peritonitis. J Vet Intern Med 19, 299.

Stoddart, C.A., Scott, F.W., 1989. Intrinsic resistance of feline peritoneal macrophages to coronavirus infection correlates with in vivo virulence. J Virol 63, 436-440.

Stout, A.E., André, N.M., Whittaker, G.R., 2021. FELINE CORONAVIRUS AND FELINE INFECTIOUS PERITONITIS IN NONDOMESTIC FELID SPECIES. J Zoo Wildl Med 52, 14-27.

Stranieri, A., Giordano, A., Paltrinieri, S., Giudice, C., Cannito, V., Lauzi, S., 2018. Comparison of the performance of laboratory tests in the diagnosis of feline infectious peritonitis. J Vet Diagn Invest 30, 459-463.

Stranieri, A., Lauzi, S., Giordano, A., Paltrinieri, S., 2017a. Reverse transcriptase loop-mediated isothermal amplification for the detection of feline coronavirus. J Virol Methods 243, 105-108.

Stranieri, A., Paltrinieri, S., Giordano, A., 2017b. Diagnosing feline infectious peritonitis using the Sysmex XT-2000iV based on frozen supernatants from cavitary effusions. J Vet Diagn Invest 29, 321-324.

Sykes, J.E., 2013. Canine and feline infectious diseases. Elsevier Health Sciences.

Takano, T., Azuma, N., Satoh, M., Toda, A., Hashida, Y., Satoh, R., Hohdatsu, T., 2009. Neutrophil survival factors (TNF-alpha, GM-CSF, and G-CSF) produced by macrophages in cats infected with feline infectious peritonitis virus contribute to the pathogenesis of granulomatous lesions. Arch Virol 154, 775-781.

Takano, T., Ishihara, Y., Matsuoka, M., Yokota, S., Matsuoka-Kobayashi, Y., Doki, T., Hohdatsu, T., 2014. Use of recombinant nucleocapsid proteins for serological diagnosis of feline coronavirus infection by three immunochromatographic tests. J Virol Methods 196, 1-6.

Takano, T., Katada, Y., Moritoh, S., Ogasawara, M., Satoh, K., Satoh, R., Tanabe, M., Hohdatsu, T., 2008a. Analysis of the mechanism of antibody-dependent enhancement of feline infectious peritonitis virus infection: aminopeptidase N is not important and a process of acidification of the endosome is necessary. J Gen Virol 89, 1025-1029.

Takano, T., Kawakami, C., Yamada, S., Satoh, R., Hohdatsu, T., 2008b. Antibody-dependent enhancement occurs upon re-infection with the identical serotype virus in feline infectious peritonitis virus infection. J Vet Med Sci 70, 1315-1321.

Takano, T., Nakaguchi, M., Doki, T., Hohdatsu, T., 2017. Antibody-dependent enhancement of serotype II feline enteric coronavirus infection in primary feline monocytes. Arch Virol 162, 3339-3345.

Takano, T., Ohyama, T., Kokumoto, A., Satoh, R., Hohdatsu, T., 2011a. Vascular

doi:10.6342/NTU202301829

endothelial growth factor (VEGF), produced by feline infectious peritonitis (FIP) virus-infected monocytes and macrophages, induces vascular permeability and effusion in cats with FIP. Virus Res 158, 161-168.

Takano, T., Tomiyama, Y., Katoh, Y., Nakamura, M., Satoh, R., Hohdatsu, T., 2011b. Mutation of neutralizing/antibody-dependent enhancing epitope on spike protein and 7b gene of feline infectious peritonitis virus: influences of viral replication in monocytes/macrophages and virulence in cats. Virus Res 156, 72-80.

Tammer, R., Evensen, O., Lutz, H., Reinacher, M., 1995. Immunohistological demonstration of feline infectious peritonitis virus antigen in paraffin-embedded tissues using feline ascites or murine monoclonal antibodies. Vet Immunol Immunopathol 49, 177-182.

Tecles, F., Caldín, M., Tvarijonaviciute, A., Escribano, D., Martínez-Subiela, S., Cerón, J.J., 2015. Serum biomarkers of oxidative stress in cats with feline infectious peritonitis. Res Vet Sci 100, 12-17.

Tekes, G., Hofmann-Lehmann, R., Stallkamp, I., Thiel, V., Thiel, H.J., 2008. Genome organization and reverse genetic analysis of a type I feline coronavirus. J Virol 82, 1851-1859.

Tekes, G., Thiel, H.J., 2016. Feline Coronaviruses: Pathogenesis of Feline Infectious Peritonitis. Adv Virus Res 96, 193-218.

Tilocca, B., Soggiu, A., Sanguinetti, M., Musella, V., Britti, D., Bonizzi, L., Urbani, A., Roncada, P., 2020. Comparative computational analysis of SARS-CoV-2 nucleocapsid protein epitopes in taxonomically related coronaviruses. Microbes Infect 22, 188-194.

Tresnan, D.B., Holmes, K.V., 1998. Feline aminopeptidase N is a receptor for all group I coronaviruses. Adv Exp Med Biol 440, 69-75.

Tresnan, D.B., Levis, R., Holmes, K.V., 1996. Feline aminopeptidase N serves as a receptor for feline, canine, porcine, and human coronaviruses in serogroup I. J Virol 70, 8669-8674.

Vennema, H., Poland, A., Foley, J., Pedersen, N.C., 1998. Feline infectious peritonitis viruses arise by mutation from endemic feline enteric coronaviruses. Virology 243, 150-157.

Vlasova, A.N., Diaz, A., Damtie, D., Xiu, L., Toh, T.H., Lee, J.S., Saif, L.J., Gray, G.C., 2022. Novel Canine Coronavirus Isolated from a Hospitalized Patient With Pneumonia in East Malaysia. Clin Infect Dis 74, 446-454.

Walter, J., Dohse, K., Rudolph, R., 1989. [A modification of the ABC method (avidin-biotin-peroxidase complex) for the detection of viral antigens in coronavirus infections in cats (FIP) and parvovirus type 2 infections in dogs]. Zentralbl Veterinarmed B 36, 321-332.

doi:10.6342/NTU202301829

Wang, M.Y., Zhao, R., Gao, L.J., Gao, X.F., Wang, D.P., Cao, J.M., 2020. SARS-CoV-2: Structure, Biology, and Structure-Based Therapeutics Development. Front Cell Infect Microbiol 10, 587269.

Wang, Y.T., Chueh, L.L., Wan, C.H., 2014. An eight-year epidemiologic study based on baculovirus-expressed type-specific spike proteins for the differentiation of type I and II feline coronavirus infections. BMC Vet Res 10, 186.

Weiss, R.C., Scott, F.W., 1981. Pathogenesis of feline infetious peritonitis: pathologic changes and immunofluorescence. Am J Vet Res 42, 2036-2048.

Wen, J., Cheng, Y., Ling, R., Dai, Y., Huang, B., Huang, W., Zhang, S., Jiang, Y., 2020. Antibody-dependent enhancement of coronavirus. Int J Infect Dis 100, 483-489.

Wolfe, L.G., Griesemer, R.A., 1966. Feline infectious peritonitis. Pathol Vet 3, 255-270.

Woo, P.C.Y., de Groot, R.J., Haagmans, B., Lau, S.K.P., Neuman, B.W., Perlman, S., Sola, I., van der Hoek, L., Wong, A.C.P., Yeh, S.H., 2023. ICTV Virus Taxonomy Profile: Coronaviridae 2023. J Gen Virol 104.

Worthing, K.A., Wigney, D.I., Dhand, N.K., Fawcett, A., McDonagh, P., Malik, R., Norris, J.M., 2012. Risk factors for feline infectious peritonitis in Australian cats. J Feline Med Surg 14, 405-412.

Yamamoto, J.K., Edison, L.K., Rowe-Haas, D.K., Takano, T., Gilor, C., Crews, C.D., Tuanyok, A., Arukha, A.P., Shiomitsu, S., Walden, H.D.S., Hohdatsu, T., Tompkins, S.M., Morris, J.G., Jr., Sahay, B., Kariyawasam, S., 2023. Both Feline Coronavirus Serotypes 1 and 2 Infected Domestic Cats Develop Cross-Reactive Antibodies to SARS-CoV-2 Receptor Binding Domain: Its Implication to Pan-CoV Vaccine Development. Viruses 15.

Yang, D.-K., Park, Y.-R., Kim, E.-j., Lee, H.J., Shin, K.-S., Kim, J.-H., Lee, K., Hyun, B.-H., 2022. Incidence and sero-surveillance of feline viruses in Korean cats residing in Gyeonggi-do. Korean Journal of Veterinary Research 62, e24.

Yen, S.J., Chen, H.W., 2021. Feline Coronaviruses Identified in Feline Effusions in Suspected Cases of Feline Infectious Peritonitis. Microorganisms 9.

Yin, Y., Li, T., Wang, C., Liu, X., Ouyang, H., Ji, W., Liu, J., Liao, X., Li, J., Hu, C., 2021. A retrospective study of clinical and laboratory features and treatment on cats highly suspected of feline infectious peritonitis in Wuhan, China. Sci Rep 11, 5208.

Yuki, M., Aoyama, R., Nakagawa, M., Hirano, T., Naitoh, E., Kainuma, D., 2020. A Clinical Investigation on Serum Amyloid A Concentration in Client-Owned Healthy and Diseased Cats in a Primary Care Animal Hospital. Vet Sci 7.

Ziebuhr, J., 2005. The coronavirus replicase. Curr Top Microbiol Immunol 287, 57-94.

Ziebuhr, J., Snijder, E.J., Gorbalenya, A.E., 2000. Virus-encoded proteinases and proteolytic processing in the Nidovirales. J Gen Virol 81, 853-879.

doi:10.6342/NTU202301829